ESTIMATION OF LONGSHORE SEDIMENT TRANSPORT AND SHORELINE EVOLUTION ALONG KUAKATA BEACH BY NUMERICAL MODELLING

DIPEN SAHA

DEPARTMENT OF WATER RESOURCES ENGINEERING

BANGLADESH UNIVERSITY OF ENGINEERING AND TECHNOLOGY

DHAKA-1000, BANGLADESH

SEPTEMBER 2021

ESTIMATION OF LONGSHORE SEDIMENT TRANSPORT AND SHORELINE EVOLUTION ALONG KUAKATA BEACH BY NUMERICAL MODELLING

DIPEN SAHA

DEPARTMENT OF WATER RESOURCES ENGINEERING

BANGLADESH UNIVERSITY OF ENGINEERING AND TECHNOLOGY

DHAKA-1000, BANGLADESH

SEPTEMBER 2021

ESTIMATION OF LONGSHORE SEDIMENT TRANSPORT AND SHORELINE EVOLUTION ALONG KUAKATA BEACH BY NUMERICAL MODELLING

Submitted by

Dipen Saha

(Student ID: 1015162026 P)

In partial fulfillment of the requirement for the degree of

MASTER OF SCIENCE IN WATER RESOURCES ENGINEERING

DEPARTMENT OF WATER RESOURCES ENGINEERING

BANGLADESH UNIVERSITY OF ENGINEERING AND TECHNOLOGY

DHAKA-1000, BANGLADESH

SEPTEMBER 2021

CERTIFICATION OF APPROVAL

The thesis titled "Estimation of Longshore Sediment Transport and Shoreline Evolution Along Kuakata Beach by Numerical Modelling" submitted by Dipen Saha, Roll No. 1015162026 P, Session: October 2015, has been accepted as satisfactory in partial fulfillment of the requirement for the degree of **Master of Science in Water Resources Engineering** on September 25, 2021.

....

Dr. Md. Ataur Rahman
Professor
WRE, BUET, Dhaka

Chairman
(Supervisor)

....

Dr. A.T.M. Hasan Zobeyer
Professor & Head
WRE, BUET, Dhaka

Member
(Ex-Officio)

....

Dr. K. M. Ahtesham Hossain
Assistant Professor
WRE, BUET, Dhaka

Member

....

Rubayat Alam
Director
Coast, Port and Estuary Division
Institute of Water Modelling, Dhaka

Member
(External)

CANDIDATE'S DECLARATION

It is hereby declared that this thesis or any part of it has not been submitted elsewhere for the award of any degree or diploma.

Signature of the Candidate

Dipen Saha

TABLE OF CONTENTS

Contents

LIST OF FIGURES

LIST OF TABLES

LIST OF SYMBOLS

$\zeta(x,y,t)$	Surface elevation (m)
$d(x,y,t)$	time varying water depth (m)
$C(x,y)$	Chezy resistance ($m^{1/2}$/s)
M	Manning's Number ($m^{1/3}$/s)
g	acceleration due to gravity (m^2/s)
$f(V)$	wind friction factor
$V, V_x, V_y(x,y,t)$	wind speed and components in x-and y-direction (m/s)
$\Omega(x,y)$	Coriolis parameter, latitude dependent (s^{-1})
$p_a(x,y,t)$	atmospheric pressure ($kg/m/s^2$)
ρ_w	density of water (kg/m^3)
x,y	space coordinates (m)
t	time (s)
$\tau_{xx}, \tau_{xy}, \tau_{yy}$	components of effective shear stress
S	source term for the energy balance equation
k_n	Bottom friction
S_{xy}	shear stress due to radiation
τ_w	wind stress
I	longshore slope of water surface
θ	angle between wind direction and coast normal
E_c	momentum exchange coefficient
ε_s	turbulent diffusion coefficient
w	fall velocity of the sediment
$Y_c(x)$	distance from the baseline to the coastline
$h_{act}(x)$	height of the active cross-shore profile
$Q(x)$	longshore transport of sediment expressed in volume
$Q_{sou}(x)$	source/sink term expressed in volume
ρ_s	sediment density
K	dimensionless empirical coefficient
H_{sb}	nearshore breaking height of significant wave
C_{gb}	wave group speed at breaking

θ_b angle breaking wave crest makes with shoreline

d_b depth of wave breaking

T_{op} breaking wave height

M_b nearshore beach gradient

α_b angle breaking wave crest makes with the shoreline

LIST OF ABBREVIATIONS

ADCP	Acoustic Doppler Current Profiler
BIWTA	Bangladesh Inland Water Transport Authority
BMD	Bangladesh Meteorological Department
BoB	Bay of Bengal
BTM	Bangladesh Transverse Mercator
BUET	Bangladesh University of Engineering and Technology
BWDB	Bangladesh Water Development Board
CERC	Coastal Engineering Research Center
DEM	Digital Elevation Model
DHI	Danish Hydraulic Institute
ECMWF	European Centre for Medium-Range Weather Forecasts
EXEN	Executive Engineer
FM	Flexible Mesh
GEBCO	General Bathymetric Chart of the Oceans
HD	Hydro-dynamic
IPCC	Intergovernmental Panel on Climate Change
IWFM	Institute of Water and Flood Management
IWM	Institute of Water Modelling
LITPACK	LITtoral Processes And Coastline Kinetics
LSTR	Longshore Sediment Transport Rate
MSL	Mean Sea Level
PWD	Public Works Datum
RMS	Route Mean Square
USGS	United States Geological Survey
WL	Water Level
WRE	Water Resources Engineering

ACKNOWLEDGEMENT

ABSTRACT

This study work has been conducted for erosion and deposition analysis of Kuakata beach, estimation of longshore sediment transport and coastline evolution as well. Satellite images of coastline during the period of 1978 to 2020 have been collected and analyzed using ArcGIS software. 24 km long Kuakata beach is subdivided into three parts like Lebur Char (13 km), Gangamatir Char (4 km) and Kawar Char (7 km) stretching from west to east. From Satellite image analysis, it is evident that Lebur Char (west part) is vulnerable to erosion, middle part of the Kuakata beach i.e., Gangamatir Char is more or less stable, and Kawar Char (east part) is accreting day by day. It is seen that 13 km long coastline has been eroded having an area of 4.8 km^2 and 7 km coastline has been accreted having an area of 3.7 km^2 has been accreted in last 42 years. During this period the average erosion rate and accretion rate are 9 m/yr and 12.2 m/yr respectively and for last it was 10 years 11.7 m/yr and 21.2 m/yr respectively. Dedicated hydrodynamic model using MIKE 21 FM (with/without wave action) is developed, calibrated and validated for studying nearshore hydrodynamic analysis. Model simulation for different critical hydrological and hydrodynamic condition reveals that there develops longshore current along the beach and eastward current magnitude dominates over westward current magnitude. Dedicated wave model has been developed using MIKE 21 SW and the simulated wave climate has been used in LITDRIFT model and LITLINE model. From wave rose analysis, it is found that waves hit the Kuakata beach angularly and eastward wave is most prominent, which generates longshore current from west to east. Simulated hydrodynamics of coupled wave-tide model are used in LITDRIFT model to estimate the rate of longshore sediment transport. It is found that overall net sediment transport occurs eastward of amount 5.94x10^5 m^3/yr and 1.46x10^5 m^3 is eroded for Lebur Char area and 2.36x10^5 m^3 deposited in Kawar Char area per year, estimated by LITDRIFT model of LITPACK module under MIKE. Coastlines have been simulated by LITLINE model, which is calibrated and validated with the real filed data of coastline extracted from the satellite images of the year 2018 and 2016. LITLINE model has been simulated over the year 2010 to 2018 for erosion prone area of Kuakata. It is observed that coastline is moving towards land with time. Future caostline position is also simulated up to the year 2024. It is predicted that western part (Lebur Char area) of Kukata beach will further erode at a rate of 9.6 m/yr up to the year 2024.

CHAPTER ONE

INTRODUCTION

1.1   General

The Bay of Bengal (BoB) is bordered by eastern coast of Srilanka and India on the west, Bangladesh coast to the north, western coast of Myanmar (formerly known as Burma) and northwestern part of Malay Peninsula to the east (Uddin et al., 2014) which is shown in the **Figure 1.1**. There is a submarine canyon, also known as swatch of no ground, in the central northern part of the BoB. Coastal zone of Bangladesh is located in the northern part of BoB. There are 19 districts in the coastal zone. Coastal zone of Bangladesh is very important due to biodiversity and economic aspects (Islam and Ahmad, 2004).
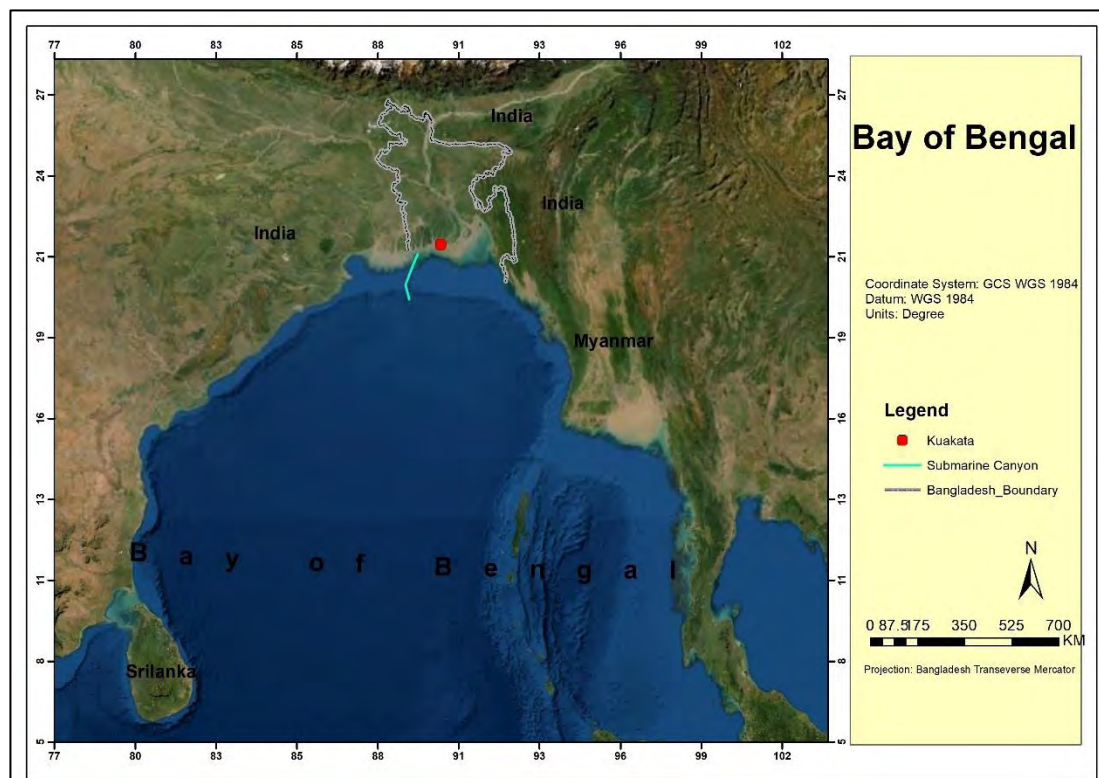
Figure 1.1: Map Showing Bay of Bengal (BoB)

Coastal erosion is one of the big challenges in Bangladesh. Many reasons are responsible for coastal erosion, among them strong tidal current, wave action, cyclonic storm surge and human interventions are prime reasons. Erosion has been happening in some places along the coastline of Bangladesh. Kuakata is one of those. There has

been happening erosion along the main beach of Kuakata for last decades. This study has been conducted to analyze the nearshore hydrodynamics and estimation of sediment transport along Kuakata beach.

1.2   Study Area

This study is conducted for Kukata beach area and coastline. Kuakata is located in the southern part of Banaladesh and northern part of BoB. It is situated 320 km south of capital city Dhaka and 70 km away from Patuakhali district headquarter. The area lies between latitudes $21^0 48^'$ and $21^0 55^'$ N and longitudes $90^0 03^'$ and $90^0 15^'$ E. Kuakata is under Kalapara upazila of Patuakhali district. Study area (Kuakata) is shown in the **Figure 1.2**.
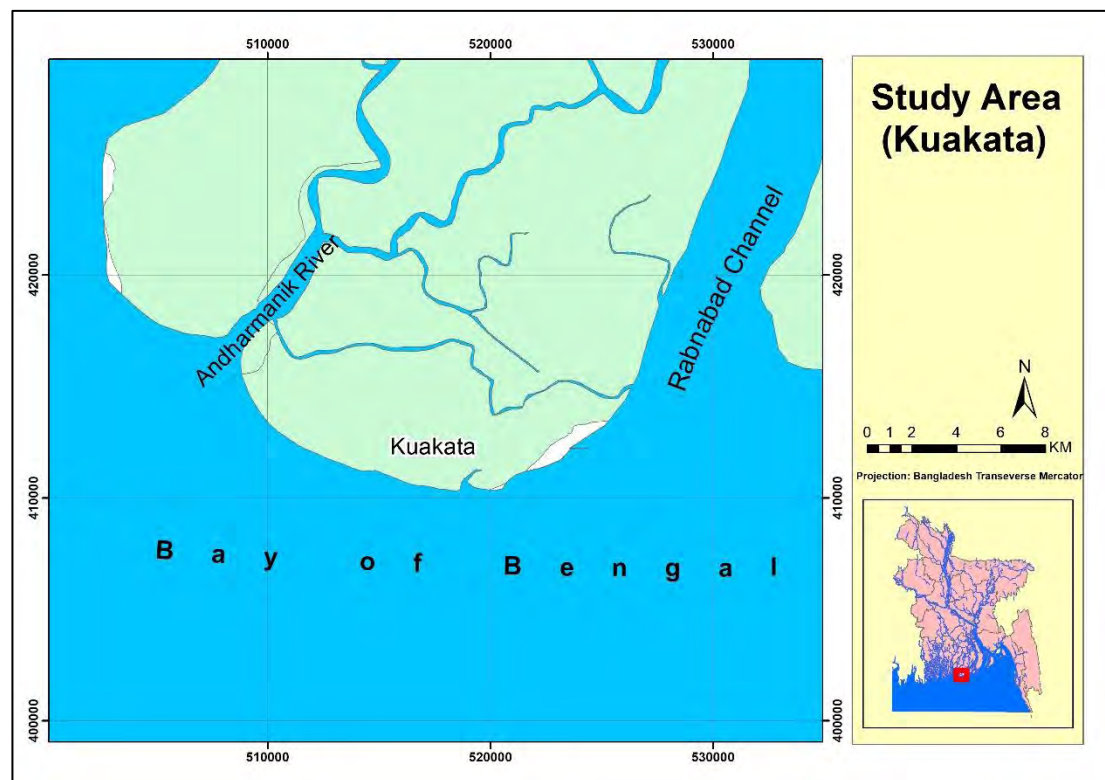
Figure 1.2: Map showing study area

Bangladesh has an area of about 1,47,570 square kilometers and a population of more than 160 million, of which 32% of the total population lives in the coastal region. About 710 km long coast of Bangladesh comprising the complex delta of the Ganges-Brahmaputra-Meghna River system has immense resources for development. Kuakata, also popularly known as Sagar Kannya (daughter of sea queen), located on

the coastal zone of Bangladesh (**Figure 1.3**). It is the only place of Bangladesh from where sun set, and sun rise can be enjoyed.
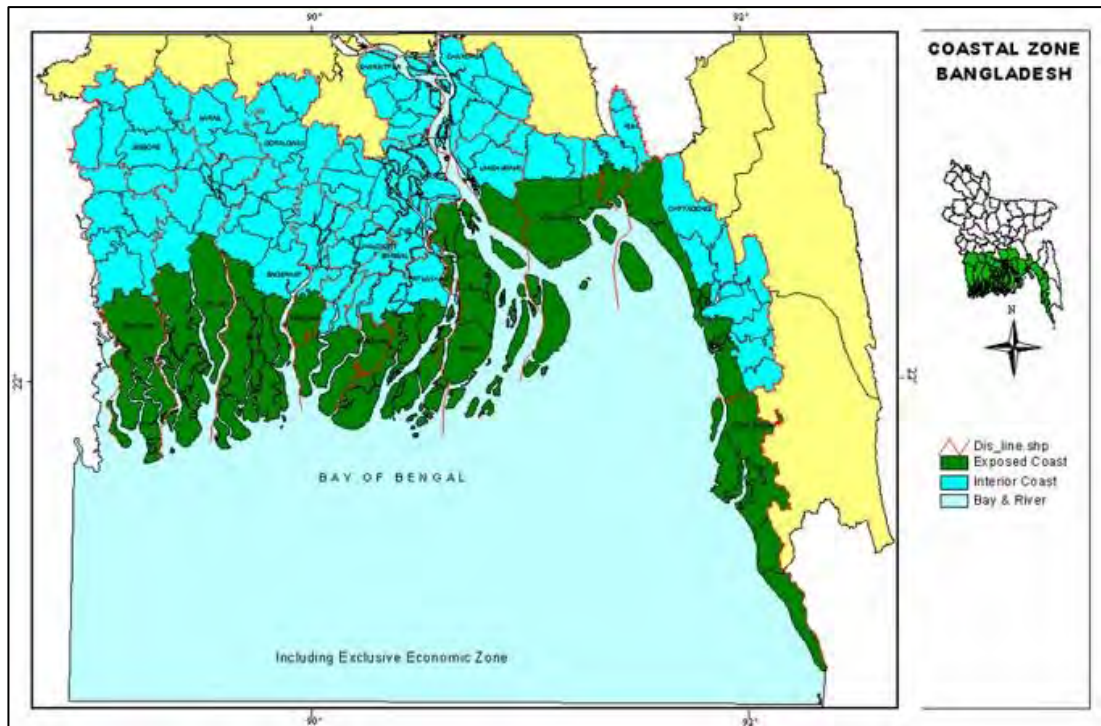
Figure 1.3: Coastal zone of Bangladesh (Source: Islam and Ahmad, 2004)

Kuakata beach is an important place for tourism and thereby plays a vital role for national economy. But beach erosion is becoming a serious problem day by day. Kuakata beach is about 24 km long stretching from west to east. West part of the beach, named Lebur Char which is the main attractive place of the tourists has been suffering from erosion for last few decades. Middle part, named Gangamatir Char is relatively stable. Whereas, the east part of the beach, named Cowar Char has been accreting for last few decades. The beach is bounded by the Andharmanik river estuary at the west and Rabnabad river estuary at the east. There are 139 polders in the coastal zone of Bangladesh to protect the area from tidal flooding and salinity intrusion. Kuakata is under polder-48 which is shown by red circle in the map (**Figure 1.4**).

A long narrow linear beach present in Kuakata. Kuakata beach is characterized by ridge and runnel topography. Deposits of the beach are mostly composed of sand. A dominant strong wind is present toward the onshore direction. A well-developed dune is present in Cowar Char area (Rashid and Mahmud, 2011).
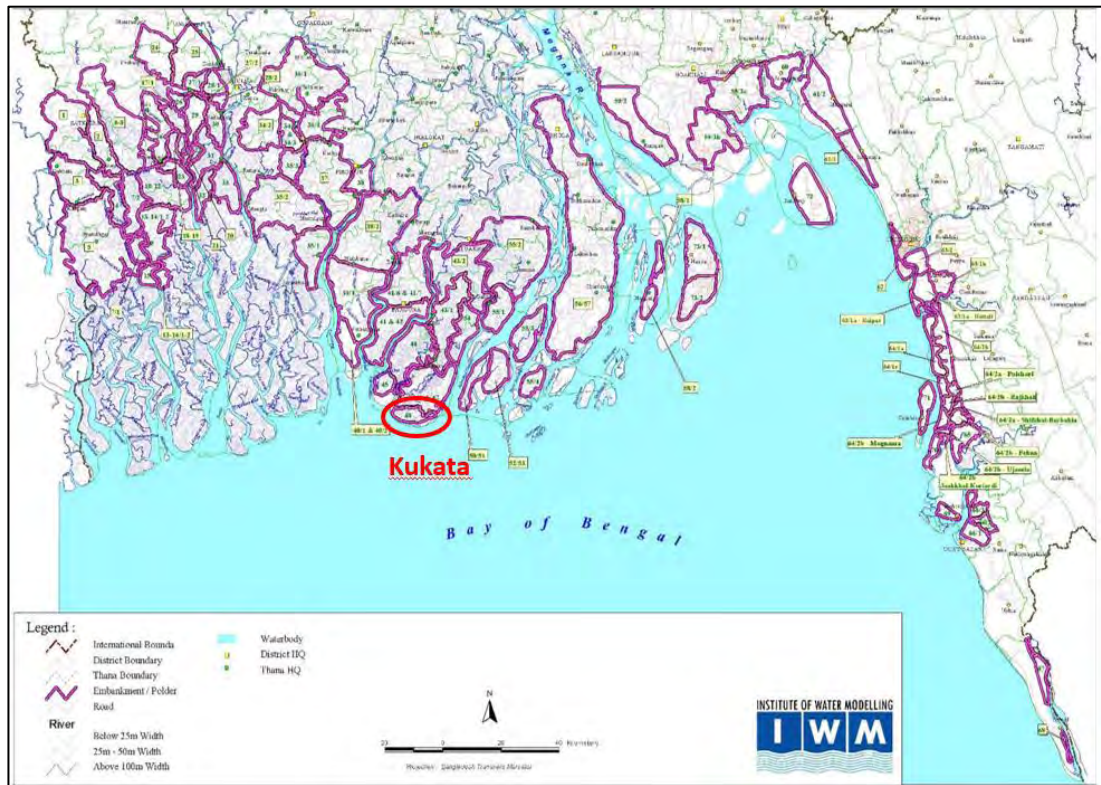
Figure 1.4: Polders along coastal zone of Bangladesh (Map Source: IWM)

Kuakata beach is facing significant amount of erosion. This study aims to assess erosion coastline shifting, hydrodynamics for occurring erosion, sediment budget assessment which are explained in detail in chapter 3 and 4.

1.3 Background and Present State of the Problem

After Cox's Bazar Kuakata is the 2nd attracted place for tourists. There is a huge impact of tourism on the society and economy of the country. It fortifies the country socially as well as economically. Bangladesh tourism industry contributes to healthy GDP and employment opportunities. According to the World Travel and Tourism report of 2011, 1.9 % of total employment is generated by tourism industry and it is expected to reach 29.3 % by 2021.

| Kuakata beach under erosion threat | Human chain to save Kuakata beach |

Figure 1.5: Kukata beach erosion at Lebur Char area (left), people demand to save Kukata beach from erosion (right) (Source: Internet)

So, in tourism aspect Kuakata has remarkable value. Though having tremendous possibilities in tourism, Kukata has beach erosion problem, shown in the **Figure 1.5**. People of Kuakata have been demanding to protect the beach from erosion for many days. In some places hard structure like revetment is provided by BWDB to protect the embankment along beach but it is not continuous. Moreover, in some places revetment have been damaged due to wave action.

| Kukata Coastline, 2000 | Kuakata Coastline, 2020 |
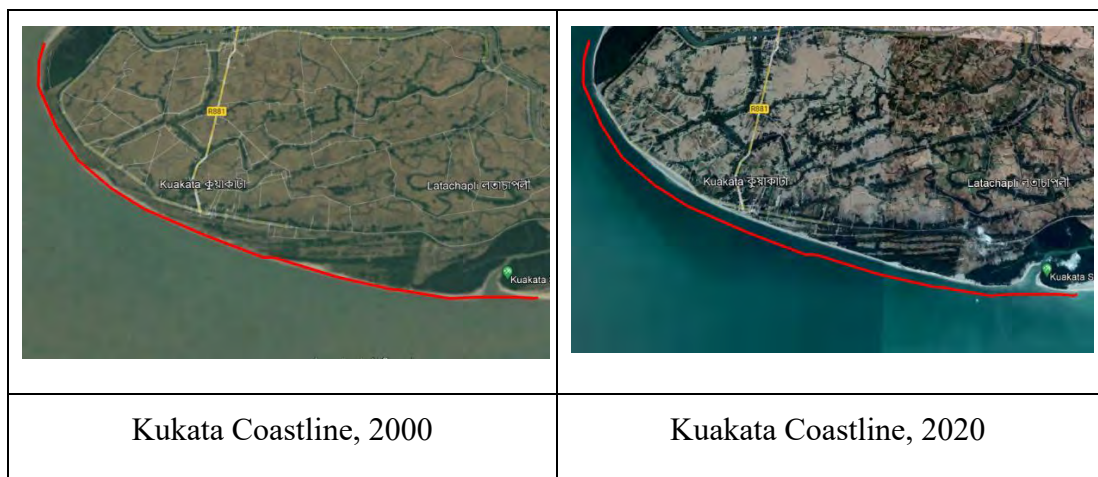
Figure 1.6: Coastline Shifting in Last 20 Years (Digitized in google earth pro)

The western part of Kuakata beach, which is the main tourist attraction, has been suffering erosion for last few decades. **Figure 1.6** is comparison of two satellite images for the year 2000 and 2020. Coastline has been digitized in google earth pro which is shown by red line for the year 2000. Same line is superimposed for the image-

2020. This figure gives us a qualitative idea about erosion in the beach over 2(two) decades.

Figure 1.7: Protection by geo-tube and geo-bag to combat erosion in Kuakata beach (Photograph Courtesy: Engr. M.H Salehy, EXEN, BWDB; May 28,2021)

So many protection measures can be deployed to combat beach erosion by break water, groyne, geo-bag, geo-tube, sea wall, beach nourishment, revetment. In some places geo-bag and geo-tube have been placed temporarily by BWDB to protect beach from erosion (**Figure 1.7**). But for sustainable solution proper protection measures should be undertaken based on intensive research.

Rahman et.al (2013) studied that in 23.56 km long Kuakata shoreline, erosion occurs in 13.59 km reach and deposition occurs in 9.97 km using satellite images from 1973 to 2010. In this study coastline shifting assessment is done using satellite image from 1978 to 2020. Longshore sediment transport rate and erosion-accretion pattern along Kuakata beach and shoreline position prediction for eroding part of Kuakata beach are done in this study which have not been done yet for Kuakata beach so far.

This study aims to identify whether longshore or cross shore current is dominant. Historical satellite images have been analyzed to understand erosion, accretion and shifting of coastline. Longshore sediment transport has been estimated by Littoral Processes FM. Coastline evolution has been estimated and verified with satellite image coastline for a particular year. Assessment of the longshore sediment transport and simulation of shoreline changes along Kuakata beach are the main output of this research work which will help coast management authority to take necessary protection measures.

1.4   Objectives

The specific objectives of this study are as follows:

i.   To assess the shoreline change along Kuakata beach from historical (1978-2020) satellite images.

ii.   To setup, calibrate and validate hydrodynamic and wave model of MIKE 21 FM/SW and simulate the near shore wave-tide hydrodynamics.

iii. To estimate longshore sediment transport rate using LITDRIFT model for the study area.

iv.   To simulate the shoreline evolution along the study area using LITLINE model which will be verified with real time coastline position for a particular year.

1.5   Scopes of the Study

This study focuses on some specific analysis by computer-based modeling and GIS tool. Shoreline shifting assessment and quantifying erosion and accretion area along Kuakata beach have been done. With the aid of hydrodynamic model simulation nearshore hydrodynamics (current direction and speed for different tidal condition) has been analyzed. At the same time a wave model coupled with HD result has been simulated and dominant sediment transport has been identified. Moreover, longshore sediment transport has been estimated, and shoreline changes has been simulated along the Kuakata beach which will help coast management authority to take necessary protection measures.

1.6   Outline of the Report

Considering literature review, location of the study area, mathematical modeling, data analysis, model calibration, results, and discussions the thesis has been organized under five chapters which are described below:

Chapter One, describes the background, highlights the objectives of the study, and contains outlines of the report.

Chapter Two, describes definition, classification of important terminology and literature review on hydrodynamic, wave and littoral transport related study.

Chapter Three, describes the methodology of the total research works including data collection, calibration, and validation of Hydrodynamic, coupled Wave model separately. It also describes the LITDRIFT model and coastline evolution model (LITLINE).

Chapter Four, describes the erosion analysis of Kuakata beach, current analysis, wave rose analysis, result from LITDRIFT model, manual calculation of annual littoral transport and comparison with simulated littoral transport, shoreline simulation by LITLINE, calibration and validation of LITLINE model, future shoreline prediction.

Chapter Five, provides the overall conclusions of the study and also some recommendations for further study.

CHAPTER TWO

LITERATURE REVIEW

2.1   General

Literature review is of paramount importance prior to conduct a study whether it is research based or project-based study. A significant number of journals, conference papers, project studies and M.Sc. thesis are explored which are relevant to current study. Many studies were conducted for different coastline all over the world. As substantial portion of Kukata beach is vulnerable to erosion so this study can play vital role to mitigate the erosion problem and obviously help the coast management authority in decision making. There is a range of options that may be considered for possible coastal protection works. These may be summarized under the general headings as follows:

- ➢ Do Nothing.

- ➢ Re-nourish the beach to maintain beach and shingle volumes.

- ➢ Use groynes or artificial headlands to control sediment drift.

- ➢ Install revetments to protect against wave attack.

- ➢ Build a series of offshore breakwaters to protect the shoreline and build up the beach.

- ➢ A combination of one or more of the above.

The choice of options is governed by a number of issues including, value of assets to be protected, impact on the coastal processes, cost of the works, environmental impact of the works and the ongoing maintenance requirements. The estimated annual longshore sediment transport will help in devising coastal protection. The review of past studies will enable to enhance the understanding on problem analysis, use of modeling tools and different protective measures and their effects.

2.2 Salient Definition and Classification

Wind-generated currents are caused by the direct action of the wind shear stress on the surface of the water. The wind-generated currents are normally located in the upper layer of the water body and are therefore not very important from a morphological point of view. In very shallow coastal waters and lagoons, the wind-generated current can, however, be of some importance. Wind-generated current speeds are typically less than 5 percent of the wind speed.

Nearshore mean currents which occur within the surf zone are principally driven by the breaking waves. For purposes of simplification, nearshore mean currents are usually separated into their cross-shore and longshore components: Undertows and rip currents have their principal axes oriented perpendicular to the beach (offshore) while longshore currents act parallel to the beach. These currents are all driven by cross- and/or longshore components of radiation stress gradients (in practice wave energy gradients) that arise through wave breaking. Thus, Wind-generated currents classified into two types (i.e., longshore current and cross-shore current)

A **longshore current** is an ocean **current** that moves parallel to shore. It is caused by large swells sweeping into the shoreline at an angle and pushing water down the length of the beach in one direction. it also moves sediment parallel to the shoreline.

A cross-shore current is an ocean current that moves perpendicular to shore. Cross-shore current can be further classified into two types like undertow and rip currents.

Longshore drift from **longshore current** is a geological process that consists of the transportation of sediments (clay, silt, sand and shingle) along a coast parallel to the shoreline, which is dependent on oblique incoming wind direction. Oblique incoming wind squeezes water along the coast, and so generates a water current which moves parallel to the coast. Longshore drift is simply the sediment moved by the longshore current. This current and sediment movement occur within the surf zone.
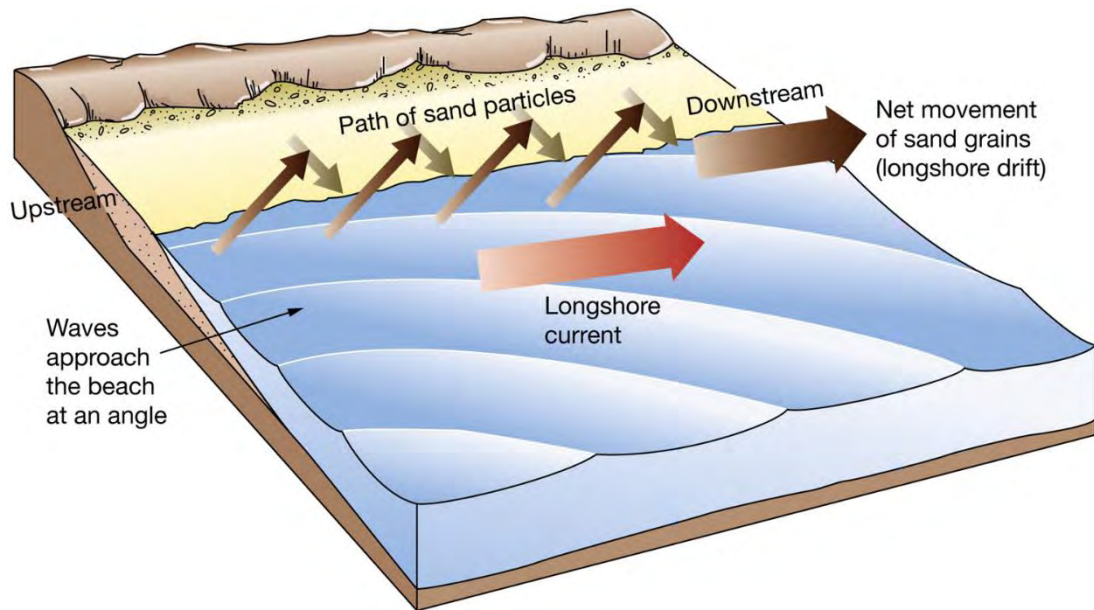
Figure 2.1: Schematic diagram depicting longshore drift (Source: https://www.davidegaeta.com/post/la-longshore-current)

Beach sand is also moved on such oblique wind days, due to the swash and backwash of water on the beach. Breaking surf sends water up the beach (swash) at an oblique angle and gravity then drains the water straight downslope (backwash) perpendicular to the shoreline. Thus, beach sand can move down beach in a zig zag fashion many tens of meters (yards) per day. This process is called "beach drift" but some workers regard it as simply part of "longshore drift" because of the overall movement of sand parallel to the coast.

A **groyne** (in the U.S. **groin**) is a rigid hydraulic structure built from an ocean shore (in coastal engineering) or from a bank (in rivers) that interrupts water flow and limits the movement of sediment. It is usually made out of wood, concrete or stone. In the ocean, groynes create beaches or prevent them being washed away by longshore drift.

Breakwaters are structures constructed near the coasts as part of Coastal management or to protect an anchorage from the effects of both weather and longshore drift.

Breakwaters reduce the intensity of wave action in inshore waters and thereby reduce coastal erosion or provide safe harborage. Breakwaters may also be small structures designed to protect a gently sloping beach and placed one to three hundred feet offshore in relatively shallow water.

2.3   Relevant Studies

A number of previous literatures are studied especially bankline/coastline shifting or erosion related study, hydrodynamic and wave model related study and longshore sediment transport and coastline/shoreline evolution related study. The prime objective of this study is to find longshore sediment transport rate and observe the shoreline changes with time. To facilitate this hydrodynamic and wave model related knowledge and model results are prerequisite. In the following sections previous literatures with brief discussion are arranged which really helped to execute this study.

2.3.1   Bankline Shifting or Erosion Related Studies

Rahman et al., (2013) Studied that in 23.56 km long shoreline, erosion occurs in 13.59 km reach and deposition occurs in 9.97 km during the period of 1973 to 2010 in Kuakata. Maximum width of beach area, which has been eroded, is about 450 m and accreted is about 1075 m during last 37 years. Kuakata coastline shifting is shown in the **Figure 2.2**.
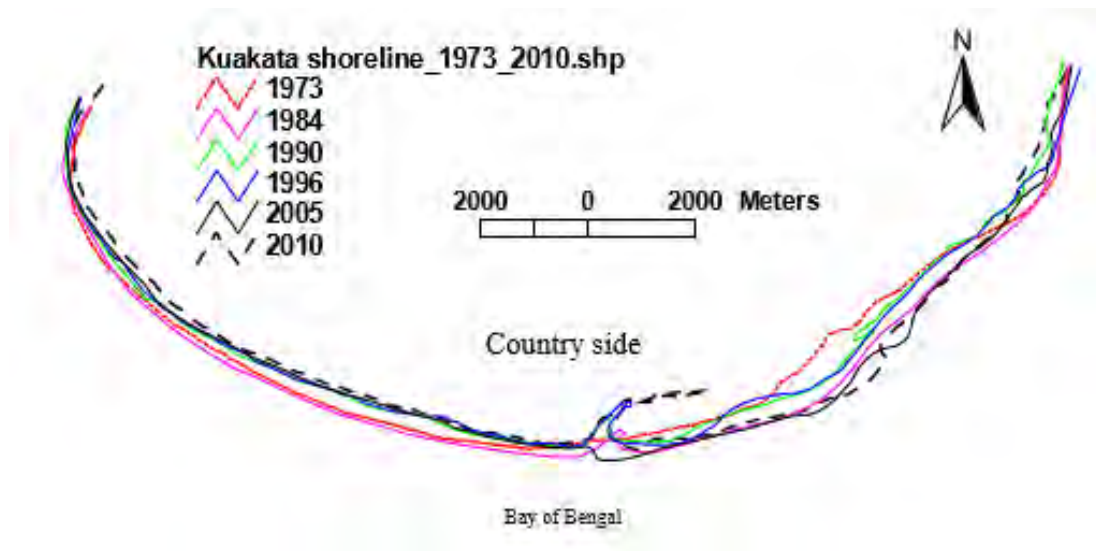
Figure 2.2: Kuakata shoreline shifting from 1973 to 2010 (Source: Rahman et al., 2013)

To protect the central 5 km reach of eroded beach this study also investigates the design aspects of protection work using artificial beach nourishment with Dean's equilibrium beach profile method considering intersecting and non-intersecting

profiles. The design volume of nourished sand required for per unit length of Kuakata beach has been estimated as 1433 m^3 /m, 934 m^3 /m and 761 m^3 /m for fill grain size of as 0.15 mm, 0.20 mm and 0.25 mm respectively. The study also calculates the half-life of the designed nourished sand, which is estimated as 4.62 years.

IWM, (2014) carried out a study on the Cox's Bazar-Teknaf Marine Drive Road (MDR) which was built to facilitate tourism opportunity, development fishing industry, enhancing regional connectivity and improved management of natural resources. The road construction was started during 1993-94. In June 2008, the first phase of the Marine-Drive Road of 24 km from Kalatali to Inani was completed. In the second phase, another 24 km road is being constructed from Inani to Shilkhali from July 2008 and still under construction. The objective of the study is to investigate the coastal erosion processes along the Marine-drive, review of existing erosion protection measures and to devise immediate and long-term erosion mitigation measures. The changes in shoreline along Maine Drive were assessed by analyzing satellite images which were collected under this study from secondary sources. The images were collected for the year 1972, 1980, 1989, 2000 and 2012. Time series satellite image analysis (2000 and 2012) was made to examine the shifting characteristics of the shoreline along Phase-I and Phase-II. The state-of the art mathematical modeling technology has been used under this study for the establishment of current speed, water level, wave dynamics, longshore sediment transport and sedimentation-erosion pattern along the Marine Drive. To accomplish the above-mentioned activities three types of models were used such as Hydrodynamic Model, Spectral Wave Model and Littoral Drift Model. The Hydrodynamic model gives the pattern of water level variation and current speed, wave model gives the pattern of wave dynamics and wave parameter, and Littoral Drift model gives the quantification of longshore sediment transport along the Marine Drive.
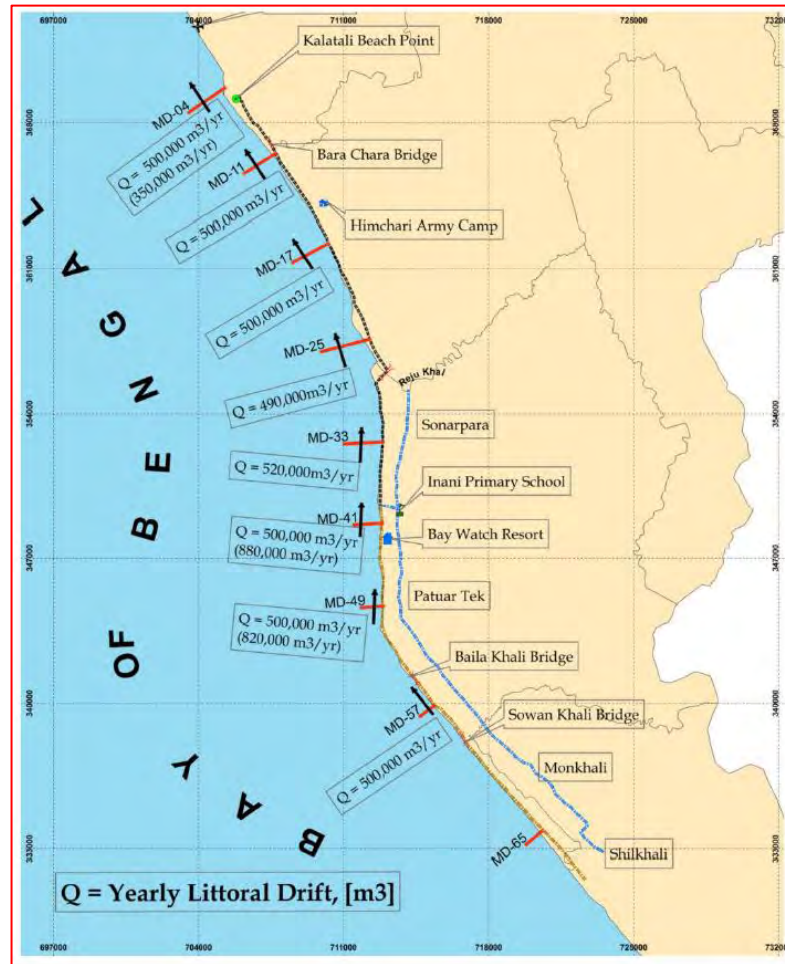
Figure 2.3: Yearly littoral transport along marine drive road, Cox's Bazar (Source: IWM,2014)

It is seen that the calculated littoral transport/longshore sediment transport close to 500,000 m^3 per year at all profiles along the Marine Drive, except at Profiles MD-41 and MD-49 which are located north of the point Patuar Tek, where a considerably higher transport rate above 800,000 m^3 was found (**Figure 2.3**). This higher transport rate is mainly due to the concentration of wave energy around the point and the large angle between the incoming waves and the orientation of the shoreline and has caused a considerable erosive pressure. This section of the coast is protected by the presence of hard erosion-resistant rocks (presumably relict corals) in the profile; the actual transport is therefore smaller than the calculated capacity (given in parentheses) because there is a lack of sand in the profile. This part of the coast (and in particular the point at Patuar Tek) is therefore under erosive pressure and is only stable because it is protected by the hard material in the profiles.

Bushra, (2013) studied on detecting changes of shoreline at Kuakata coast using RS-GIS techniques and participatory approach. The land-water interface is of great importance due to its significance in resource extraction, coastal management, and climate change vulnerability analysis. In the recent years, determination of shoreline requires more concern as the coast of Bangladesh is vulnerable to anticipated sea level rise due to climate change. Region specific shoreline determination is needed for resource extraction, coastal risk management and landuse planning. This report is produced to address the areas of erosion, accretion, and stable shoreline along the coast of Kuakata for providing a basis to describe the extent of economic and environmental effects of present shore erosion and accretion. In this study, the shoreline change is primarily detected for three decades by comparing satellite imagery of 1989, 2003 and 2010, using Landsat TM 30mresolution images. Band Combination, Ratio Transformation, Normalized Difference Vegetation Index (NDVI) and Normalized Difference Water Index (NDWI) algorithms are used to extract shoreline from land water boundary. Later Band Combination (BC) is specifically used to measure the differences from year to year. These change detections were compared and verified by using Participatory Rural Appraisal (PRA) tools like- Transect Walk, Timeline Analysis, Cause and Effect Diagram, Key Informant Interview and Focus Group Discussion. Application of these tools also reveals the impacts due to this change. The study area, Kuakata, is a dynamic coast. Comparison of distances between derived shorelines and reference shorelines consistently shows that from 1989 to 2010 total 11.81 km^2 coastal land has been eroded and 2.34 km^2 land has been accreted. The coastline is retreating about 4.7 km^2 per decade. Information from the Participatory Rural Appraisal (PRA) implies that, at the coast of Kuakata, the rate of erosion is higher than the rate of accretion. This result validates the finding of image interpretation from RS-GIS method. It shows that mainly fisheries and tourism is affected by the shoreline change. Marine and climatic factors are the main causes of this change. This complex shoreline change has great significance since it is one of the major tourist spots in Bangladesh.

Corbella and Stretch, (2012) studied that storms and water levels are subject to seasonal variations but may also have decadal or longer trends that need to be included

when estimating risks in the coastal zone. They propose a non-stationary multivariate generalized extreme value model for wave height, wave period, storm duration and water levels that is constructed using Archimedean copulas. The statistical model was applied to a South African case study to test the impacts of decadal trends on beach erosion. Erosion was estimated using three process-based models like SBEACH, XBEACH and the Time Convolution model. The XBEACH model provided the best calibration results and was used to simulate potential future long-term trends in beach erosion. Based on the simulated erosion results of 5 beach profiles for storms with 25, 50- and 100-year return periods, it was estimated that the erosion rate could increase by 0.20%/year/storm and should therefore be a significant factor in long-term planning. The predicted future erosion due to storm and sea level trends was estimated to increase at a rate of 0.14%/year/storm and 0.20%/year/storm as a result of the 0.0057 m/yr and 0.02 m/yr increase wave height respectively. It has been estimated that storm trends are unlikely to contribute to long term erosion prior to the year 2100 while it is plausible that sea level rise is already contributing to long term erosion. The methods presented in this paper should be useful for medium to long term planning by coastal managers and decision makers.

Frihy and Deabes, (2012) showed that the rate of shoreline changes, seabed morphology and coastal processes are integrated to assess erosion resulting from construction of a series of jetties and groins built in stages to support recreation facilities at the Marina Resort Center at El Alamein historic site on the western Mediterranean coast of Egypt. Analysis of shoreline changes using satellite images spanning between 1988 (pre-construction) and 2011 (present situation) indicates that coastal stretch with these hard structures, 8 km long, has experienced a state of stability with a general tendency toward accretion (2.1–16.4 m/yr), mostly occurring to the west of these structures under the action of the prevailing easterly longshore current. As a consequence, the accretion systematically continues eastward for a 3.5 km distance and then reverses to erosion between −1.2 and −3.9 m/yr, threatening the adjacent resort beaches. Annual sand nourishment operations undertaken downcoast of these structures between 1989 and 2009 were unsuccessful in maintaining stability of this eroded sector because of its steeply sloped beach face and incompatibility of

borrowed sand for nourishment. Therefore, establishing a sustainable erosion mitigation with minimum impacts has been the ultimate goal to stabilize the area and also to create a calm beach safe enough for recreation and swimming. As a practical response, an environmentally acceptable "Perched Beach" was designed in 2011 and is now under construction.

2.3.2 Hydrodynamic and Wave Model Related Studies

Haque, (2018) conducted a study to assess the hydrodynamic changes during construction of a closure in a 4 km wide tidal channel between Subornachar and Swarnadip island located in the Meghna Estuary. Two construction methods have been considered vertical and horizontal closing method. A developed hydrodynamic model was used for the simulations of different construction stages of these two closing techniques using MIKE-21FM model. For the horizontal closing method, the channel was narrowed down from the sides and for vertical closing method it was raised from the bottom of the bed at regular intervals by varying sill levels. For the horizontal closing method, nine construction stages were considered and for the vertical closing method five construction stages were considered. The construction stages for horizontal closing method were H1(3650 m opening), H3(2850 m opening), H5(2050 m opening), H6(two 250 m openings and one 1050 m opening), H7(two 250 m openings and two 300 m openings), H8 (two 300 m openings) and H9 (two 250 m openings). The five construction stages for vertical closing method were V1 at sill level -5 mPWD, V2 at sill level -3 mPWD, V3 at sill level -1 mPWD, V4 at sill level +1 mPWD and V5 at sill level +5mPWD. For the horizontal closure the model was run by keeping the sill level fixed at +7.5 m PWD and the channel was narrowed down from the sides at regular intervals. Model simulation shows that the maximum flow velocities during the construction of the closure were obtained during flood tide as 1.43 m/s (H1), 1.7 m/s (H3), 2.28 m/s(H5), 2.56 m/s (H6), 4.36 m/s (H7), 4.58 m/s (H8) and 4.76 m/s (H8). **Figure 2.4** illustrates flow speed and direction for H1.
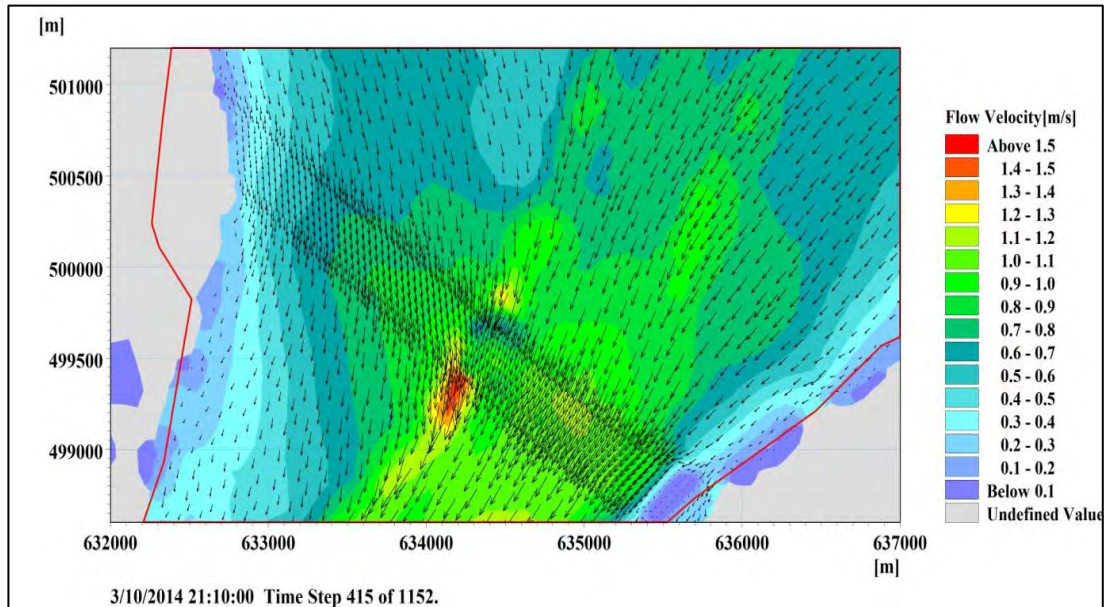
Figure 2.4: Current direction speed diagram with direction and corresponding WL condition during construction of closure H1 (source: Hauque, 2018)

It is suggested that the channel should be closed at once after H7 stage, because as the opening becomes smaller (H8 or H9) the velocities are seen to be increasing. For the vertical closing method, the flow velocity over the sill was calculated using the Weir and Villante Formula. The maximum flow velocity initially increases for V1 (2.76 m/s), V2(3.07 m/s) and V3 (3.88 m/s) and then decreased for V4 (3.14 m/s) and V5 (2.9 m/s). These flow velocities were found during flood tide. This gradual drop in flow velocities occur as the flow becomes supercritical. As the channel was vii closed the flow velocity at north of the closure were found to be decreasing and that south of the closure were found to be increasing. Since the channel has a width of about 4000m, constructing the tidal closure poses severe challenges. The construction period is

desired to be during neap tide of a dry season (preferably December which has the lowest tidal range of all times based on the water level data for Swarnadip).

However, the construction would require a series of neap tidal cycles with spring tides coming in between and pausing the construction period. Therefore, flow velocities for spring tide have been also determined, so that sufficient material could be used to bear the increased flow velocity due to narrowing down of the channel. For such a long channel having a width of 4000m, the vertical closing method seems more feasible as it has lower flow velocities during construction than horizontal closing method and narrowing down such a wide channel from the sides is practically difficult than closing it from the bottom.

A study work has been conducted by Nahiduzzamn, (2018) for simulation of storm surge level at a tidal channel due to coastal cyclone along the Bangladesh coast. Bay of Bengal hydrodynamic model (BoB) of IWM has been updated with finer mesh resolution at Baleshwar channel and it has been calibrated and validated for water level using the measured data of the year 2017 and 2015 respectively. Moreover, cyclone model of MIKE-21 maintained by IWM has been calibrated for measured wind speed at several locations for cyclone 1991, cyclone SIDR (2007) and cyclone AILA (2009). These two calibrated models (hydrodynamic and cyclone model) have been coupled together and storm surge model has been developed for Bangladesh coastline. Finally, this storm surge model has been calibrated and validated using the measured storm surge levels for cyclone SIDR (2007) and cyclone AILA (2009). This calibrated and validated storm surge model has been further verified with the storm surge level during Cyclone SIDR-2007 measured by Japan Society of Civil Engineers (JSCE) team. Wave model needs to simulate wave height during the cyclone period. Therefore, both storm surge and wave model has been simulated for cyclone SIDR-2007. Both storm surge and wave model result has been used to verify the maximum observed water elevation during cyclone SIDR-2007 at three locations of Baleshwar River namely Southkhali, Rayenda Bazar and Solombaria. Simulated storm surge level of calibrated storm surge model (under this research work) shows a difference of (+)10.7%, (-)11.5% and (-)18.4% at Solombaria, Rayenda Bazar and Southkhali respectively with the field investigation of JSCE team for cyclone SIDR-2007 (

Figure 2.6). This may happen due to some measurement uncertainty of the JSCE team. Maximum wave height in Baleswar Channel is shown in the **Figure 2.5**.
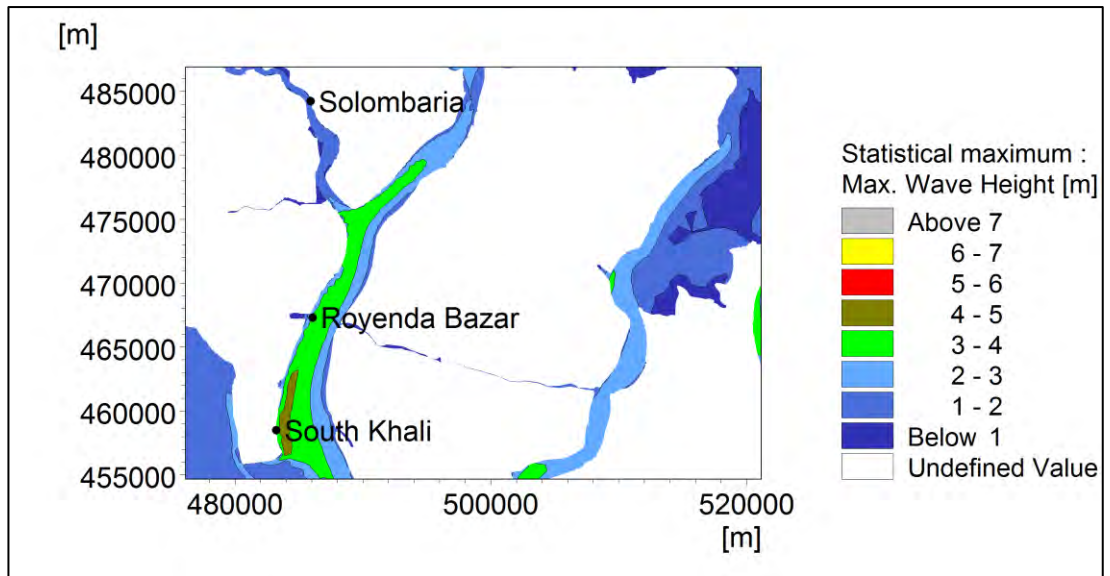
Figure 2.5: Maximum wave height along Baleshwar Channel (Source: Nahiduzzaman, 2018)

The model simulated result of storm surge level is then further compared with the existing storm surge model simulations of IWM. The result shows a little difference in the surge level compared to the simulation result of IWM. It is to be mentioned that IWM storm surge model is developed by coupling of calibrated hydrodynamic model and cyclone model (calibrated with the pattern of satellite image). It is seen that simulated storm surge level under this study is found to be decreased by a range of 13 to 24 cm at different locations of Baleshwar channel and estuary compared to IWM model simulation results.
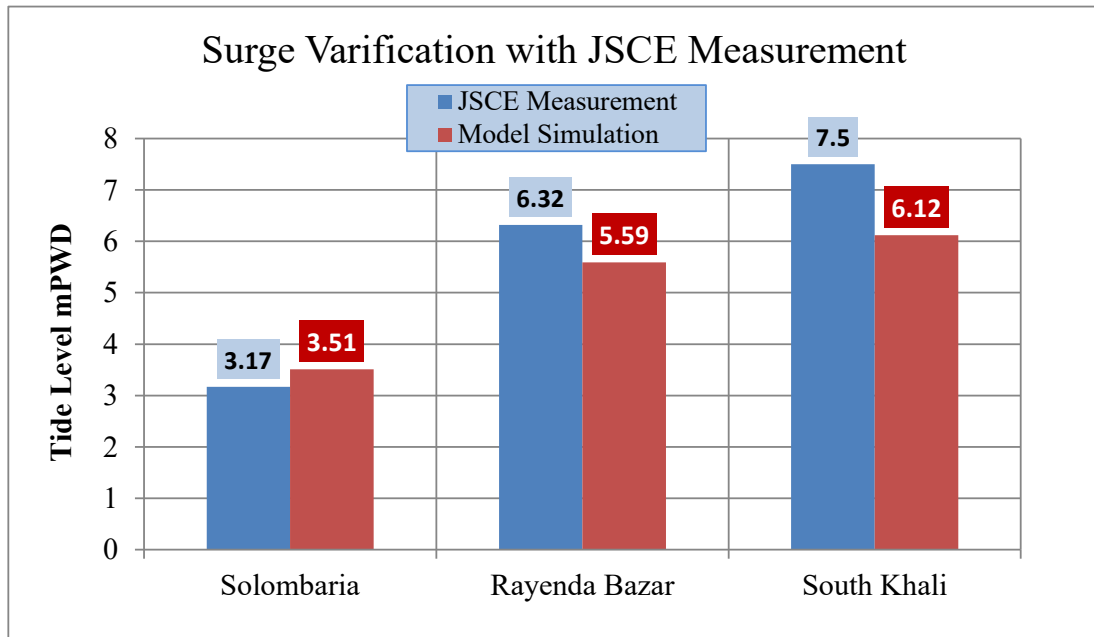
Figure 2.6: Surge verification with JSCE measurement (Source: Nahiduzzaman, 2018)

The calibrated and validated storm surge model has been simulated for five different water level and five different wind speed conditions to see the impacts of water depth and wind speed on storm surge height at Baleshwar estuary. The simulation result shows that storm surge height is a power function of wind speed. Storm surge height increases with the increase of wind speed for constant water depth and cyclone track. Again, it also found that storm surge height is inversely proportional to water depth for constant wind speed and cyclone track. These analysis results have been used to establish a relation between cyclone parameter and storm surge height at Baleshwar estuary. An equation has been developed for estimating the storm surge height at Baleshwar estuary which is further verified with the simulated surge height of IWM and shows good agreement.

Uddin et al., (2014) updated the BOB model with recent bathymetry data and shoreline of islands and coastline and upgrading from rectangular grid to finer size of mesh grids by using latest version of MIKE21 FM modeling system. This model is very useful for the hydrodynamic study in the coastal region of Bangladesh. Their paper also presents the model set-up, boundary condition and few calibration results of the

model. The mathematical model presented in this study includes the area of northern part of the Bay of Bengal from latitude 17.65˚ to the coast of Bangladesh and longitude 94.57˚ at Gawa beach to 83.28˚ at Vishakhapatnam (**Figure 2.7**).
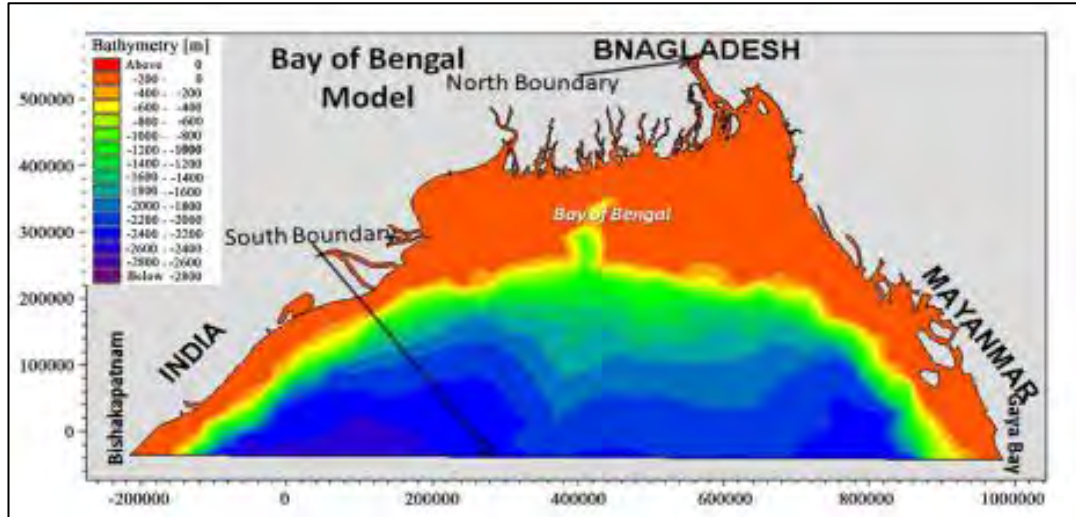
Figure 2.7: Bathymetry and open boundaries of BoB Model (Source: Uddin et al., 2014)

The hydrodynamic factors that are playing dominant role in morphological development along coastline of Bangladesh are enormous volume of river water flow, sediment transport, strong tidal and wind actions, wave, salinity, and cyclonic storm surge. These hydrodynamic factors and their interactions shape the morphology of the estuary. A complicated interplay between the forces of the river, tide and the waves create a complex pattern of sediment displacement in the estuary. Large quantities of sediment are transferred continuously towards the shallow coastal region of Bangladesh. The displacement of sediment is a part of continuous process of the estuarine landscape striving to achieve dynamic equilibrium between morphology and the continuously changing river discharge conditions and tidal flows. Keeping this background in mind, in order to have the essential comprehension of the flow pattern in the Bay of Bengal which is highly affected by above mentioned natural and many other man-made activities, the authors realized to have an accurate hydrodynamic model. Scientifically based mathematical modelling is an efficient tool for establishing hydraulic and morphological conditions, reliable evaluation of coastal development plan for maximizing the benefit integrating the coastal systems incorporating upstream and downstream hydraulic conditions.

2.3.3 Longshore Sediment Transport and Shoreline Changes Related Studies

Rajab and Thiruvenkatasamy, (2017) carried out a study in estimating longshore sediment transport along Puducchery Coast, India. Measured waves at 15 m water depth off Puducherry coast were used to estimate the longshore sediment transport along the Puducherry coast based on empirical methods and surf zone model. Comparison of longshore sediment showed that transport rate estimates gave wide variation among the empirical methods and surf zone model. Transport rate estimates using CERC gave higher (factor 2.5) and Kamphuis gave factor 1.5 when compared to VanRijn transport estimates. Estimated longshore sediment transport using surf zone model was close agreement with estimated littoral transport using VanRijn method. Estimated annual longshore sediment transport based on surf zone model along the Puducherry coast show that the highest northerly transport occurred in the month of May, followed by September, July, June, and August. Highest southerly transport was observed in December followed by November. Net monthly transport was northerly from March to October and southerly during the remaining months. Transport rate was found to be low in February. Volume of annual gross transport was estimated as 0.40 x 10^6 m³/year and the volume of annual net transport was 0.13 x 10^6 m³/year (towards north).

Appendini et al., (2012) published a paper which presents a qualitative assessment of coastal processes along the Northern coast of Yucatan based on a method to estimate the potential longshore sediment transport. Despite the deep-water low-energy wave conditions (Hs=1 m) in the study area, the erosion is critical in many locations including the urbanized stretches of coast. The waves were characterized using a 12-year (1997- 2009) deep-water wave hindcast (WAVEWATCH III) as forcing for a spectral wind-wave numerical model (MIKE 21 SW) used to propagate the waves to the coast. Simulated time series of significant wave height, peak period, and direction are compared against *in situ* measurements at 10 m water depth. Numerical results are further employed for estimation of the nearshore wave climate along the coast. Wave conditions are strongly affected by the wide continental shelf in front of the northern Yucatan Peninsula, with an increase of wave energy at the eastern part of the peninsula

where the shelf narrows. The nearshore wave climate is employed for the qualitative assessment of potential longshore sediment transport (LITDRIFT Model) in the study area. The sediment transport calculations are consistent with both volume impoundment estimations at a groin and dredging estimates at a harbor (-35,000m3/year). A net westward potential longshore sediment transport is found along the entire coast, ranging between -20,000 and -80,000 m^3/year, except West of Holbox, where longshore transport direction is inverted. Based on sediment transport gradients, potential erosion and deposition areas are identified. Erosion/accretion patterns at non-urbanized areas are consistent with field observations. This dominant westward longshore transport suggests an extremely sensitive shoreline to littoral barriers, as supported by observations in the most urbanized areas. These areas show no gradients on longshore sediment transport whereas beach erosion is a common feature enhanced by littoral barriers. Shore protection should then be oriented towards sediment management strategies.

Thanch et al., (2007) studied shoreline change by using LITPACK mathematical model for Cat Hai Island. Nowadays, there are many methods to study shoreline change in coastal engineering. Among them, mathematical methods are considered as effective ones that have been used for a long time. LITPACK is a numerical model in MIKE software package, developed by Danish Hydraulic Institute (DHI), for simulating non-cohesive sediment transport in wave and currents, littoral transport, coastline evolution and profile development along quasi-uniform beaches. In this paper, the authors apply the model for studying shoreline change in Cat Hai Island, Hai Phong City. Cat Hai is a famous island with dense population working with various coastal tradition works locating at the center of Hai Phong, where coastal line is changing with high speed and complicated cycles. Based on the analysis of hydrodynamic-lithologic conditions in this area, a coast protected structure system has been proposed, consisting of revetments, groynes, submerged breakwaters and emerged breakwaters. Results derived from LITPACK model show that they are reliable enough and suitable for use as remedial protecting measures.

Hossain, (2015) made an assessment of sediment movement pattern along nearshore coastal water of Cox's Bazar in his M.Sc. thesis work. Cox's Bazar is the most important Coastal district of Bangladesh. Coastal resources provide here the opportunities to use the coast in different ways within the hazard prone environment. The shape and orientation of the coastal landforms near Cox's Bazar is primarily based on sediment transport. Mathematical model can be used successfully to forecast this sediment movement pattern in nearshore coastal water of Cox's Bazar. Validity of forecast in sediment transport depends on both mathematical modeling technique and boundary conditions. In this research a numerical two-dimensional hydrodynamic Depth Integrated Velocity and Solute Transport Model (DIVAST) has been set up at nearshore coastal water of Cox's Bazar to assess the sediment movement pattern. An observation was made on the condition of suspended sediment and bed load along the study area by changing wave angle for 2 cases, one is for the boundary condition generated within the study area (case 1) and another is for the boundary condition generated outside of the study area from deep sea (case 2). The model output for both suspended and bed load is representing here one by one plotting them in surfer software to visualize and assess the sediment movement pattern in nearshore coastal water of Cox's bazar covering three very important beach of Bangladesh, Kolaboti beach, Laboni beach and Inani beach and the adjacent area of Moheshkhali channel. At first, the model was run for the wave angle 230o. Gradually it was changed for every 10o and the model output is presented here up to wave angle 290^0. Some selected model output for wave height and radiation stress is also presented in this thesis paper. The wave angle 230^0 for case 1 and 240^0 for case 2 were found most critical because of a considerable amount of suspended and bed load movements occur with these wave angles. The amount of sediment concentration has found to be negligible for incoming wave angle of 260^0, 270^0 and 280^0. After 290^0 the suspended sediment movement and after 270^0 the bed load movement was found insignificant. The sediment concentration is higher along the shore line than the other point of the study area.

Safak, (2006) conducted a study where a numerical model is developed to determine shoreline changes due to wind wave induced longshore sediment transport, by solving

sediment continuity equation and taking one-line theory as a base, in existence of seawalls, groins, Tgroins, offshore breakwaters and beach nourishment projects, whose dimensions and locations may be given arbitrarily. The model computes the transformation of deep-water wave characteristics up to the surf zone and eventually gives the result of shoreline changes with user-friendly visual outputs. A method of representative wave input as annual average wave characteristics is presented. Compatibility of the currently developed tool is tested by a case study, and it is shown that the results, obtained from the model, are in good agreement qualitatively with field measurements. In the scope of this study, input manner of long-term annual wave data into model in miscellaneous ways is also discussed.

Hendriyono et al., (2015) studied sediment transport modeling for Batang, Central Java. The presence of newly-built infrastructures along the coast of Batang, Central Java, has inherent effects on coastal hydrodynamics and natural equilibrium of annual sediment transport near the coastline. Retreating coastline as a result of severe erosion continuously occurs at some locations in recent years.
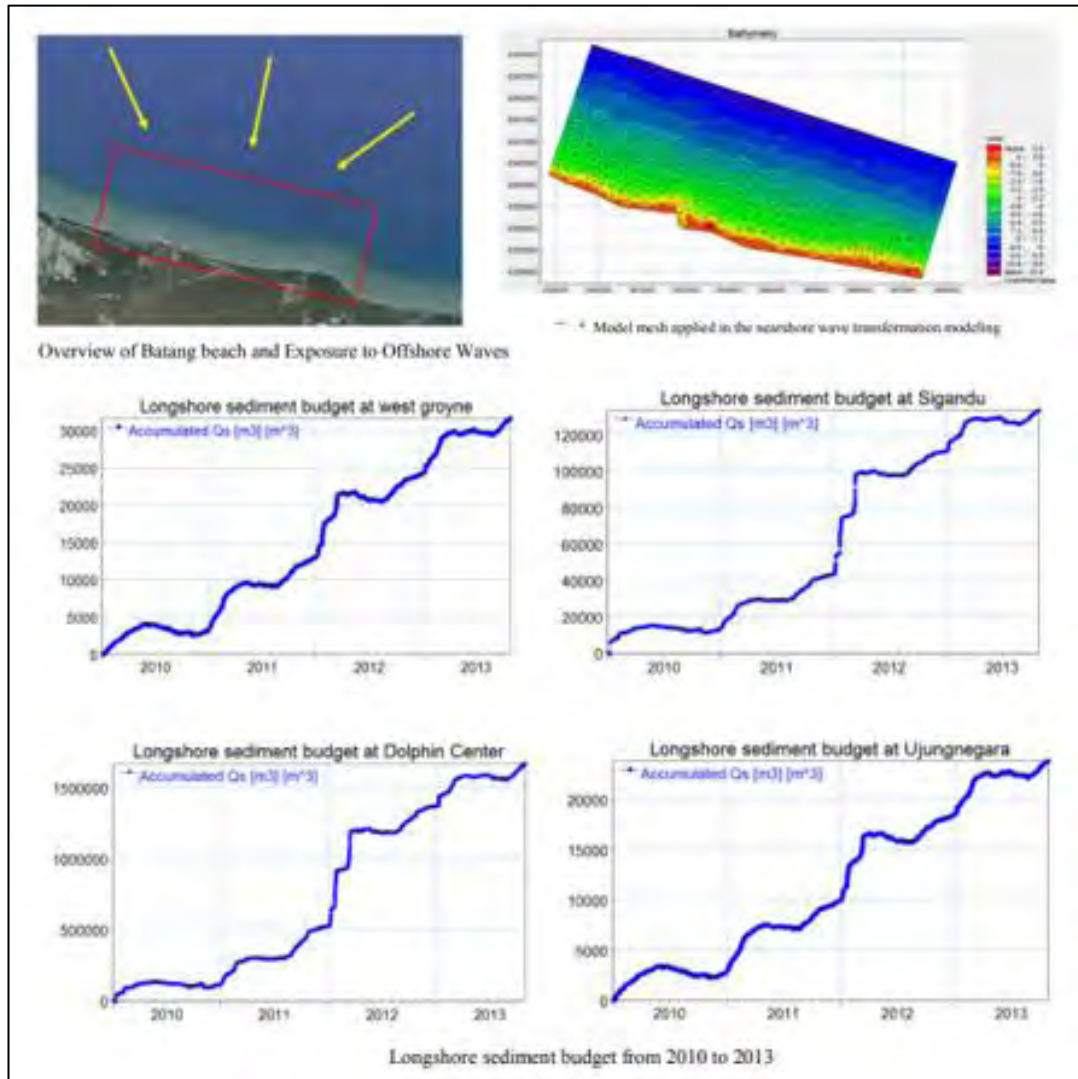
Figure 2.8: Model domain and longshore sediment transport (Source: Hendriyono et al. 2015)

This study aims to calculate the sediment transport behavior along the coast of Batang, Central Java, by considering the presence of infrastructures. Modeling was done by means of a commercially available software package MIKE21, especially the LITPACK module, developed by DHI Water and Environment, Denmark. The model shows that sediment drift parallel to the coastline occurs primarily within the distance of 300 meters from the coast. From 2010 to 2013, the general trend of sediment transport in the area is that there is a net sediment transport from the west to the east direction in the early months of the year, followed by a shorter period of transport in opposite direction (westward) for a few months. The in balance of this sediment

transport capacity is suspected to be responsible for the changes in coastline morphology in Batang.

Shetty and Jayappa, (2020) studied the Karnataka coast which is subjected to high wave activity during the southwest monsoon when most of the sandy beaches undergo erosion. Based on the littoral cell concept, the Karnataka coast is broadly divided into 14 major littoral cells and 26 stations are selected in the present study. Wave Watch III global wave model data at 0.5^0 interval were used to derive the nearshore wave characteristics from XBeach numerical model. The model results were validated with the measured wave rider buoy data of the Indian National Centre for Ocean Information Services. The beach orientation, nearshore slope, median sediment size, significant wave height, mean wave direction, and the
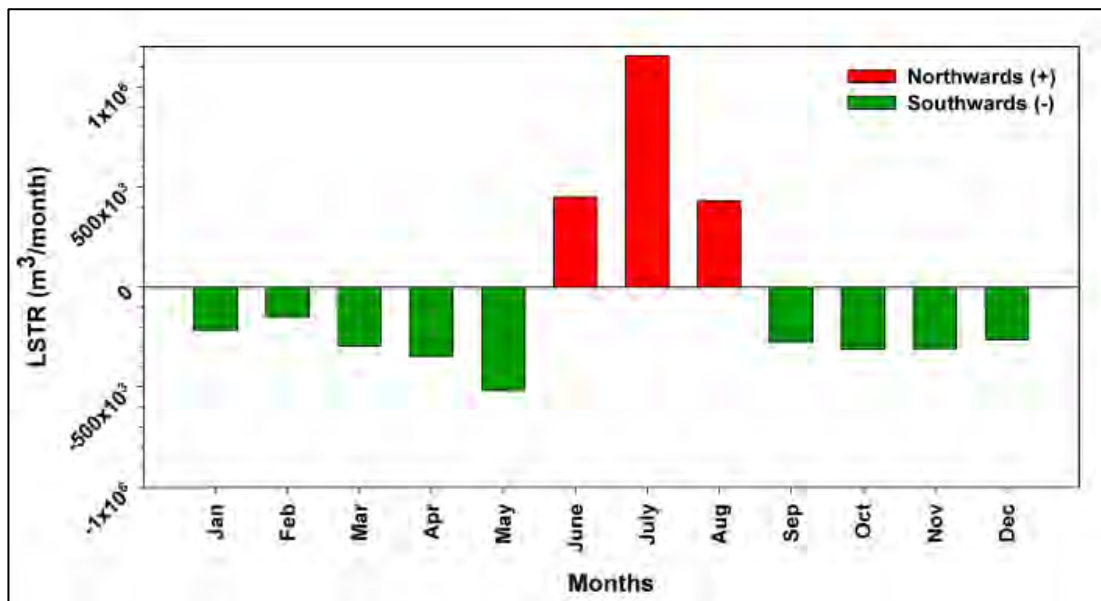
Figure 2.9: Monthly variation of longshore sediment transport rate (source: Shetty and Jayappa, 2020)

peak wave period were used in the estimation of longshore sediment transport rate. The mean significant wave height along the Karnataka coast was about 0.86 m, wave direction was about 210^0 and peak wave period was about 13 sec. The wave height during southwest monsoon (June–September) was higher, post-monsoon (October–December) was moderate and pre-monsoon (January–May) was the calmest period. Direction of longshore sediment transport was southwards during pre- and post-

monsoons when waves were from the south–southwest. Whereas northwards during monsoon when the wave approach from west–southwest to west. The annual net longshore sediment transport rate estimated was about 0.65×10^6 m^3 towards the south and the sediment budget investigation depicts the loss of 0.067×10^6 m^3 during the study period.

Shi et al., (2015) conducted a study to determine of critical shear stresses for erosion and deposition based on in situ measurements of currents and waves over an intertidal mudflat. The studies reveal that bed shear stress is one of the main governing factors of sediment transport. Under this study the effect of critical shear stresses on erosion and deposition based on in-situ measurements of currents and waves over an intertidal mudflat. Accurate determination of the critical shear stress associated with the erosion and deposition of sediments is an important component of numerical models used to predict and quantify sediment behavior and transport across intertidal flats. In the study, water depth, wave parameters, near-bed turbulent velocity, suspended sediment concentration (SSC), and intertidal bed-level changes were measured to determine the erosion (τ_{ce}) and deposition (τ_{cd}) thresholds of sediments on an intertidal mudflat at Jiangsu, China. Based on integrated field measurements of bed level changes and hydrodynamics, the bed shear stresses of currents (τ_c), waves (τ_w), and combined current-wave action (τ_{cw}) were calculated. During field measurements, deposition occurred ($\tau_{cw} < \tau_{cd}$) when current action exceeded wave energy ($\tau_c > \tau_w$) during calm weather, whereas erosion occurred ($\tau_{cw} > \tau_{ce}$) when wave action increased drastically during rough weather. The field data showed that high current velocities lead to low τ_c, possibly because high SSC reduced the drag coefficient, which is variable during a tide, and further caused low τ_c under high current velocities. Additionally, bedforms characteristic of intertidal mudflat (e.g., gullies, small creeks, ripples, or saltmarsh) had a significant influence on the drag coefficient of the bed. This study demonstrated that the in-situ determination of the parameters that control erosion and deposition is a useful approach to obtaining values of τ_{ce} and τ_{cd}, which provide the basis for a mechanistic understanding of the morphological evolution and development of predictive sediment transport and erodibility models.

Shi et al., (2012) studied accretion and erosion at an exposed tidal wetland to the bottom shear stress of combined current–wave action. To understand the nature of sediment behavior under combined current–wave action at an exposed tidal wetland, the waves, currents, water depths, bed-level changes, and sediment properties at a mudflat–salt marsh transition on the Yangtze Delta, China was measured, during five consecutive tides under onshore winds of around 8m/s, and calculated the bed shear stresses due to currents(τ_c), waves (τ_w), combined current-wave action (τ_{cw}), and the critical shear stress for the erosion of the bottom sediment (τ_{ce}) .The bed shear stresses under combined current–wave action τ_{cw}) were approximately five times higher on the mudflat than on the salt marsh. On the mudflat τ_{cw} was larger than the critical erosion shear stress for 70% of the period of submergence whereas τ_{cw} was always lower than τ_{cw} at the salt marsh site. This result indicated that the sediment dynamics on the mudflat were dominated by erosion, whereas at the salt marsh they were governed by deposition, which conforms the observed bed- level change during the study period. Overall, it was concluded that τ_{cw} in combination with τ_{ce} is useful in assessing the hydrodynamic mechanisms that underlie the morphological evolution of exposed tidal wetlands

José et al., 2012 in their study presented a new large-scale experimental data which showed evidence of a link between the swash zone dynamics and the surf zone morpho dynamics. Two sets of large-scale experiments were presented. The first set of experiments investigates the swash and surf dynamics under the same hydrodynamic forcing but with two different swash zone morphological conditions, one of which was created by manual reshaping of the sub-aerial beach face. It is shown that more dissipative swash zone conditions (a more mildly sloping beach face) significantly reduce the rate of seaward sandbar migration such that it almost ceases during the performed experimentation time. This behavior is compared to a second set of experiments which shows the natural sand bar offshore migration under almost identical hydrodynamic forcing. The changes in the sandbar migration were investigated in terms of the differences in the swash zone dynamics. The more reflective swash zone was characterized by more intense backwashes that, in turn, promote significant quantities of sediment suspension during the interaction of the

backwash with the subsequent bore. The dissipative swash zone leads to a larger number of waves–swash interactions, reducing the backwash magnitudes and the magnitude of suspended sediment concentration events in the swash zone, with a corresponding reduction in the offshore suspended sediment transport. The total offshore sediment transport rates were also shown to reduce, leading to the observed modification of the sandbar migration.

2.4 Summary

Several other research-works along with the studies discussed in the previous section are studied (Ariya et al., 2013; Hauque, 2018; Islam and Ahmad, 2004; Noujas and Thomas,2018; Paul, 2009; Yadav et al., 2016; and Uddin et al., 2014) which are relevant to this thesis work. From literature review it can be concluded that no in-depth study regarding longshore sediment transport and coastline evolution have not yet done for Kuakata beach. This study aims to identify dominant current (i.e., longshore, or cross shore) in the nearshore area, estimate sediment budget and simulation of coastline evolution which will help coast management authority to take right decision regarding protection measures and create scope for further study as well.

CHAPTER THREE

METHODOLOGY AND MODEL SETUP

3.1   General

Four models (i.e., Hydrodynamic, wave, littoral drift and coastline evolution) are used in this study. Both Hydrodynamic and wave model are setup, calibrated and validated. Ultimately using HD result file and wave result file sediment budget is from LITDRIFT model and coastline evolution is seen by LITLINE model for Kukakata beach. Methodology comprises literature review related to this study and data collection like bathymetry, water level, discharge, wave data, historical satellite images etc. Detail methodology is described in this chapter regarding this study. The complete methodology of the research work is presented in the flow chart which is given in **Figure 3.1.**

3.2   Data Collection

Various types of data have been collected for this study purpose like water level, wind data, satellite images,1D hydrodynamic result file for the year 2010 to 2018, wave data for the year 2010 to 2018 and wind field for the same period from different sources. Data type, location, period, and source are shown in the following **Table 3.1.**

3.2.1   Water Level Data

Water level data in Kawar char and Fakiraghat have been collected for the year 2017 for calibration and for the year 2015 for validation. The source of water level data is IWM. Water level station is shown in the map (**Figure 3.3**). The tidal difference at Kawar Char is 2.5 meter and at Fakiraghat is 3 meter which can be measured from **Figure 3.2**.
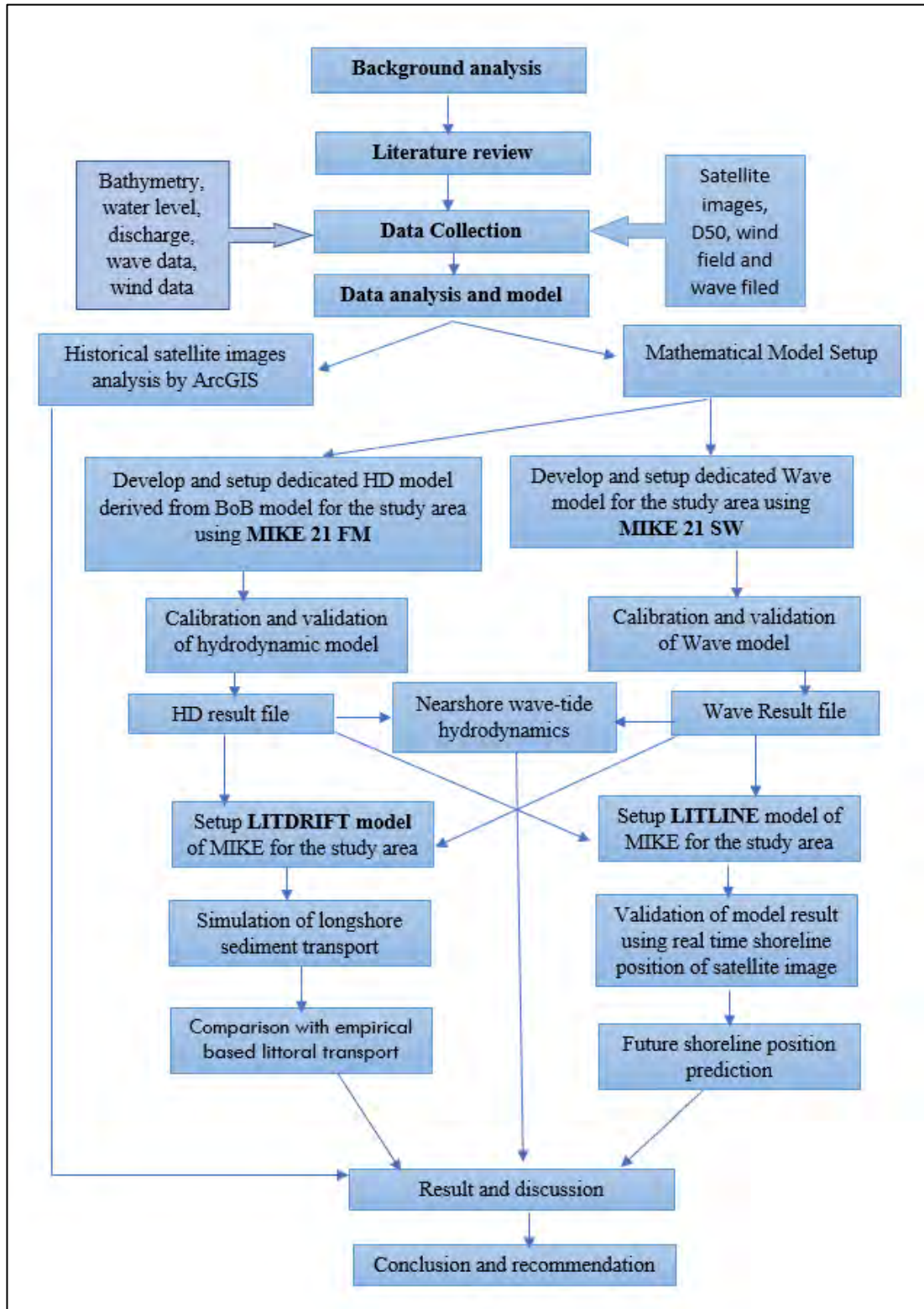
Figure 3.1: Methodology of the research work

Table 3.1: List of data collection

Data type	Place/Location	Year/Period	Data source
Water Level	Kawarchar, Fakiraghat	2015-2017	IWM
Discharge	Tumchar (Tentulia) and Bamna(Bishkhali)	11/12/2017 and 16/12/2017 11/03/2015 and 12/03/2015	IWM
Wind data	Khepupara	2017	BMD
Wind field	BoB	01-01-2008 to 01-01-2019	EMCWF
Satellite Imageries (Resolution 30m x 30m and 10mx10m)	Kukata area	1978-2020	USGS
Wave data	24 km offshore of Kuakata	07-03-2018 to 02-04-2018	IWM
Wave field	BoB	01-01-2008 to 01-01-2019	EMCWF
Sea Bathymetry	BoB	2014	GEBCO
River Bathymetry	Bishkhali, Baleswar, Rabnabad,Buriswar, Rabnabd, Andhar Manik	2019	IWM
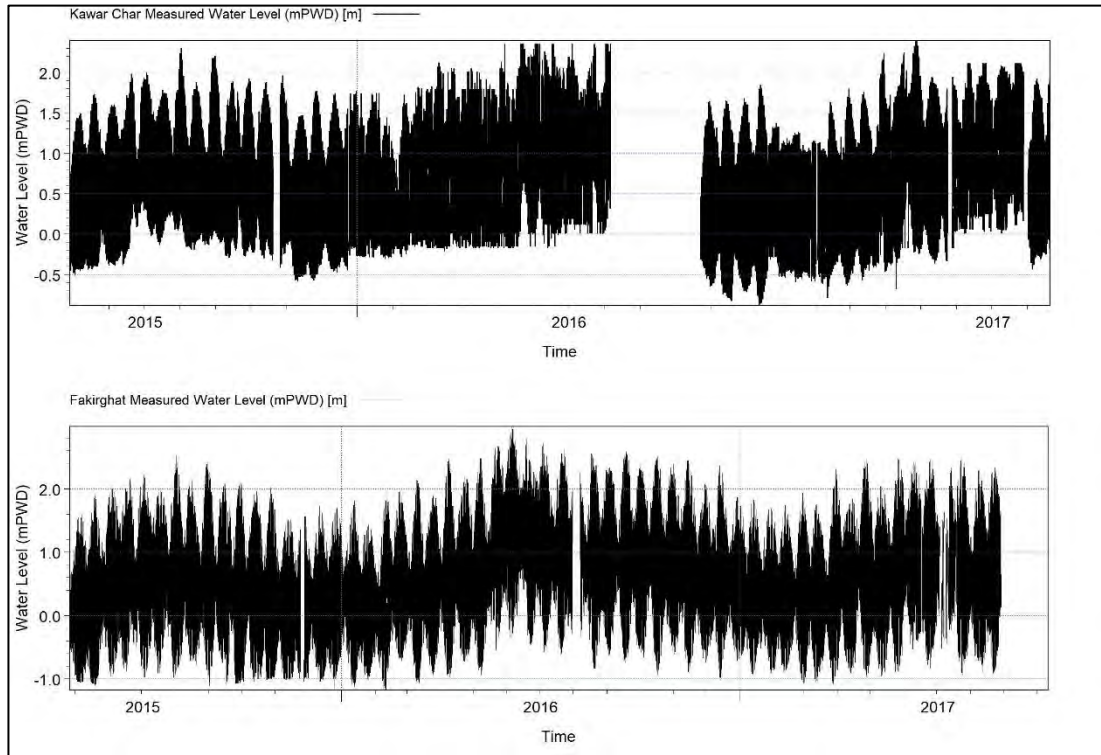
Figure 3.2: Measured water level time series at Kawar char (above) and Fakira Ghat (below)

3.2.2 Discharge Data

Measured discharge data has been collected from IWM for two station to calibrate and validate the dedicated hydrodynamic Model. Discharge information is given in the **Table 3.2** and measured discharge location is shown in the **Figure 3.3**. From the hydrograph of discharge (**Figure 3.4**) it is seen that max discharge is about 9000 and 5000 m^3/s for Tumchar and Bamna respectively.

Table 3.2: Measured discharge information matrix

Sl.	Station	River Name	Max Q (m³/s)	Time period
1	Tumchar	Tentulia River	9000	11/12/2017 and 16/12/2017
2	Bamna	Bishkhali River	5000	11/03/2015 and 12/03/2015
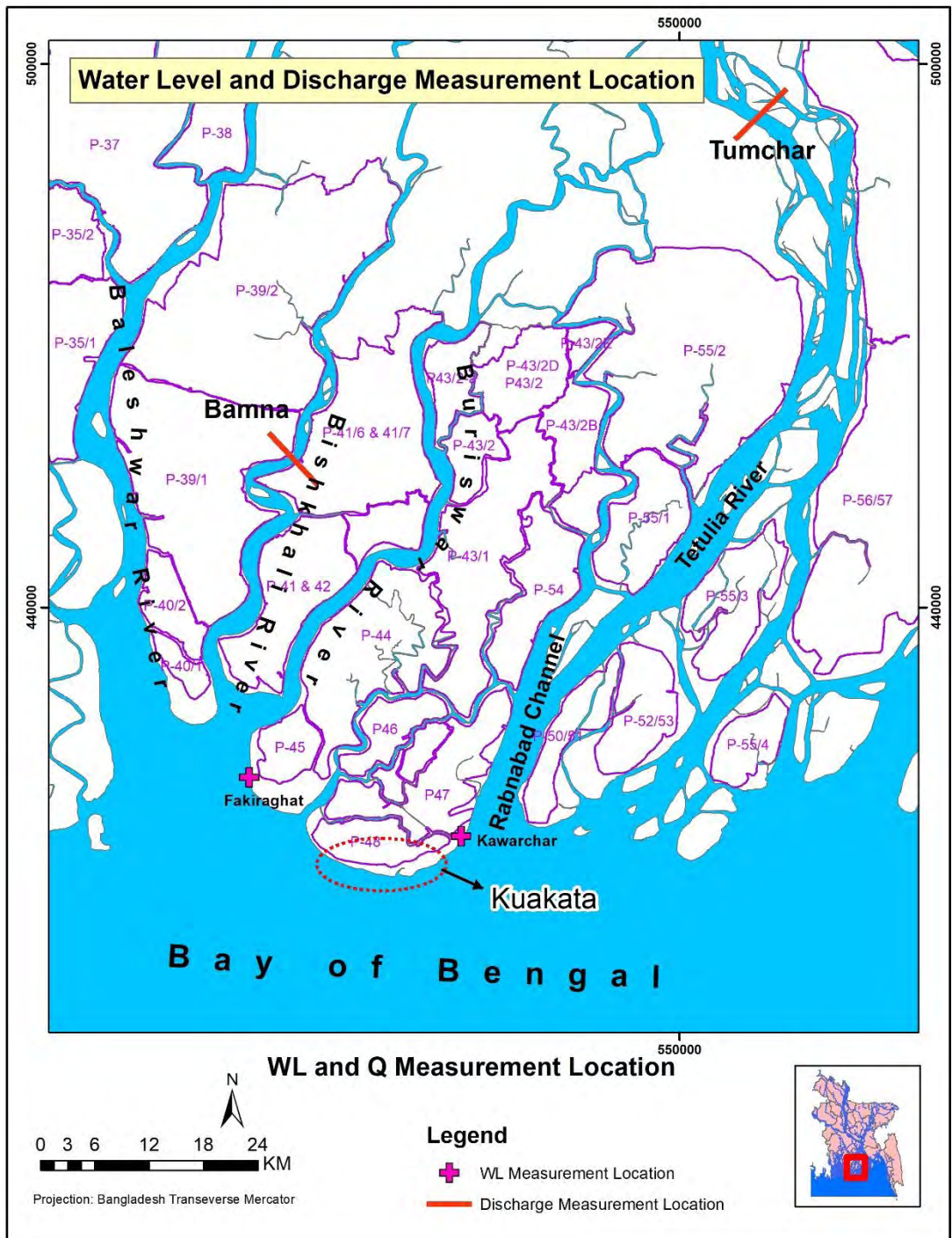
Figure 3.3: Water level and discharge measurement location
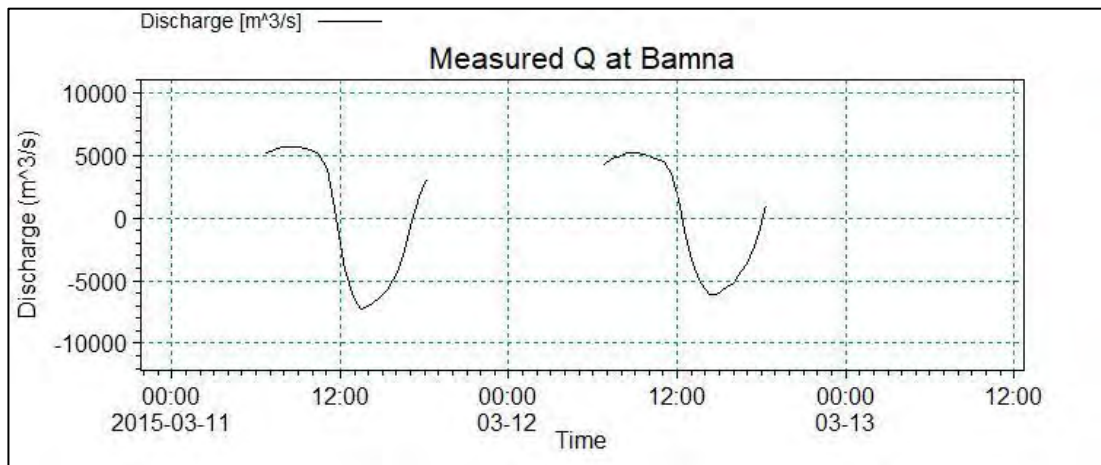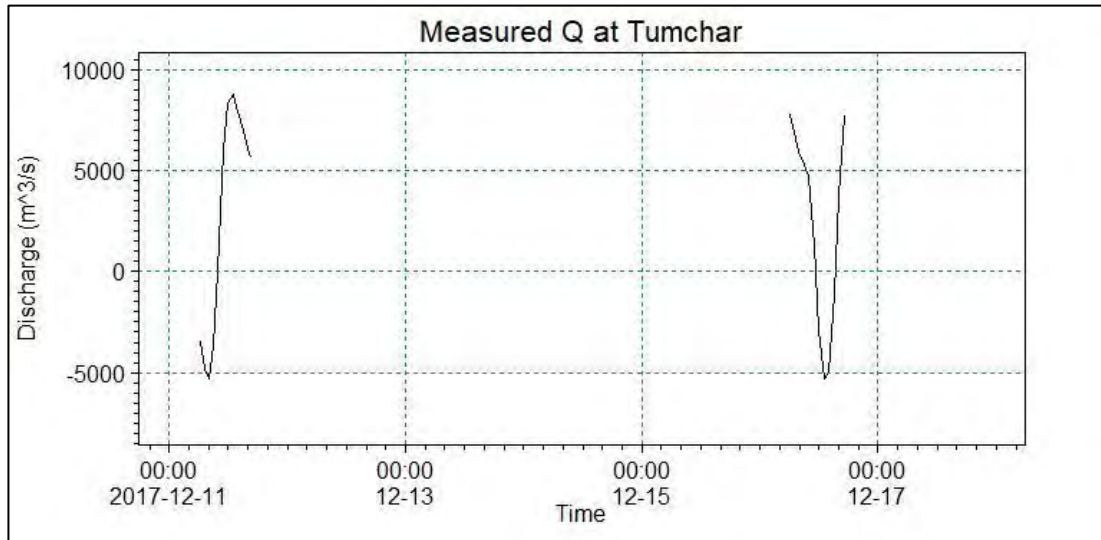
Figure 3.4: Measured discharge hydrograph at Tumchar (above) and Bamna(below)

3.2.3 Wind Speed Data from BMD

Wind data for Khepupara station (Latitude 21.9833^0, Longitude 90.2333^0), Kuakata has been collected from BMD just to observe dominant direction of wind in the study area. From **Figure 3.5** it is seen that most of the time wind flows south to north direction and about 60 % time it stays calm.
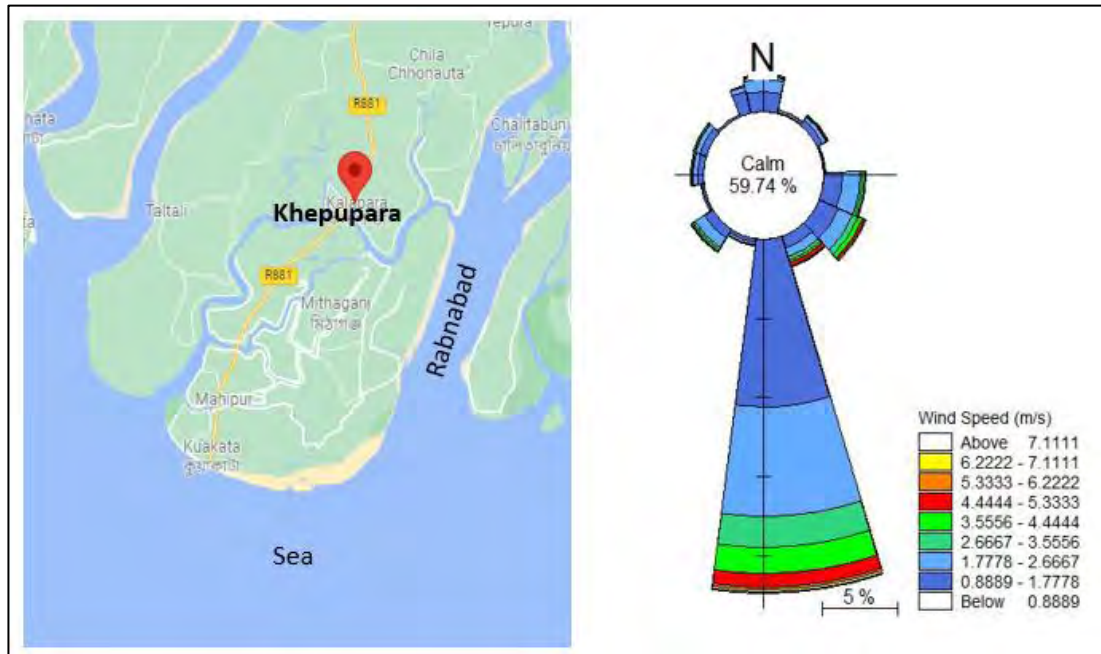
Figure 3.5: Map of wind measuring staion (left) and windrose of Khepupara (right) for the year 2017

3.2.4 Satellite Images

Satellite images for different year have been downloaded from USGS as listed in the **Table 3.3** and shown in the **Figure 3.6**. All the images are captured by Landsat satellite. Long term (10 years) shifting has been taken under consideration for coastline shifting assessment.

Table 3.3: List of satellite images

SL	Year	Satellite	Resolution
1	1978	LANDSAT	30x30 m
2	1988	LANDSAT	30x30 m
3	1998	LANDSAT	30x30 m
4	2008	LANDSAT	30x30 m
5	2018	LANDSAT	30x30 m
6	2020	LANDSAT	30x30 m
7	2016	Sentinel	10x10 m

SL	Year	Satellite	Resolution
8	2018	Sentinel	10x10 m

All satellite images are geo-referenced. Total 8 number of satellite images are used in this research works.
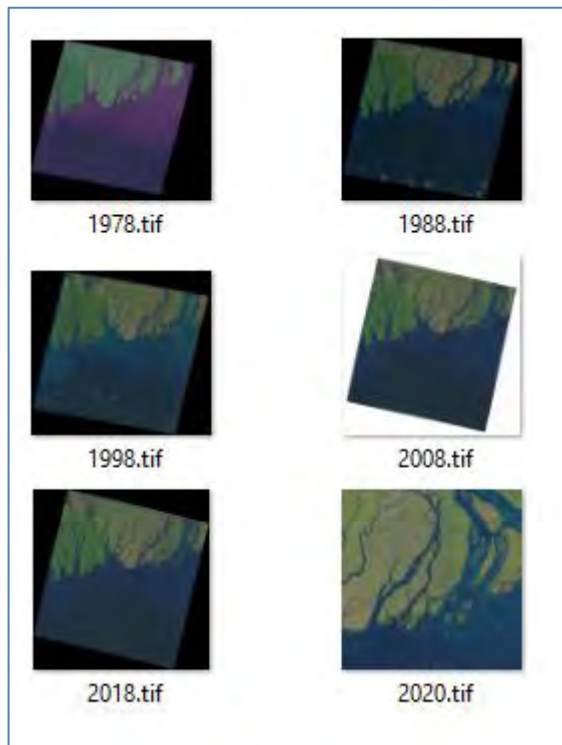
Figure 3.6: Satellite images of different year

First 6 images are used for coastline shifting assessment and quantifying erosion and accretion which are coarser resolution, and last 2 images are calibration and validation of LITLINE model.

3.2.5 HD Result File

South-west regional model (1-D hydrodynamic) is maintained by IWM. The rivers of dedicated 2D hydrodynamic of this study fall in south-west region. HD result file of south-west regional model (1-D) for the year 2010 to 2018 have been collected from IWM. From this result file discharge is extracted at Hilisha river (**Figure 3.7**) which is used for upstream boundary of 2-D hydrodynamic model.
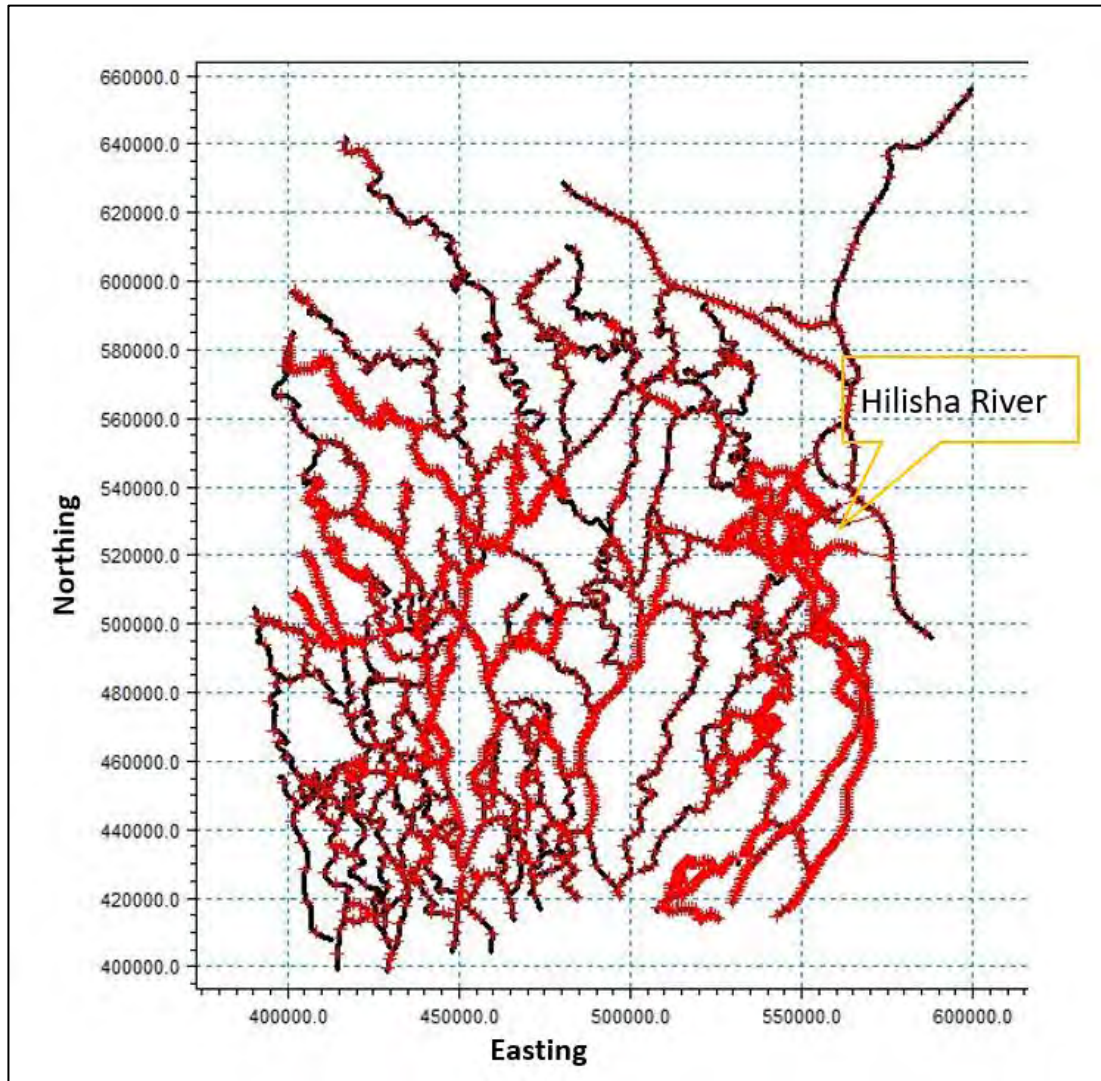
Figure 3.7: South-west regional model

3.2.6 Wave Data

Wave data of the Bay of Bengal for year 2010 to 2018 has been collected from ECMWF. This wave data is dfsu format and the resolution of wave data is 0.125^0. The boundary of BoB model is shown by red solid line in the **Figure 3.8**. The wave boundary is generated on the south boundary of BoB. The boundaries for dedicated wave model (i.e., east, west, and south boundary) have been extracted BoB wave result file, as discussed in the article 3.4.2. Measured wave data has been collected from IWM to calibrate the dedicated wave model. The measurement location (Longitude 90.255^0 and Latitude 21.649^0) is shown in the **Figure 3.9** and wave data plotting is shown in the **Figure 3.10**.
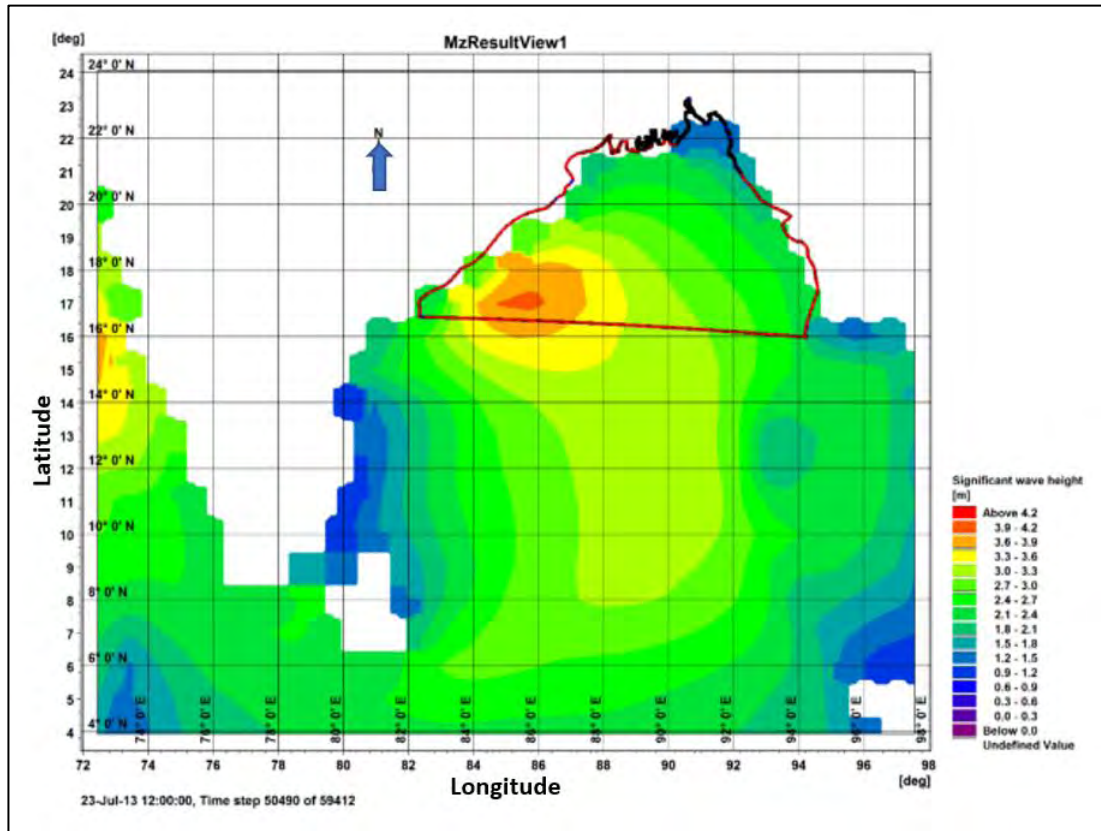
Figure 3.8: Wave data from global wave model from ECMWF (BoB coverage shown by solid line)
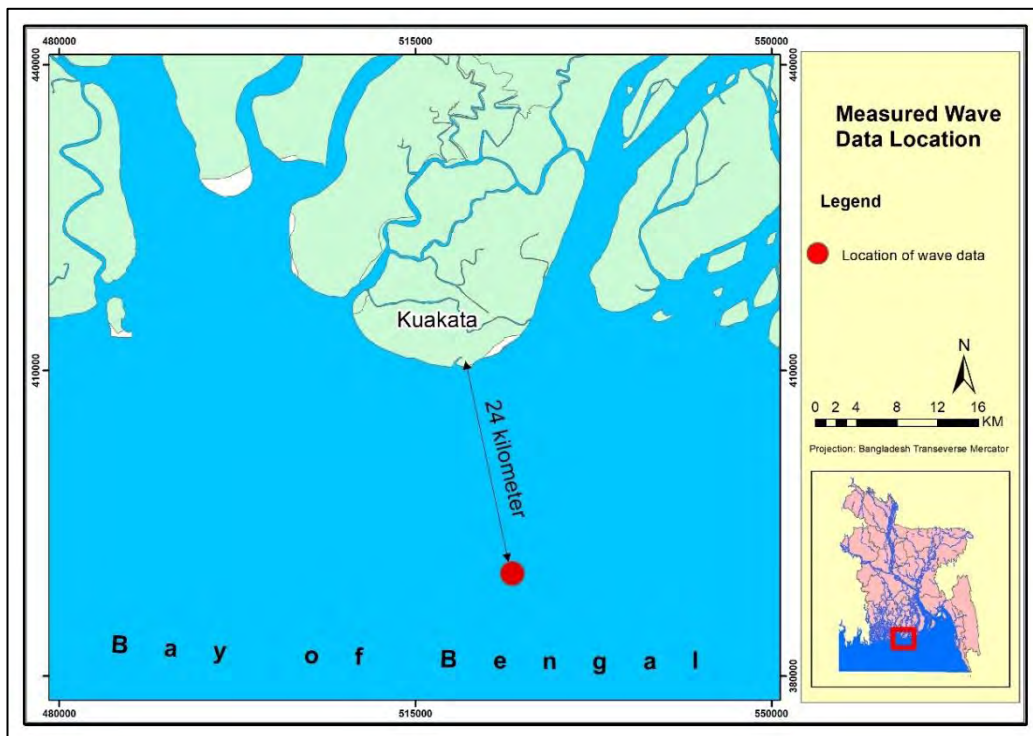
Figure 3.9: Measured wave data location
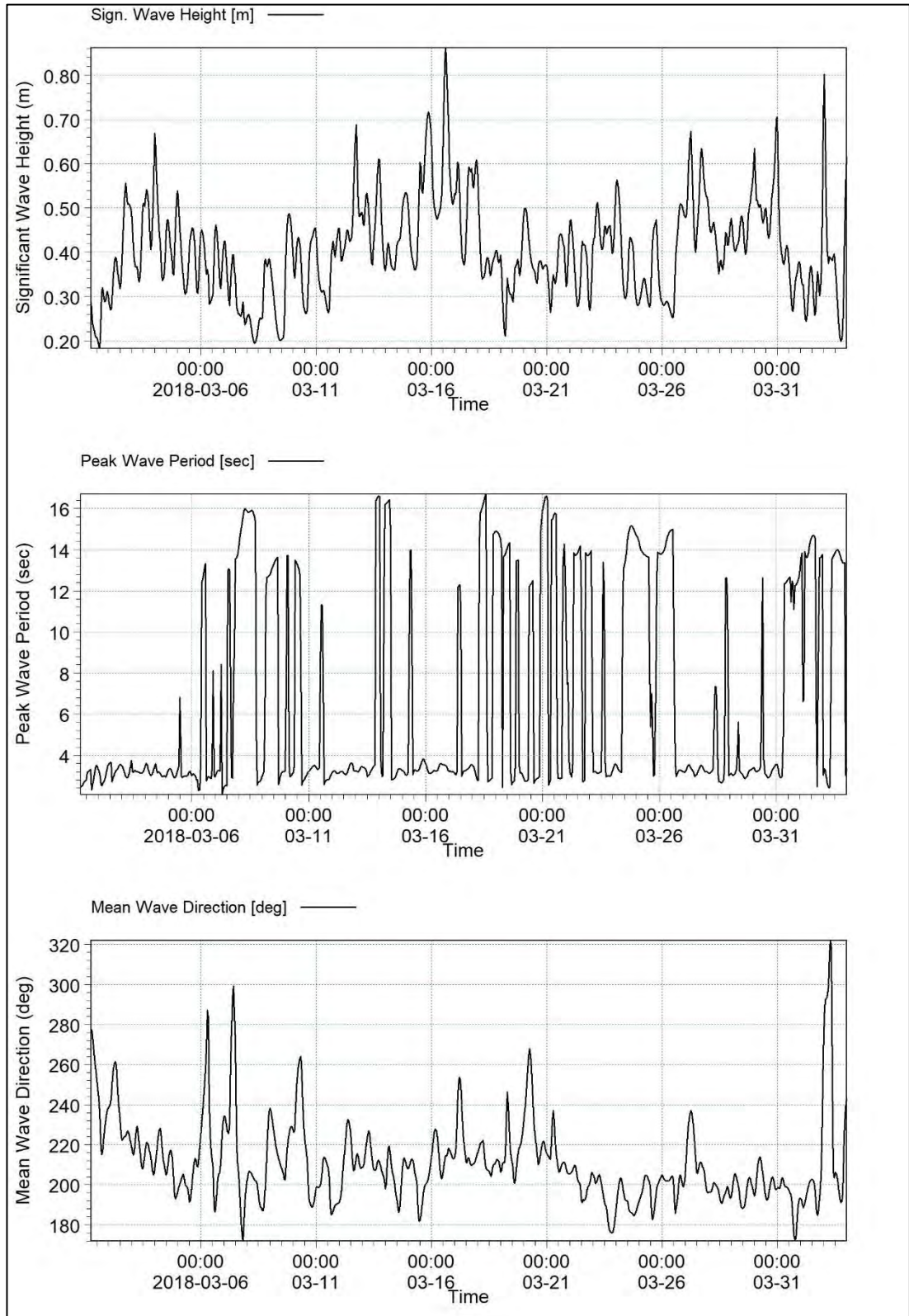
Figure 3.10: Measured wave data 24 km offshore of Kuakata

3.3   2D-Hydrodynamic Model

MIKE 21 flow model FM developed by DHI (Danish Hydraulic Institute) has been used for the Hydrodynamic Modeling of this research work. The Hydrodynamic Module is the basic computational component of the entire MIKE 21 Flow Model FM modelling system providing the hydrodynamic basis for the other Module. The Hydrodynamic Module is based on the numerical solution of the two-dimensional shallow water equations - the depth-integrated incompressible Reynolds averaged Navier-Stokes equations.

The local continuity equation is written as

$$\frac{\partial \zeta}{\partial t} + \frac{\partial p}{\partial x} + \frac{\partial q}{\partial y} = \frac{\partial d}{\partial t} \tag{3-1}$$

And the two horizontal momentum equations for the x- and y- component, respectively

$$\frac{\partial p}{\partial t} + \frac{\partial}{\partial x}\left(\frac{p^2}{h}\right) + \frac{\partial}{\partial y}\left(\frac{pq}{h}\right) + gh\frac{\partial \zeta}{\partial x} + \frac{gp\sqrt{p^2+q^2}}{C^2.h^2}$$
$$-\frac{1}{\rho_w}\left[\frac{\partial}{\partial x}(h\tau_{xx}) + \frac{\partial}{\partial y}(h\tau_{xy})\right] - \Omega q - fVV_x \tag{3-2}$$
$$+\frac{h}{\rho_w}\frac{\partial}{\partial x}(p_a) = 0$$

$$\frac{\partial q}{\partial t} + \frac{\partial}{\partial y}\left(\frac{q^2}{h}\right) + \frac{\partial}{\partial x}\left(\frac{pq}{h}\right) + gh\frac{\partial \zeta}{\partial y} + \frac{gq\sqrt{p^2+q^2}}{C^2.h^2}$$
$$-\frac{1}{\rho_w}\left[\frac{\partial}{\partial y}(h\tau_{yy}) + \frac{\partial}{\partial x}(h\tau_{xy})\right] + \Omega p - fVV_y \tag{3-3}$$
$$+\frac{h}{\rho_w}\frac{\partial}{\partial y}(p_a) = 0$$

The following symbols are used in the equation.

$h(x,y,t)$ water depth $(= \zeta - d, m)$

$d(x,y,t)$ time varying water depth (m)

$\zeta(x,y,t)$	Water surface elevation (m)
p,q (x,y,t)	flux densities in x- and y-directions (m^3/s/m) = (uh, vh); (u,v) = depth averaged velocity in x-and y-directions
$C(x,y)$	Chezy resistance (m$^{1/2}$/s)
g	acceleration due to gravity (m^2/s)
$f(V)$	wind friction factor
$V,V_x,V_y(x,y,t)$	wind speed and components in x-and y-direction (m/s)
$\Omega(x,y)$	Coriolis parameter, latitude dependent (s^{-1})
$p_a(x,y,t)$	atmospheric pressure (kg/m/s^2)
ρ_w	density of water (kg/m^3)
x,y	space coordinates (m)
t	time (s)
$\tau_{xx}, \tau_{xy}, \tau_{yy}$	components of effective shear stress

In the horizontal domain both Cartesian and spherical coordinates can be used. The spatial discretization of the primitive equations is performed using a cell centered finite volume method. The spatial domain is discretized by subdivision of the continuum into non-overlapping element/cells. In the horizontal plane, an unstructured grid is used comprising of triangles or quadrilateral element. An approximate Riemann solver is used for computation of the convective fluxes, which makes it possible to handle discontinuous solutions. For the time integration, an explicit scheme is used.

3.3.1   Existing Bay of Bengal Model of IWM

IWM has maintained the two-dimensional Bay of Bengal Model (Hydrodynamic model) since 1995. The geographical extent of the model is shown in Figure 3-6. The area covered by the model starts from Baruria on the Padma River and Bhairab Bazar on Upper Meghna River down to 16^0 latitudes in the Bay of Bengal. In the deep sea, the bathymetry is based on Etopo2 and near the coastline on local surveys. In between these areas' nautical sea-chart from C-Map has been used. Etopo2 are very accurate in deeper area. In shallow area C-Map normally is more accurate than Etopo2 due to finer resolution. As C-Map is used for navigational purpose it's not very accurate in

deep water. In the rivers and the inner part of the estuary local measurement has been used where possible. A list of bathymetric data used for Model Development is given in Table 3.4.

Table 3.4: List of bathymetric data used for model development

Sl. No.	Description of data	Period		Cruise Number/Data Source
		From	To	
	Bathymetry			
1	Bay near Sandwip Channel,Lower Meghna	07/04/2009	22/04/2009	EDP-1
2	East Shahabazpur Channel, East of Hatiya	06/05/2009	20/05/2009	EDP-2
3	Lower Meghna	16/06/2009	25/06/2009	EDP-3
4	Channel between Sandwip & Jahazer Char	01/07/2009	27/07/2009	EDP-4
5	Tentulia River	02/10/2009	17/10/2009	EDP-6
6	West Shahabazpur Channel	08/01/2010	07/02/2010	EDP-7
7	West Shahabazpur Channel, near Nijhum Dwip	15/02/2010	06/03/2010	EDP-8
8	Mainka Channel	Oct-09		IWM-survey
9	Montaz Channel			
10	Bangla Channel			
11	Tentulia-Ilisha Channel	Jan-Feb 2010		
12	Upper Meghna, Lower Meghna, Padma	2011-12		IWM-survey
13	Pussur, Sibsha, Boleswar, Kocha, Madhumoti	2011		IWM-survey

Sl. No.	Description of data	Period		Cruise Number/Data Source
		From	To	
	Bathymetry			
14	Noakhali – Urir char Channel	2012		IWM-survey
15	Sandwip-Noakhali-urir char area	2014		IWM-survey
16	Sandwip East Channel	2015		IWM-survey
17	Kobadak	2008-09		IWM-survey
18	Betna, Morirchap, Parulia-sapmara	2012		IWM-survey
19	Nabogonga, Atharabanki, Atai, Bhairab, Chitra	2011		IWM-survey
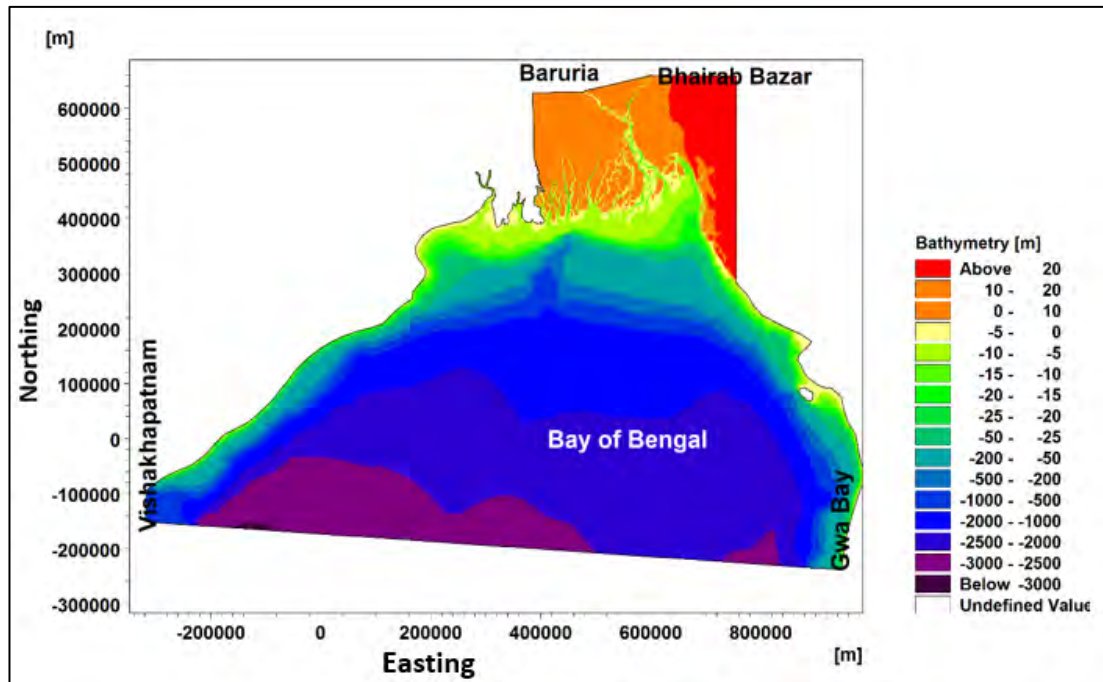
Figure 3.11: Geographical extent of the model domain (Source: IWM)

A 2D depth integrated hydrodynamic (HD) model has been setup for the channel. This 2D model is based on the hydrodynamic model of the Bay of Bengal (available in IWM), which has been used extensively in previous studies. For the present study, the

existing model has been updated and fine-tuned for the Kuakata and vicinity to the Kuakata beach using the newest available data.

3.3.2 Dedicated Hydrodynamic Model Setup

Concept of dedicated hydrodynamic model for Kuakata beach is brought under consideration because it is easy to handle, simulation time can be minimized, and high accuracy can be achieved through fine tuning of the model. Moreover, only one upstream boundary is required, which can be obtained from south-west regional model, to run the model. The flow chart of hydrodynamic model is illustrated in **Figure 3.12**.
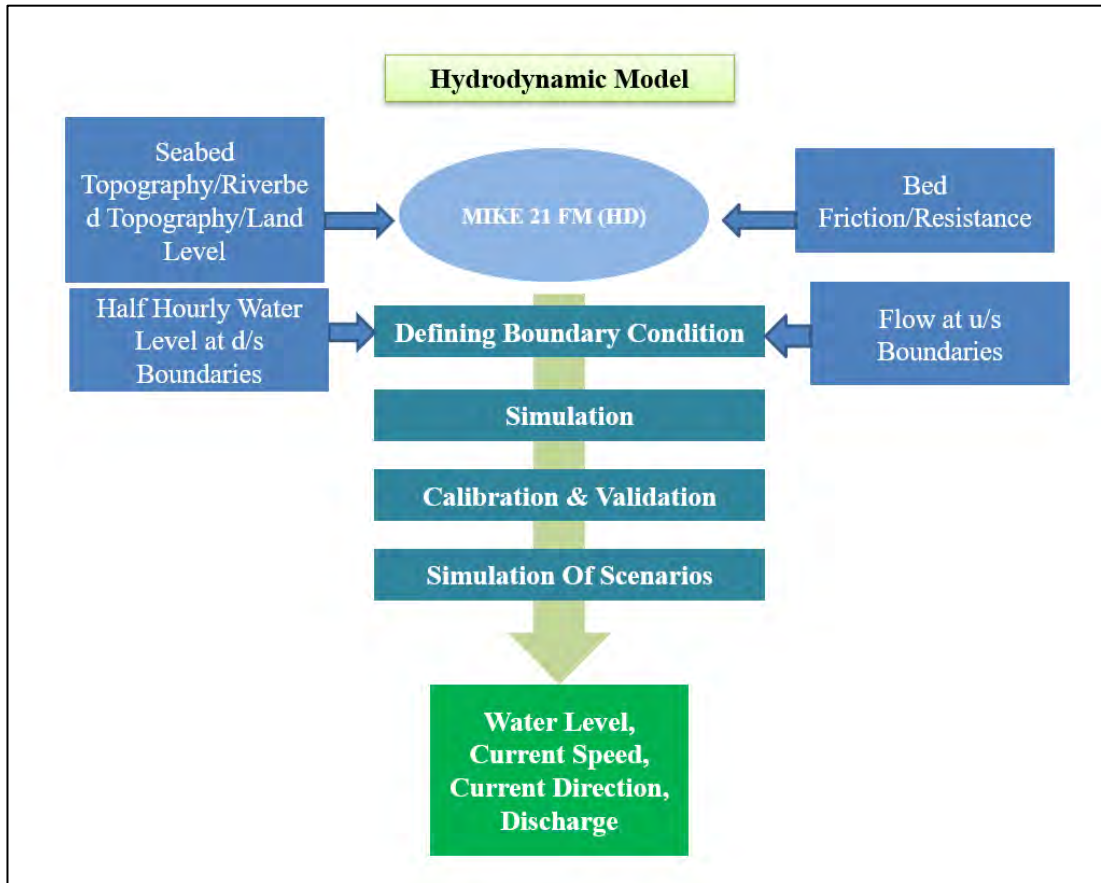
Figure 3.12: Flow chart of a hydrodynamic model

Model Domain:

A smaller domain covering the area of interest was created based on the existing HD model of the Bay of Bengal. **Figure 3.13** shows the model domain of study area. East, west and south boundary of the model domain are in the Bay of Bengal and upstream

boundary is Hilisha river which has been originated from Lower Meghna. Moreover, the important rivers in the domain are Baleswar, Bishkhali, Buriswar-Payra, Andharmanik, Lohalia, Tentulia, Rabnabad Channel etc.
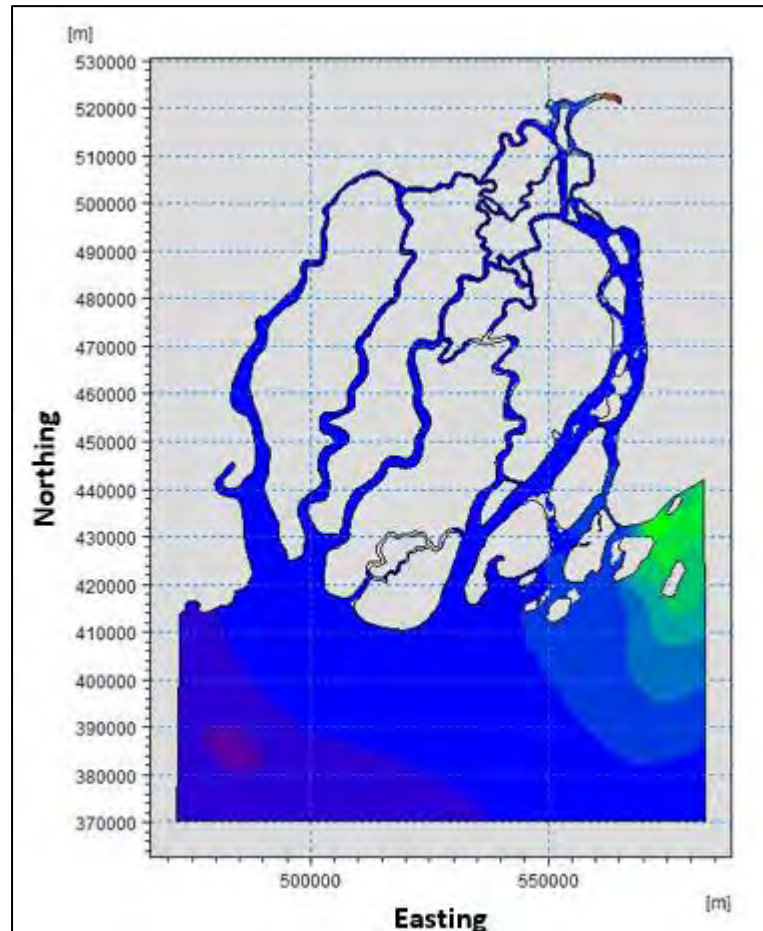
Figure 3.13: Model domain of the Kuakata study area

Model Boundaries:

This model has four boundaries. Upstream boundary is in Hilisha river, boundary is given as time series of discharge here. And discharge is extracted from the southwest regional model for the year 2015. Downstream boundaries are east west and south where water level is given as boundary here. These water levels are generated from global tide model.
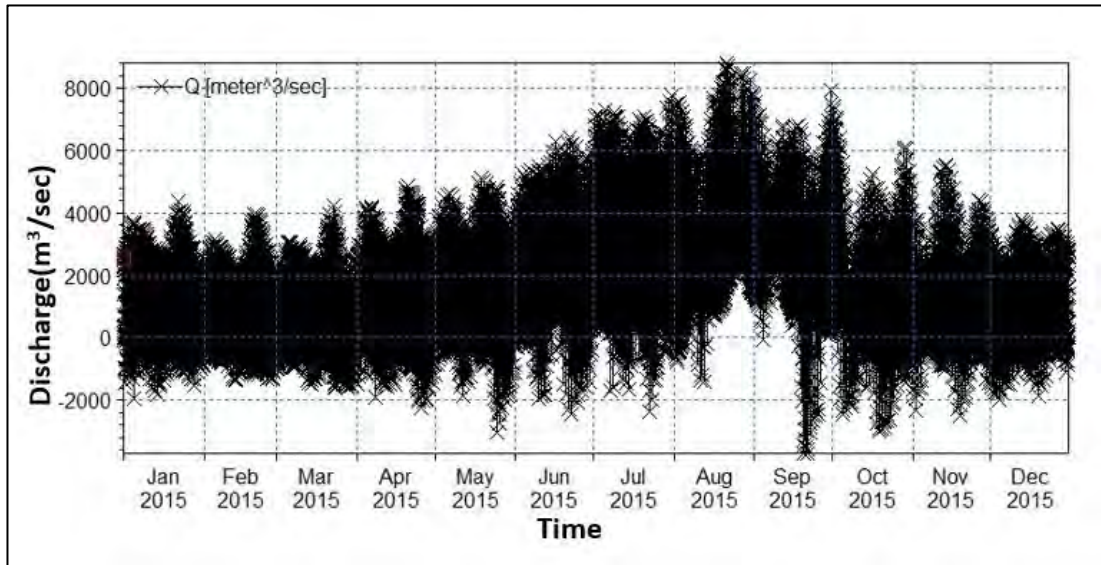
Figure 3.14: Upstream boundary of hydrodynamic model (Hilisha river)

3.3.3 Upgrading of the Hydrodynamic Model

Upgrading of the hydrodynamic model comprises the improvement of mesh resolution specially for the area of interest. This study is focused on determining sediment budget. The mesh resolution of Kuakata beach area has been decresed from 13000 meters (Max^m area 80000000 m^2) to 100 meters (Max^m area 30000 m^2) under this research work. The upgraded mesh resolution and the bathymetry has been shown in **Figure 3.16.**
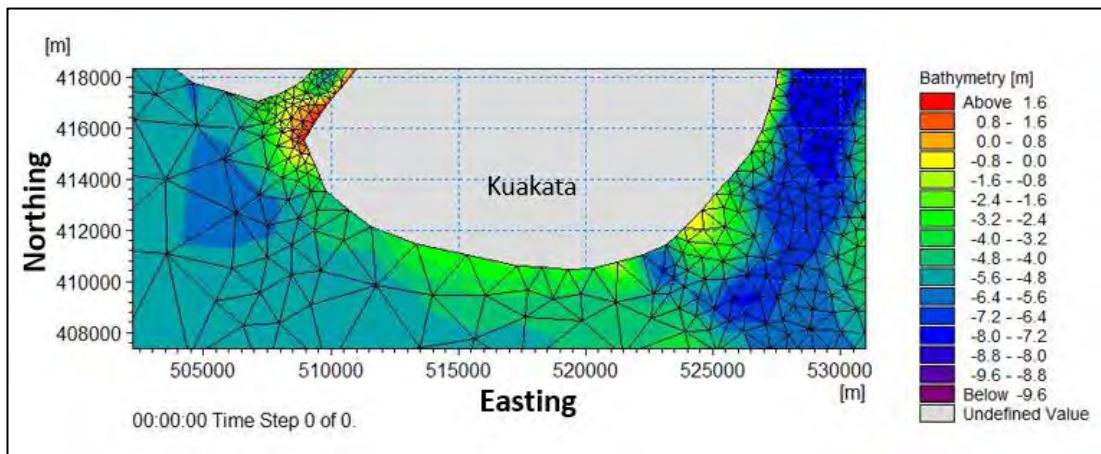
Figure 3.15: Mesh size of existing BoB model of IWM in the Kuakata beach area
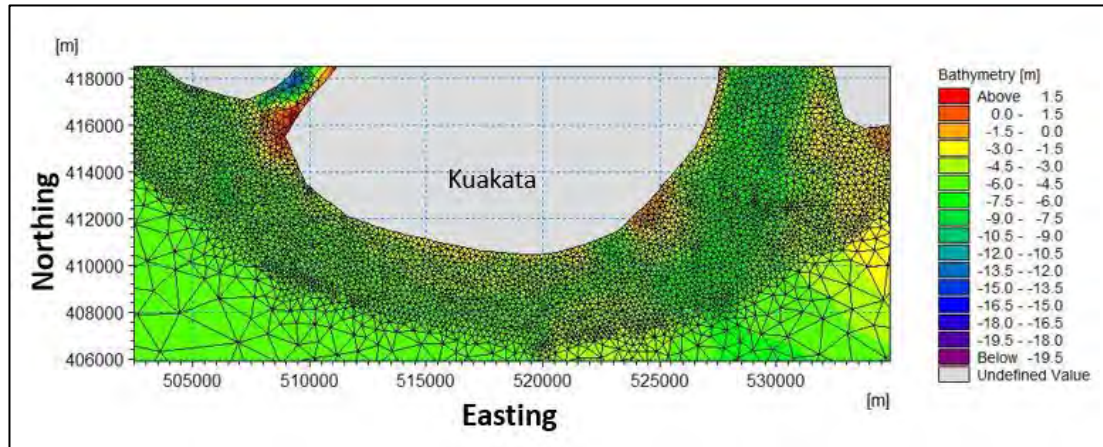
Figure 3.16: Updated fine mesh used in the dedicated model under this study in the Kuakata beach area

Bed Resistance

To calibrate the model, it is necessary to adjust the bed resistance. A spatially varying map of bed resistance has been used for this research work. The relation between Manning number (M) and bed roughness length, K_s can be estimated using the following formula:

$$M = \frac{25.4}{Ks^{1/6}} \tag{3-4}$$

Initially the manning map was prepared based on the available water depth. Further correction has been made during the calibration process of the model. The applied Manning roughness (M) in the study area which is the reciprocal value of Manning's n is shown in **Figure 3.17**.
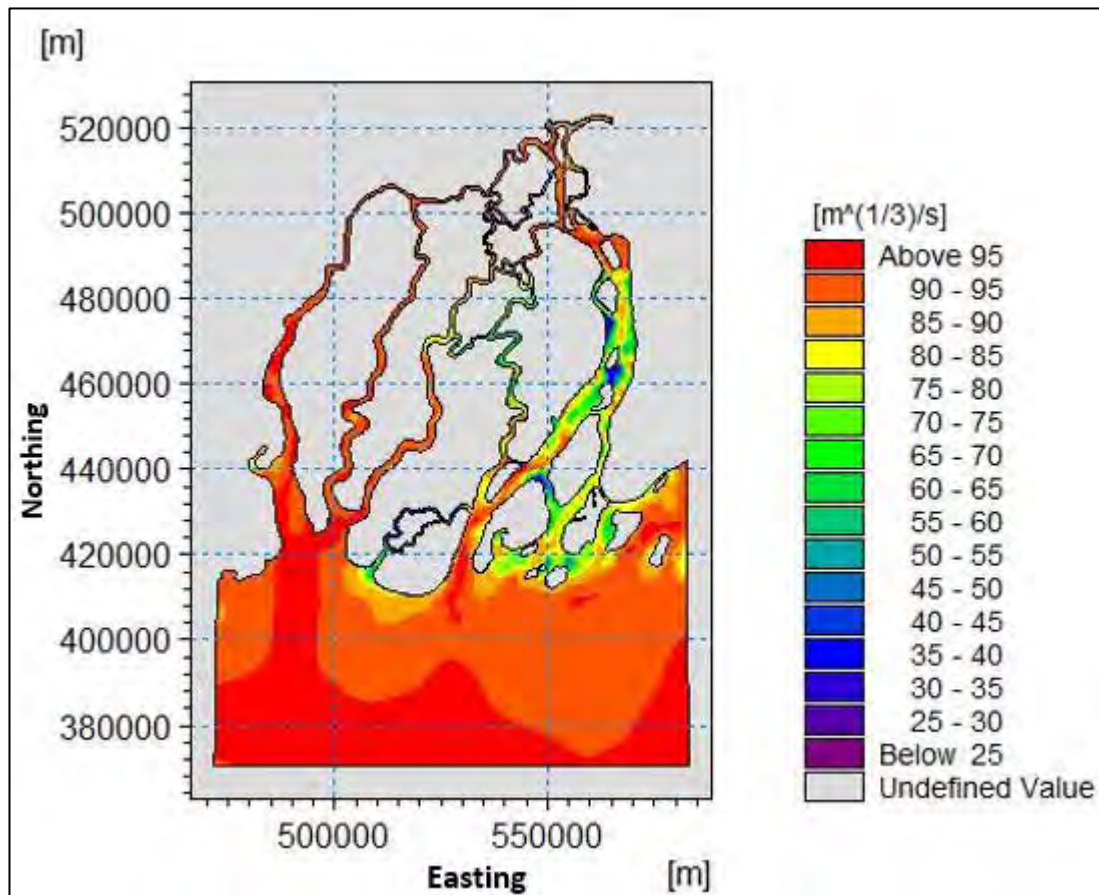
Figure 3.17: Spatially varied manning M map used for model calibration

Flood & Dry

Standard flooding & drying facility was enabled for the stability of the model.   When the water depth is less than the wetting depth the problem is reformulated and only if the water depth is less than the drying depth the element/cell is removed from the simulation. The flooding depth is used to determine when an element is flooded (i.e. re-entered into the calculation). In this simulation 0.005, 0.05, & 0.1m depth has used as the drying, flooding & wetting depth respectively.

Eddy Viscosity

Velocity based Smagorinsky formulation has been used for eddy viscosity. The proportionality factor for each area has been considered to be 0.28.

3.3.4   Calibration and Validation of Hydrodynamic Model

The hydrodynamic model has been simulated for a 20 days' period of March 2017. Model has been calibrated at two locations, i.e Fakira Ghat and Kawar Char. **Figure 3.18** shows the model calibration and validation locations.
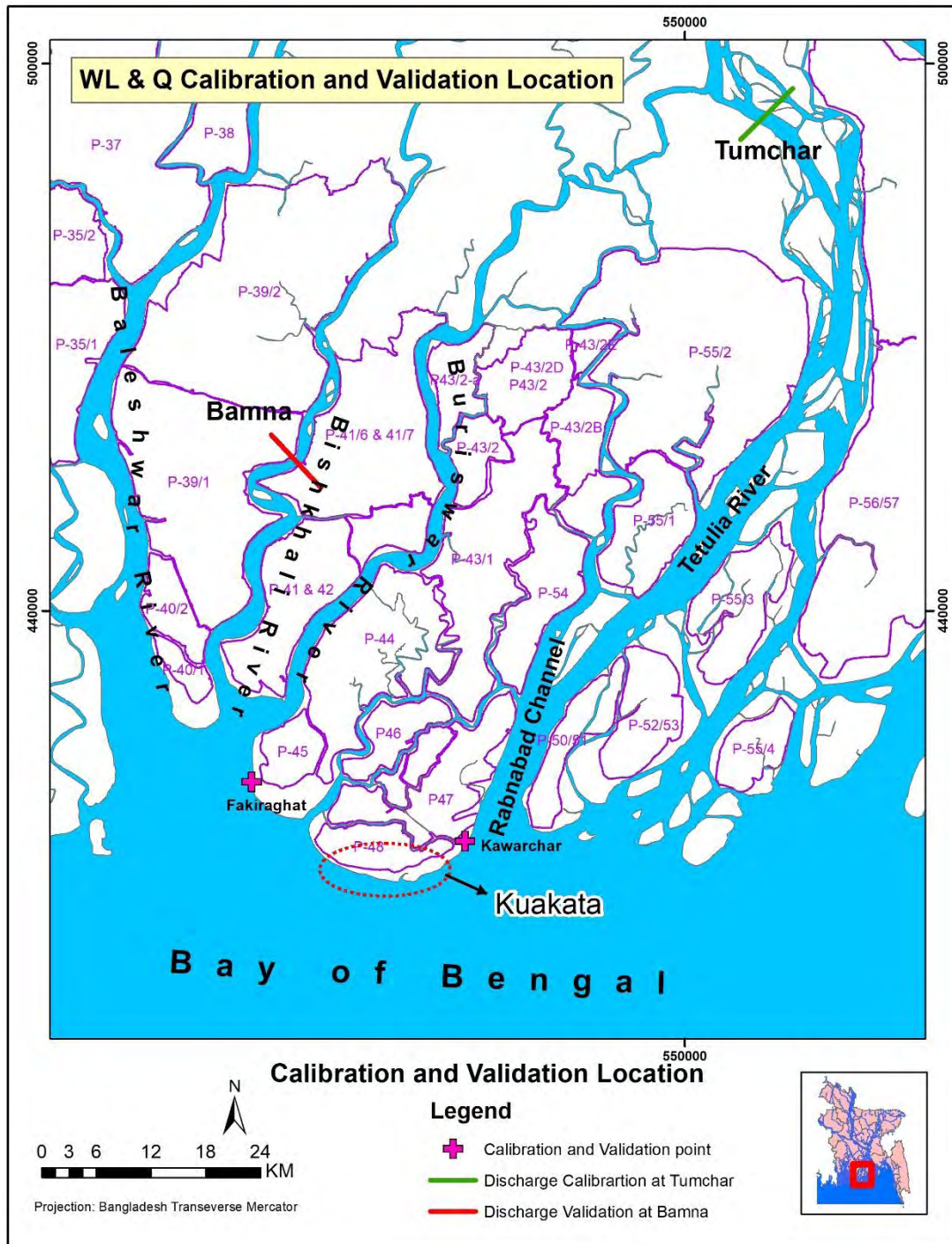
Figure 3.18: Hydrodynamic model calibration and validation locations

Model Parameter

The main model parameter used for the calibration of the hydrodynamic model is shown in the **Table 3.5**.

Table 3.5: The model parameters used for hydrodynamic calibration

Model Parameter	Value
Numerical Scheme	Low
Eddy Viscosity	Smagorinsky formulation constant 0.28
Bed Resistance	Constant in time, varying in domain
Coriolis force	Varying in domain

An appropriate internationally accepted standard values of model parameters for the validation of hydrodynamic model performance can be found in the UK Foundation for Water Research Publication named "A framework for marine and estuarine model specification in the UK".

In broad terms, this can be categorized by the following performance limits:

- Tidal elevations: Root Mean Square (RMS) error < 15% on spring tide and 20% on neap tide ranges (maximum deviation 0.1 m at marine estuarine boundary, 0.3 m at estuary head);

- Current speed deviation RMS error < 10 to 20% (maximum deviation 0.2 m/s);

- Direction error RMS error < 20 deg; and

- Timing of high water at marine estuarine boundary 15 minutes, 25 minutes at estuary head.

Calibration results of water level at different locations are shown in **Figure 3.19**. From this figure it is seen that simulated water level and observed water level matched well.
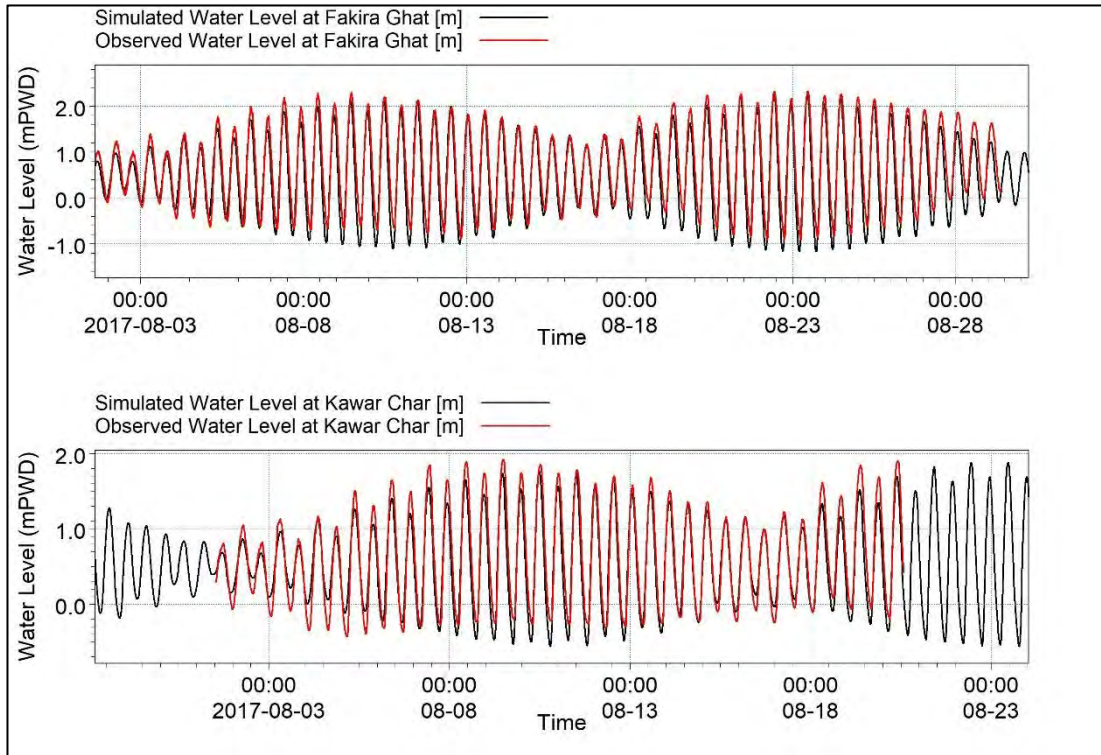
Figure 3.19: Water level calibration at Fakirghat and Kawar Char
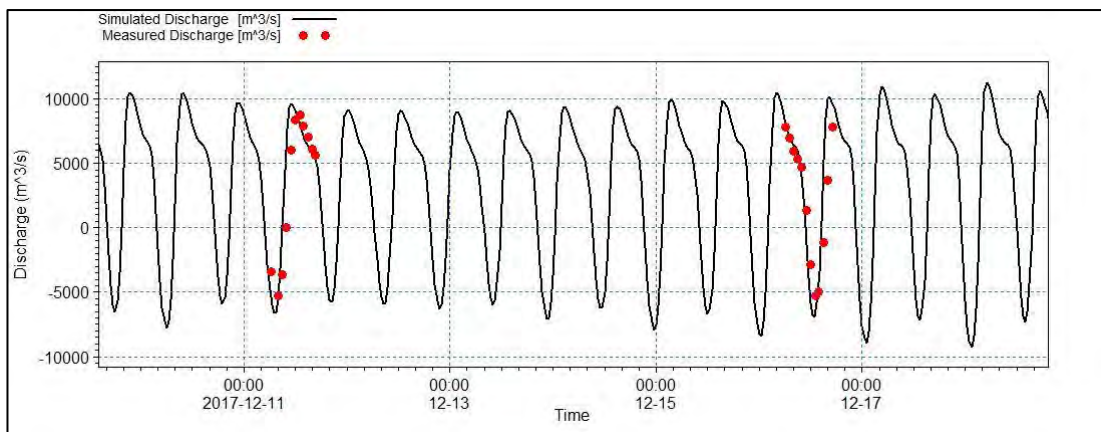
Figure 3.20: Discharge calibration at Tumchar in Tentulia river

To validate the hydrodynamic model performance, some statistical parameters such as mean, bias, RMS, scatter index and correlation coefficient have been determined with updated model results. Also, these parameters have been determined by the comparison of the measured or predicted water level and the simulated water level to

see the development of the updated model in terms of calibration. The quality indices are calculated by the following Eq. (3-5 to Eq. (3-11.

mo_i = Model Simulated Water Level

me_i = Measured or predicted Water Level

dif_i = Difference between model simulated and measured water level

$\overline{me}$ = Mean value

RMS = Root Mean Square value

BI = Bias Index

SI = Scatter Index

ρ = Corelation index

$$dif_i = mo_i - me_i \tag{3-5}$$

$$\overline{me} = \frac{1}{N}\sum_{i=1}^{n} me_i \tag{3-6}$$

$$bias = \overline{dif} = \frac{1}{N}\sum_{i=1}^{n} dif_i \tag{3-7}$$

$$RMS = \sqrt{\frac{1}{N}\sum_{i=1}^{n} dif_i{}^2} \tag{3-8}$$

$$BI = \frac{bias}{me} \tag{3-9}$$

$$SI = \frac{RMS}{me} \tag{3-10}$$

$$\rho = \frac{\sum_{i=1}^{n}(me_i - \overline{me})(mo_i - \overline{mo})}{\sqrt{\sum_{i=1}^{n}(me_i - \overline{me})^2 \sum_{i=1}^{n}(mo_i - \overline{mo})^2}} \tag{3-11}$$

Different quality indices parameters at different locations for the predicted and measure water level are summarized in **Table 3.6**.

Table 3.6: Correlation factors for hydrodynamic model calibration

Parameter	Mean	Bias	RMS	Bias/Mean	Scatter Index	Correlation	No. of Time Steps
Fakirghat	0.52	-0.01	0.16	-0.02	0.30	0.84	3930
Kawar Char	0.51	-0.04	0.18	-0.07	0.35	0.85	2532
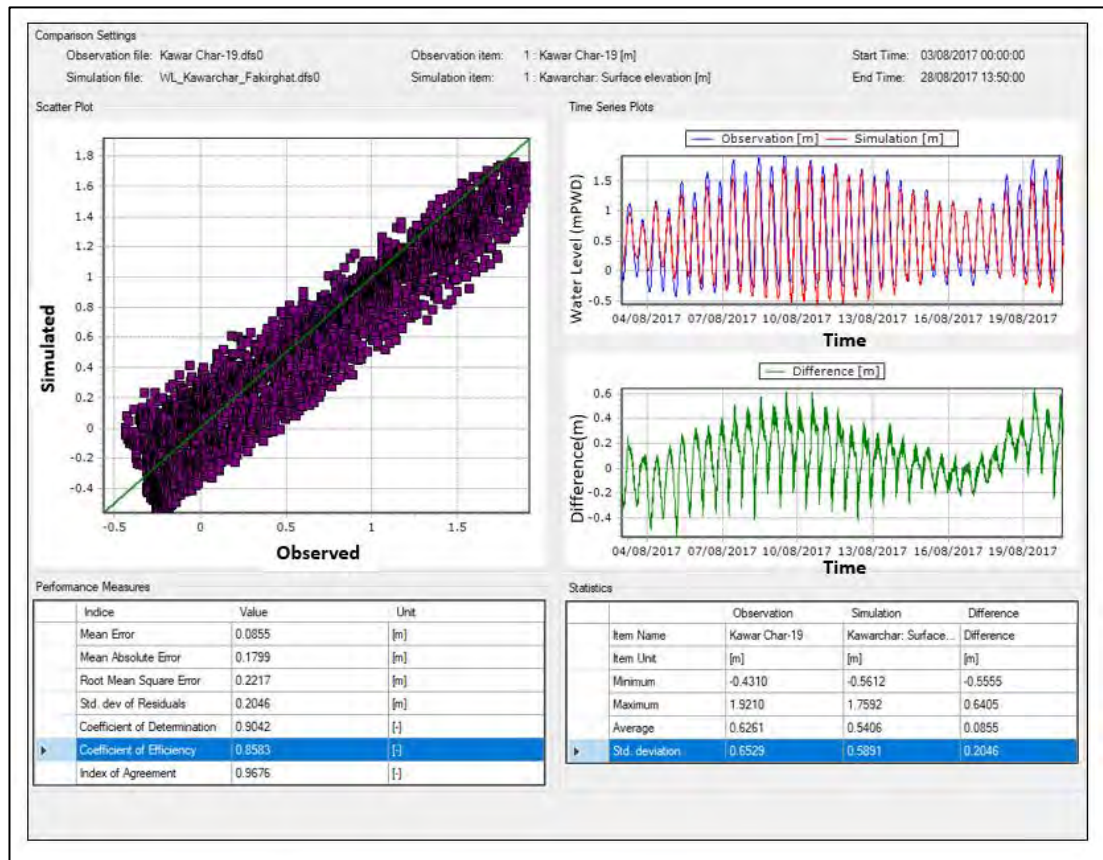
Figure 3.21: Performance measures for Kawar Char calibration

There is tool named timeseries comparator which exists in MIKE Zero. By this tool performance measures can easily be found out. The performance measures result for Kawar Char calibration by time series comparator tool is shown in the **Figure 3.21** and result has good agreement. The performance measures result for Fakira Ghat calibration by time series comparator tool is shown in the **Figure 3.22** and result has good agreement also.
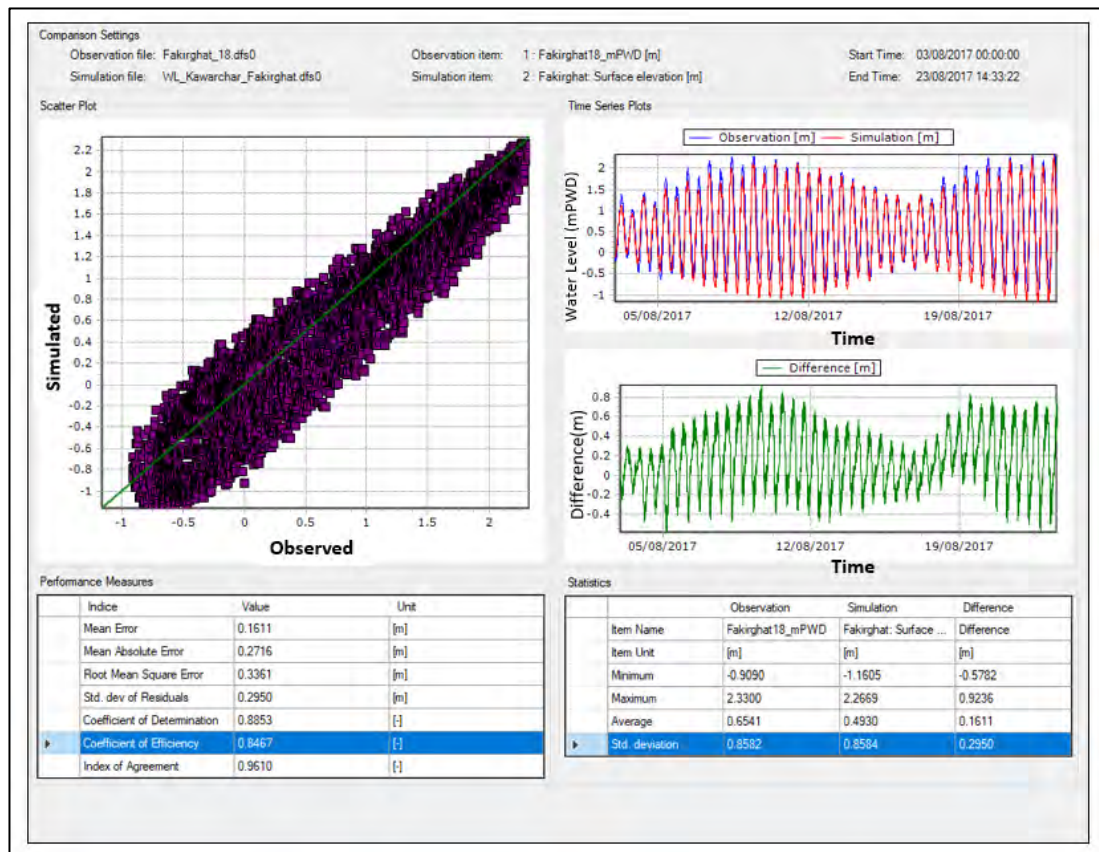
Figure 3.22: Performance Measures for Fakira Ghat Calibration

We have discharge measurement at Tumchar in Tentulia river of the year 2017. Discharge is calibrated with this measurement which is shown in the **Figure 3.20**. It is seen from the time series plot that simulated discharge and observed discharge matched well.

Validation of Hydrodynamic Model

Validation for hydrodynamic model is required to verify the model or to validate that the model works good in a different year time period rather than calibration period. The model has been validated for tidal water level at different locations for the year 2015. Validation locations are shown in **Figure 3.18**. Usually, validation location is chosen such way that it differs from calibration locations. In this study water level calibration and validation locations are same that means calibration and validation have been done for same location. Validation Results are shown in **Figure 3.23.** From this time series plot it seen that for both locations (i.e., Fakira Ghat and Kawar Char) simulated and observed water level matched well. Correlation factors for

hydrodynamic model validation are found out by previously mentioned formulae which is shown in the **Table 3.7.**
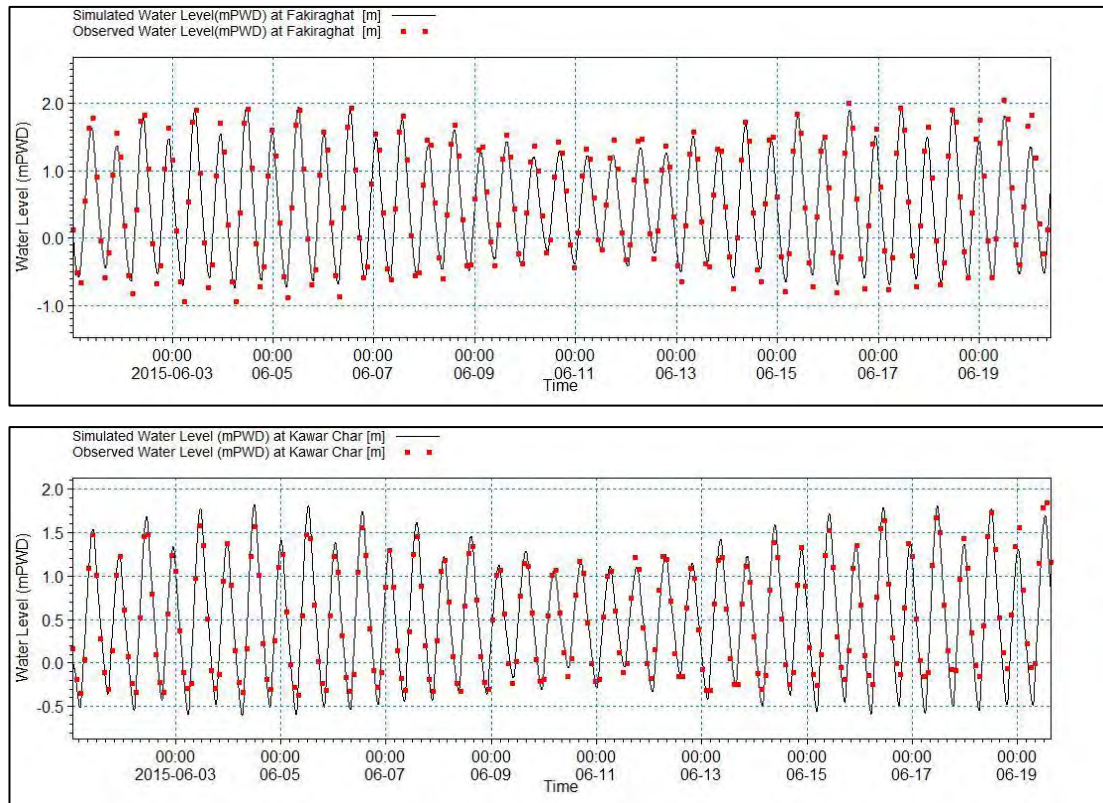
Figure 3.23: Water level validation at Fakiraghat and Kawar Char
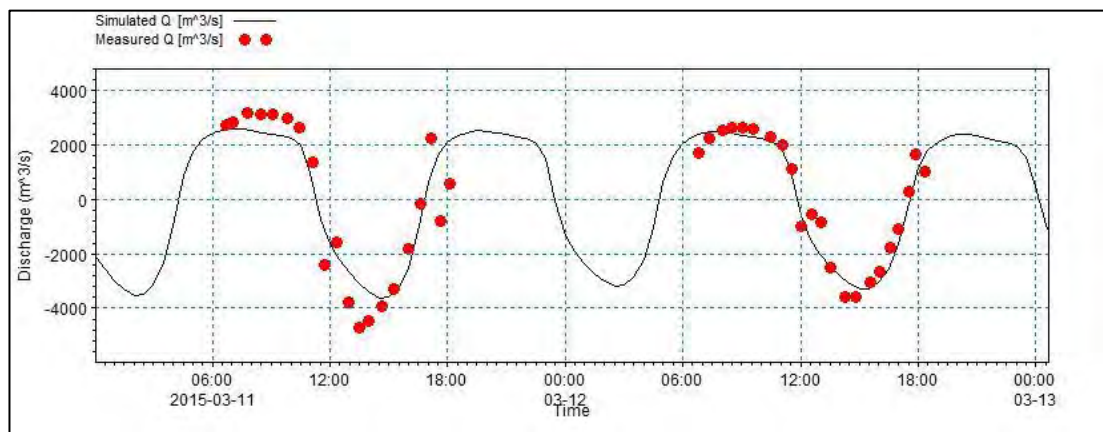
Figure 3.24: Discharge validation at Bamna of Bishkhali river

Moreover, the performance measures result for Fakira Ghat validation by time series comparator tool is shown in the **Figure 3.25** and result has good agreement. The performance measures result for Kawar Char validation by time series comparator tool is shown in the **Figure 3.26** and result has good agreement also.

Table 3.7: Correlation factor for hydrodynamic model validation

Parameter	Mean	Bias	RMS	Bias/Mean	Scatter Index	Correlation	No. of Time Steps
Fakiraghat	0.53	0.01	0.10	0.02	0.19	0.94	2737
Kawar Char	0.57	0.02	0.10	0.03	0.17	0.93	2740
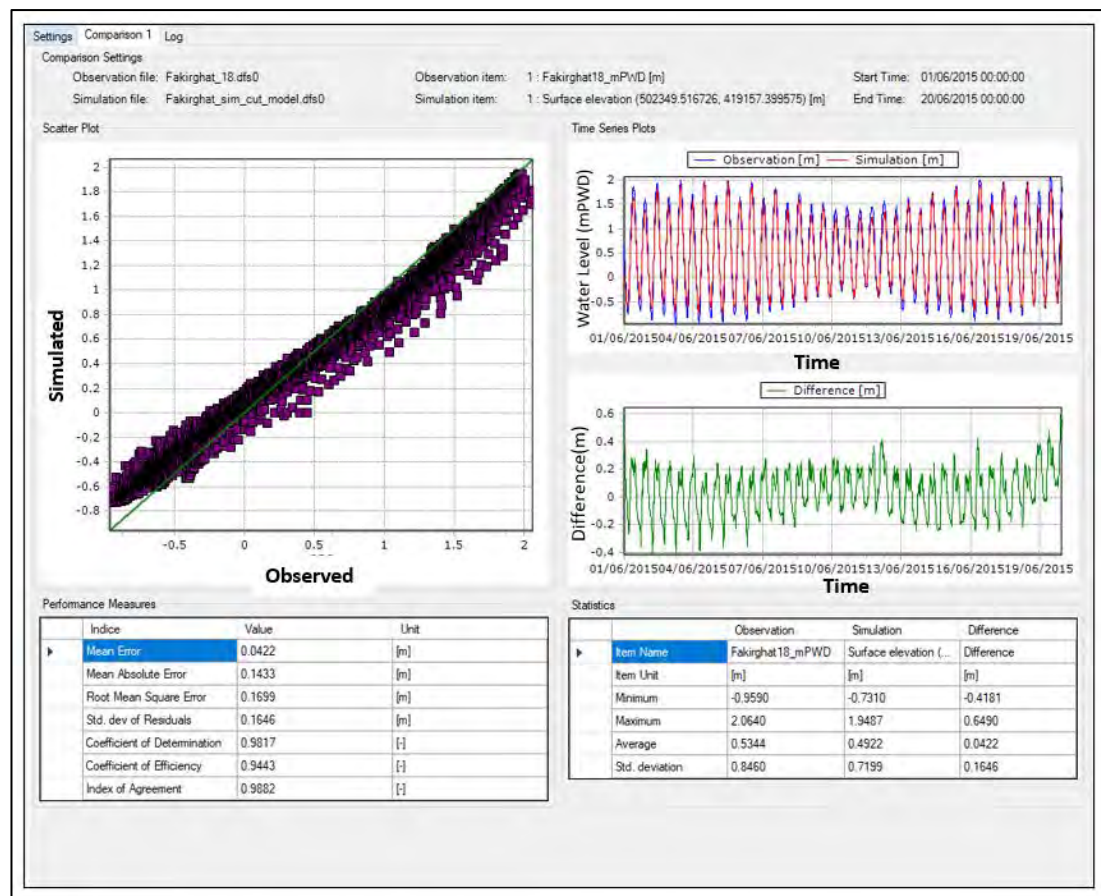
Figure 3.25: Performance Measures for Fakiraghat Validation

Discharge Validation is done at Bamna in Bishkhali river. Time series plot of simulated and observed discharge is shown in the **Figure 3.24**. It can be concluded from this figure validation for discharge has good agreement also as simulated and measured discharge matched well.
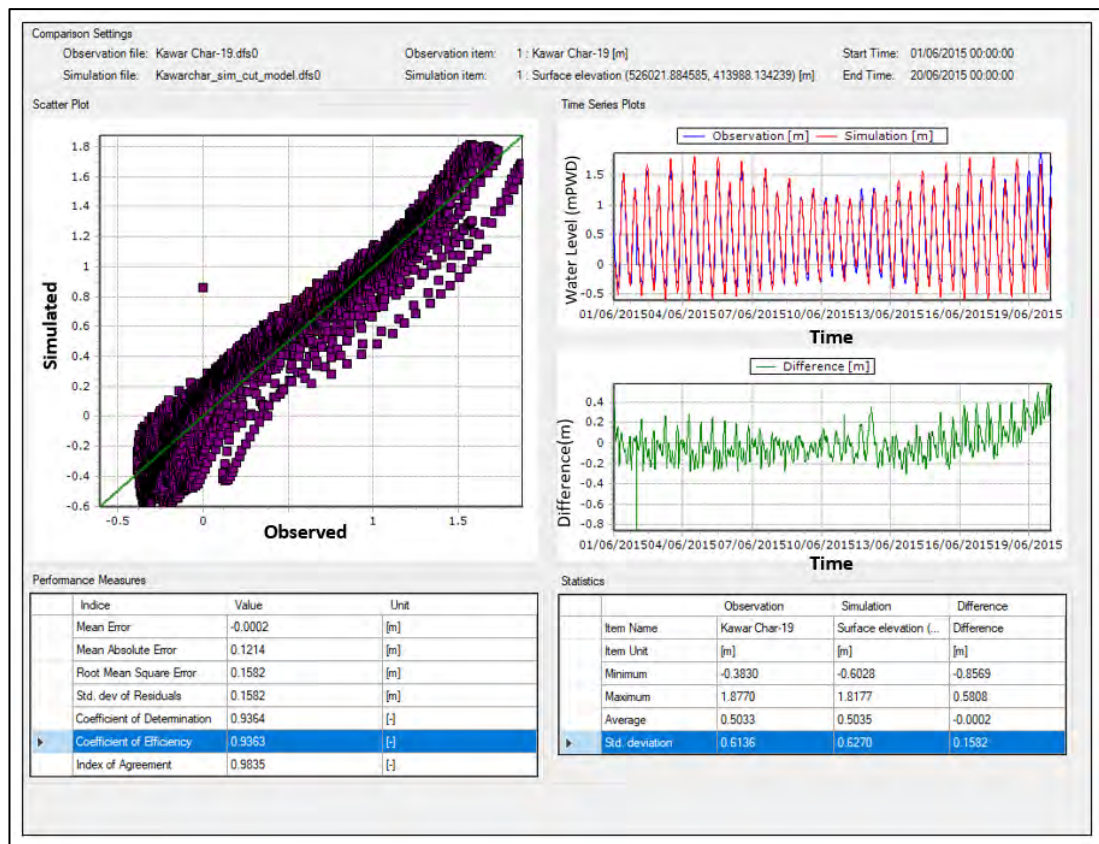
Figure 3.26: Performance Measures for Kawar Char Validation

3.4 Wave Model

The spectral wave module of Mike 21 (MIKE 21 SW) is based on the wave action balance equation where the wave field is represented by the wave action density spectrum $N(\sigma, \theta)$. The relation between the wave energy density spectrum $E(\sigma, \theta)$ and the wave action density spectrum is given by

$$N = E/\sigma \qquad \text{(3-12)}$$

The spectral wave module includes two different formulations

- Directionally decoupled parametric formulation

- Fully spectral formulation

The fully spectral formulation is based on the wave action conservation equation as described in e.g., Komen et al. (1994) and Young (1999), where the directional-frequency wave action spectrum is the dependent variable.

In horizontal Cartesian co-ordinates, the conservation equation for wave action can be written as

$$\frac{\partial N}{\partial t} + \nabla \cdot (\vec{v}N) = \frac{S}{\sigma} \qquad \text{(3-13)}$$

Where, $N(\vec{x}, \sigma, \theta, t)$ is the action density,

t is the time, $\vec{x} = (x, y)$ is the Cartesian co-ordinates,

$\vec{v} = (c_x, c_y, c_\sigma, c_\theta)$ is the propagation velocity of a wave group in the four-dimensional phase space $\vec{x}$, σ and θ, and

S is the source term for the energy balance equation.

∇ is the four-dimensional differential operator in the $\vec{x}$, σ, θ-space

3.4.1 Existing Wave Model of IWM

Spectral Wave module has been applied for the study. MIKE 21 SW is a new generation spectral wind-wave model based on unstructured flexible mesh. The model simulates the growth, decay and transformation of wind generated waves and swells in the offshore and coastal areas. MIKE 21 SW includes the following physical phenomena:

- Wave growth by action of wind
- Non-linear wave-wave interaction
- Dissipation due to white capping
- Dissipation due to bottom friction
- Dissipation due to depth-induced wave breaking
- Refraction and shoaling due to depth variation
- Wave-current interaction

- Effect of time varying water depth.

The existing bathymetry that has been used for wave model are given in **Figure 3.27**.
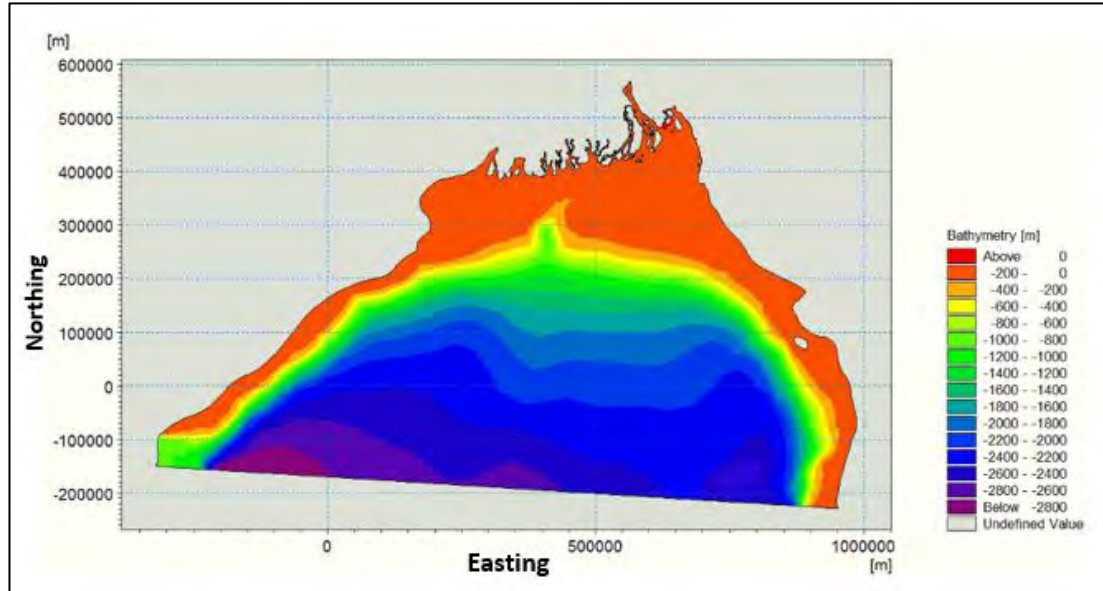
Figure 3.27: Bay of Bengal Spectral Wave Model

The existing mesh resolution has been further upgraded for the study area and also bathymetry is updated in Rabnabad Channel, Andharmanik River and the vicinity of Kuakata beach under this research work. The boundary conditions for the upgraded model are extracted from the existing Wave Model of IWM.

A dfs1 file as wave boundary of Bay of Bengal (BoB wave model domain) is collected from IWM for the year 2008 to 2018. This dfs1 file is actually prepared from ECMWF. Existing BoB wave model is run using this boundary for long term. For dedicated wave model east west and south wave boundary is created from simulating BoB model. Dedicated wave model result is more accurate as higher resolution mesh is used and bathymetry is updated in the study area. Then wave result is analyzed and used for littoral drift and coastline evolution model. Parameters used at the boundary data for the upgraded wave model are significant wave height, peak wave period, mean wave direction and directional standard deviation.

3.4.1.1 Model Parameters

For the local spectral wave model, the model parameters are shown in **Table 3.8**. MIKE 21 SW includes two different formulations: 1) Directional decoupled parametric formulation and 2) Fully spectral formulation. The directional decoupled parametric formulation is based on a parameterization of the wave action conservation equation. The parameterization is made in the frequency domain by introducing the zeroth and first moment of the wave action spectrum as dependent variables following Holthuijsen (1989). The fully spectral formulation is based on the wave action conservation equation, as described in e.g., Komen et al. (1994) and Young (1999), where the directional-frequency wave action spectrum is the dependent variable. The number of discrete directions should be large enough to resolve the directional variation of the waves. For swell with a relative narrow directional distribution of the wave action/energy a relatively small directional resolution is needed.

Table 3.8: Model parameters for local wave model.

Model Parameter	Value
Basic equations	Fully spectral formulation Instationary formulation
Spectral discretization	16 directions
Solution technique	Low order fast algorithm Max. number of levels in transport calculation = 32 Minimum time step = 0.01 sec Maximum time step = 600 sec
Water level conditions	Calculated using HD model
Wind forcing	U and V wind field from ECMWF
Wave breaking	Specified gamma Gamma = 0.8 Alpha = 1 Gamma (wave steepness) = 1 Effect on mean frequency not included
Bottom friction	Nikuradse roughness height. Kn = 0.04 m Effect on mean wave frequency was included
Current conditions, ice coverage, diffraction	Excluded

The discretization in geographical and spectral space is performed using a cell-centered finite volume method. In the geographical domain, an unstructured mesh is used. The spatial domain is discretized by subdivision of the continuum into non-overlapping elements. The convective fluxes are calculated using a first order upwinding scheme. Depth-induced wave breaking is the process by which waves dissipate energy when the waves are too high to be supported by the water depth, i.e., reach a limiting wave height/depth-ratio. The formulation used in the spectral wave module is based on the formulation of Battjes and Janssen (1978). This model has been used successfully in the past in fully spectral models as well as in parameterized versions. As waves propagate into shallow water, the orbital wave velocities penetrate the water depth, and the source function due to wave-bottom interaction become important. The dissipation source function used in the spectral wave module is based on the quadratic friction law and linear wave kinematic theory.

3.4.2 Dedicated Wave Model

Concept of dedicated wave model is deployed in this study due to ease of handling the model, it minimizes the simulation time, provides good result incorporating the finer mesh. Plenty of scenarios can be investigated in limited time. The flow chart in the **Figure 3.28** indicates how a wave model works by MIKE 21 SW.
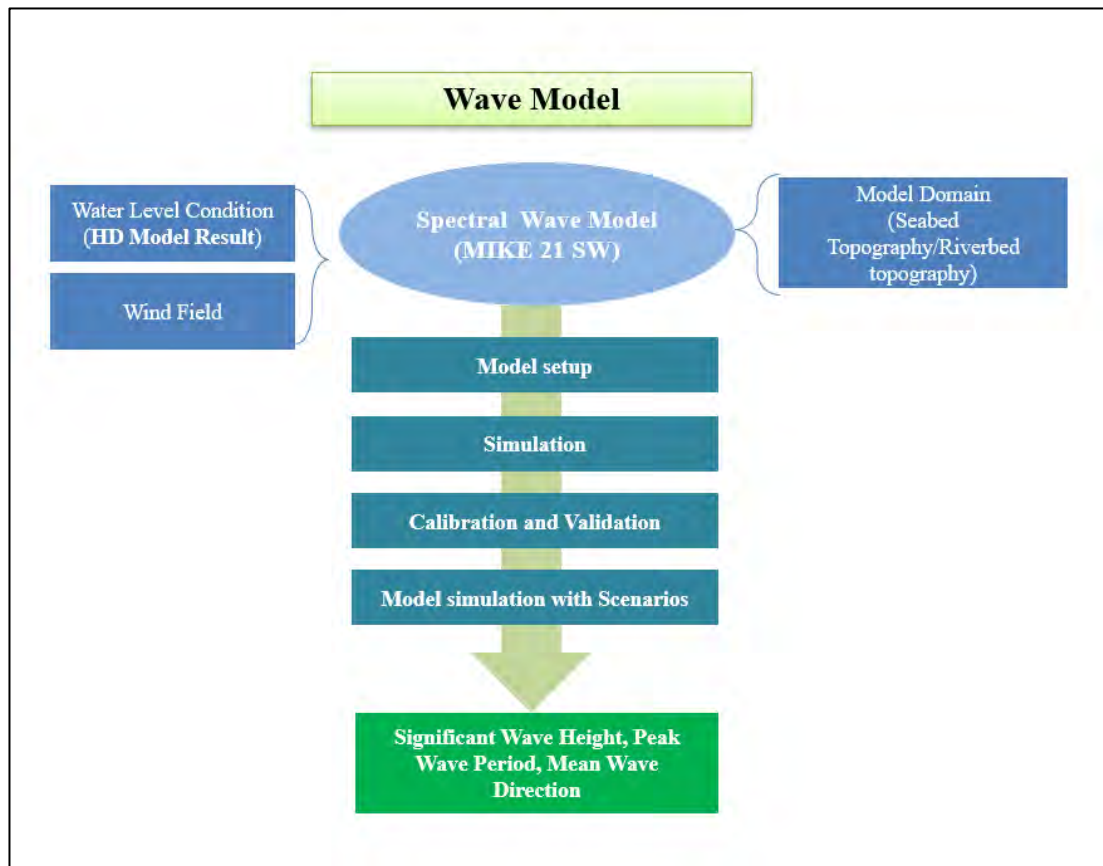
Figure 3.28: Flow chart of wave model using MIKE 21 SW

Model Domain:

In the present study, a dedicated model has been developed which is cut from the existing IWM wave model. Mesh is improved in the vicinity of Kuakata beach. In IWM wave model very coarse mesh was used, here in this study finer mesh is used as sediment budget calculation is involved.

Figure 3.29 shows the model domain of study area. East, west and south boundary of the model domain are in the Bay of Bengal and upstream boundary is Hilisha river which has been originated from Lower Meghna. Moreover, the important rivers in the domain are Baleswar, Bishkhali, Buriswar-Payra, Andharmanik, Lohalia, Tentulia, Rabnabad Channel etc.
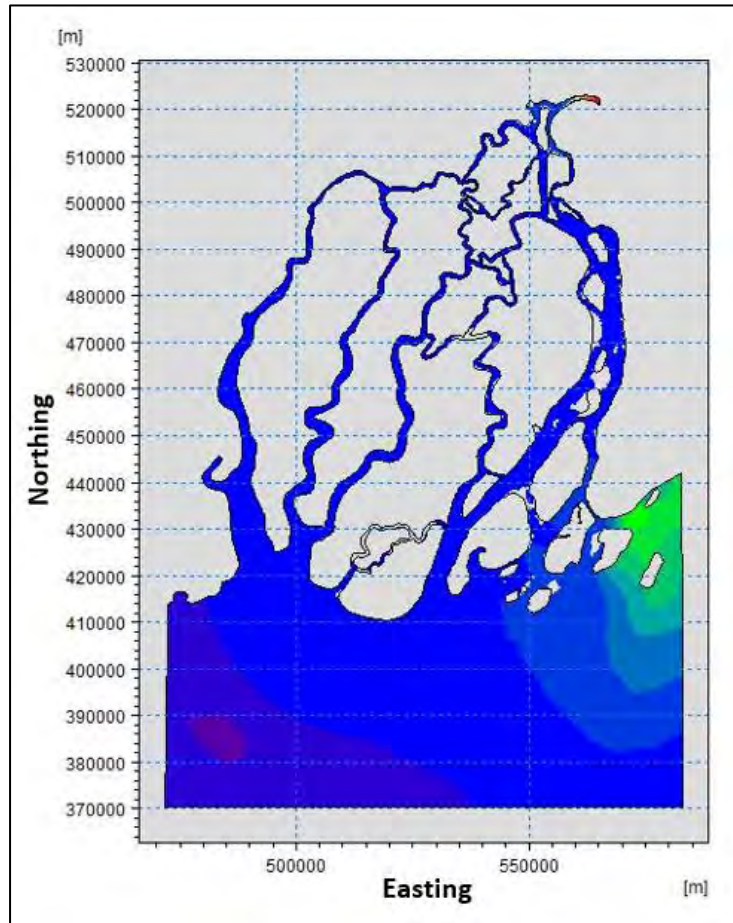
Figure 3.29:Dedicated wave Model domain of the Kuakata study area

Water level conditions:

For the same domain hydrodynamic model was run for the year 2018. Result file of hydrodynamic simulation is used as water level condition. So, Water level is used as varying in time, varying in domain.

Wind:

Accurate predictions of extreme values of waves are essential when determining design data for marine structure. The safety of structures, as well as the possibility of developing an economic design, relies above all on reliability and accuracy of the underlying design data. European Centre for Medium-Range Weather Forecasts (ECMWF) has carried out global forecast model for different part of the world. In this study, wind and wave data will be extracted from this global model from ERA5 for forecasting wind and wave in the project area. **Figure 3.30** shows the coverage of the

global model data for existing Bay of Bengal model. The detailed description of the wind field data is furnished below:

Area: 81⁰E to 95⁰E and 16⁰N to 25⁰N

Period: 1 Jan 2008 to 1 Jan 2019 with resolution 0.125 x 0.125 degrees

Parameters: Atmospheric pressure and wind components (X and Y)

Format: DFS2 (structured grid)

The wind data is variable in space/time and inserted in the model as velocity components. **Figure 3.30** shows y component of a sample wind data.
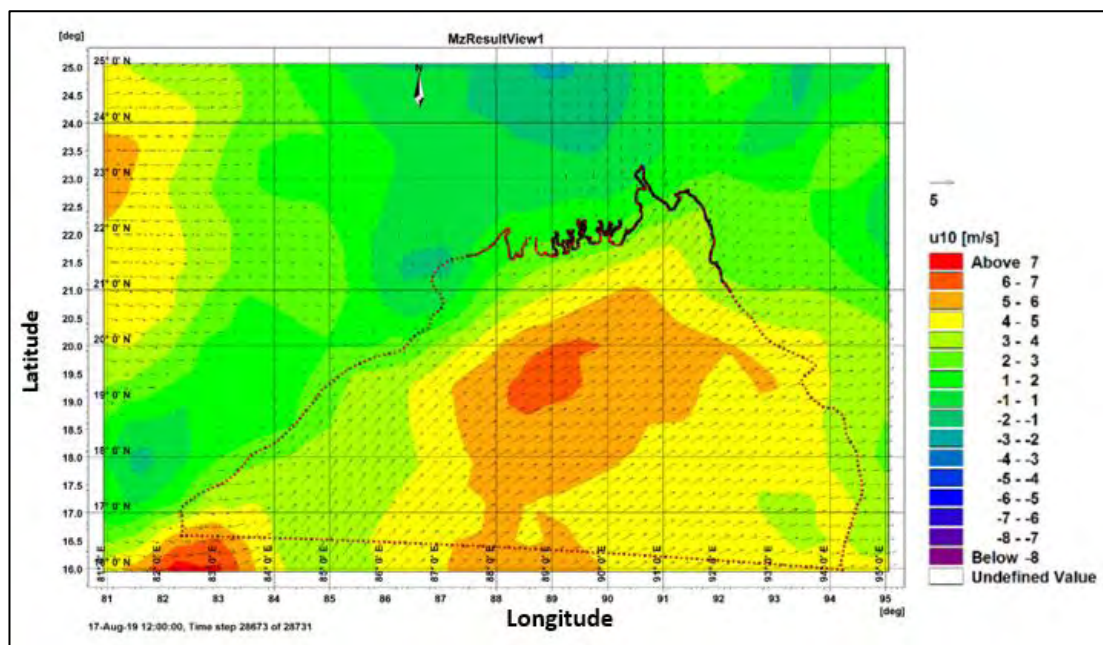
Figure 3.30: Y-component of wind speed at a particular time covering the Bay of Bengal model area

Development of Boundary condition:

The model has three open boundaries namely the south, west and east boundary where offshore wave conditions are specified for the period 2008-2018 and the other boundary is absorbing land boundary. The offshore wave conditions defined in the Mike 21 SW model are

- Significant wave height (meters)

- Peak wave period (seconds)

- Mean wave direction (degrees)

- Directional standard deviation (degrees)

This integrated wave parameters have been extracted from Global wave Model.

3.4.3 Calibration of Dedicated Wave Model (MIKE 21 SW)

Simulation:

A number of simulations were carried out to establish the nearshore wave conditions in the study area. The simulations have been carried out using the following conditions:

- Fully spectral formulation

- Quasi-stationary time formulation

- Directional discretization 360 degrees

- Bottom friction $k_n = 0.015$

- Wave breaking $\gamma = 0.8$ and $\alpha = 1.0$

The bottom friction is specified as Nikuradse roughness, k_n. The default value k_n is 0.04 m which is usually too high for nearshore applications using the fully spectral formulation. The value of k_n is selected 0.015 m for the SW model of Kuakata beach by trial and error process.

Calibration:

Calibration means adjustment of the model parameters so that simulated and observed data match within the desired accuracy. The spectral wave model was calibrated using recorded wave data from 7th March – 2nd April of year 2018. The location of the wave measurement was 24 km offshore from Kuakata beach and is illustrated in **Figure 3.9**. The simulated significant wave height, peak wave period & peak wave direction is compared with the observed data at the available location in **Figure 3.31**. It is seen in **Figure 3.31** that the significant wave height, peak wave period & peak wave direction is well represented by the spectral wave model.

For validation the wave model no observed wave data is found for the study area. So, it can be treated as a limitation of this thesis work.
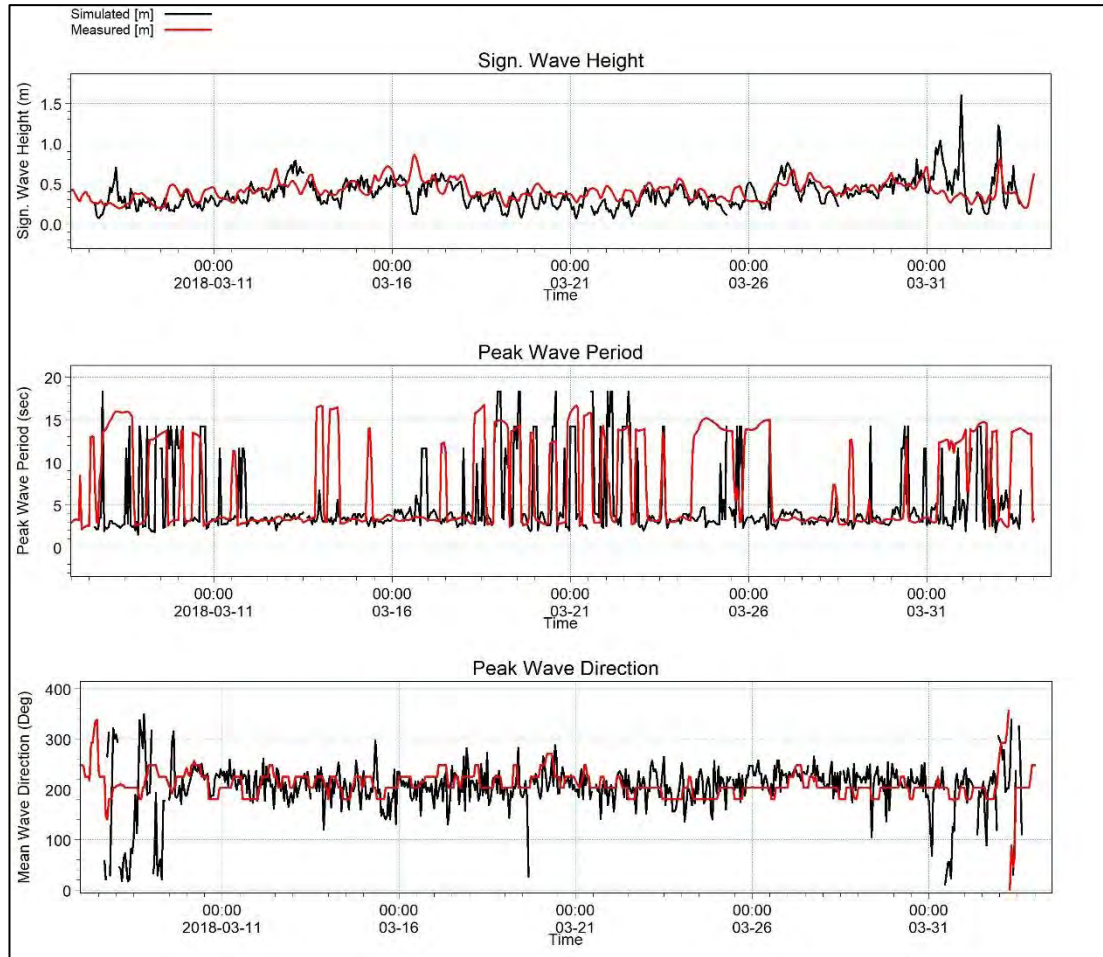
Figure 3.31: Calibration plot of significant wave height, peak wave period and peak wave direction

3.5 LITDRIFT Model

LITDRIFT simulates the littoral drift or shore parallel sediment transport, and it is a part of the software package LITPACK developed by DHI Water & Environment. The output from the model is the littoral transport for the individual wave situations and the total sediment budget for any time period.

LITDRIFT consists mainly of two calculation parts:

- longshore current calculation

- sediment transport calculation

The cross-shore distribution of longshore current, wave height and setup for a coastal profile, is found by solving the long and cross shore momentum balance equations. The longshore current model includes a description for regular and irregular waves, the influence of tidal current, wind stress and non-uniform bottom friction, as well as wave refraction, shoaling and breaking.

The sediment transport is calculated by the Sediment Transport Program (STP) of DHI based on the local wave, current and sediment conditions. STP is a detailed intra-wave-period model which describes the time-varying distribution of both suspended load and bed load within the wave period in combined wave and current motion, including the effect of wave breaking when relevant. The transport rates are found directly by calls to STP. As a result, LITDRIFT is able to give a deterministic description of the cross-shore distribution of longshore sediment transport for an arbitrary, non-uniform, bathymetry and sediment profile, as well as a detailed description of the sediment budget. The structure of LITDRIFT is shown in **Figure 3.32.**
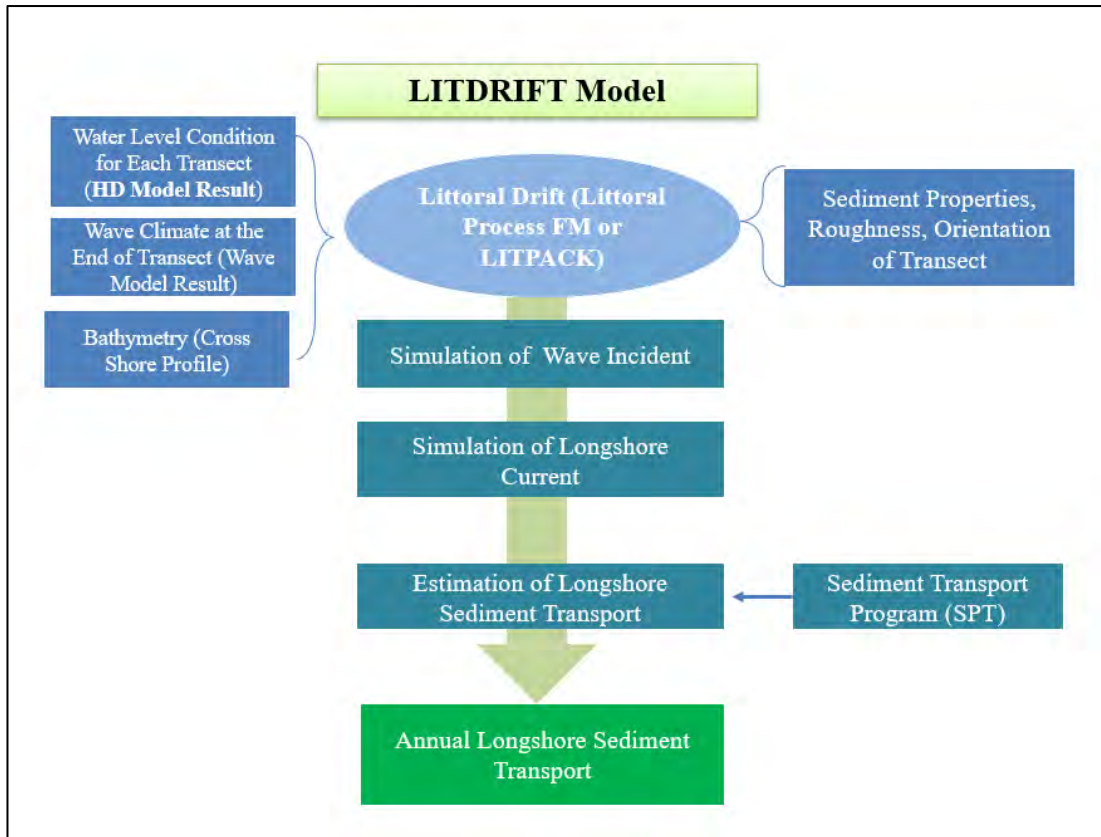
Figure 3.32: Structure of LITDRIFT model

3.5.1 Governing Equations of LITDRIFT Model

The Littoral Processes FM module is an integrated modelling system that simulates non-cohesive transport in points and along quasi-stationary coastlines using an n-line approach.

The Littoral Processes module provides a powerful tool for sediment budget analysis, which is of paramount importance to all coastal morphology studies. The Littoral Processes FM module combines a technically strong deterministic sediment transport model with a very user-friendly graphical interface. It simulates a wide range of wave and current scenarios along straight or nearly straight coastlines.

For some applications it may be necessary to go into detail for the individual wave period, why the simulation of the transport for a single point provides an intra-wave period output functionality.

The system of numerical models available in Littoral Processes FM (popularly known as LITPACK) enables one to determine longshore current and distribution of sediment concentration in vertical direction which ultimately determines sediment transport. Litdrift model is one of the modules under Littoral Process of FM (LITPACK) by which longshore drift can be estimated. Longshore sediment transport primely depends on wave climate, sediment characteristics and orientation of coastline.

The littoral current computation in LITPACK is based on the equation,

$$-\frac{1}{\rho}\frac{\partial S_{xy}}{\partial x} + \frac{1}{\rho}\tau_w sin\theta + gDI = \frac{V^2}{C^2} - \frac{\delta}{\delta x}\left(E_c D \frac{\delta v}{\delta x}\right) \qquad \text{(3-14)}$$

Where,

ρ density of sea water

D   water depth

V   mean velocity over depth

c   resistance factor

S_{xy} shear stress due to radiation

τ_w wind stress

I   longshore slope of water surface

θ   angle between wind direction and coast normal

E_c momentum exchange coefficient

G   acceleration due to gravity

x   longitudinal coordinate along the coastline

Sediment concentration is determined by vertical turbulent diffusion equation as mentioned below:

$$\frac{\delta c}{\delta t} = \frac{\delta}{\delta x}\left(\epsilon_s \frac{\delta c}{\delta z}\right) + W \frac{\delta c}{\delta x} \tag{3-15}$$

Where,

c   sediment concentration

t   time

z   vertical coordinate

ϵ_s turbulent diffusion coefficient

w   fall velocity of the sediment

x   longitudinal coordinate

Total sediment load (q_T) is computed by adding bed load(q_b) and suspended load (q_s). Bed load is determined by deterministic approach of Engelund Fredsoe (1976) model while suspend load is calculated by the following equation

$$q_s = \frac{1}{T}\int_0^T \int_{2d}^D (uc)\,dz\,dt \tag{3-16}$$

Where, q_s is the suspended load, u is the velocity, x is the vertical coordinate, T is the wave period, D is the local depth, c is the reference concentration, t is the time and d is the sediment size.

3.5.2 Estimation of Longshore Sediment Transport

The annual drift is found by the contribution of transport from each of the wave incidents occurring during the year.

When calculating the annual drift, the wave climate in the calculations is described in a time series file where each set of items describe the characteristics of one wave incident and the bathymetric conditions at that time. In addition, the duration of the individual wave incident considered.

Thus, the total annual drift Q_{annual} is found as the sum of the contributions from all wave incidents.

$$Q_{annual} = \sum_{i=1}^{NSETS} Qs(i).Duration(i) \qquad \textbf{(3-17)}$$

Where NSETS is the total number of wave incidents and Duration(i) is the duration of the wave incident. The definition of annual drift Q_{annual} is provided that the total duration in the wave climate file is one year. Otherwise, the total drift is found per design period (i.e., total duration in simulation).

3.5.3   Model Development

The Litdrift model for the study area covers the coastline of Kuakata beach. Total of six transects are selected to obtain the longshore sediment transport in the shoreline stretching from Lebur Char to Kawar Char, as shown in **Figure 3.33** and **Figure 3.34**. The six transects are established by taking into account the wave climate, shoreline orientation and the erosion and deposition pattern of the shoreline. The cross-sectional profile along the above mentioned six transects are shown in the **Figure 3.35**.
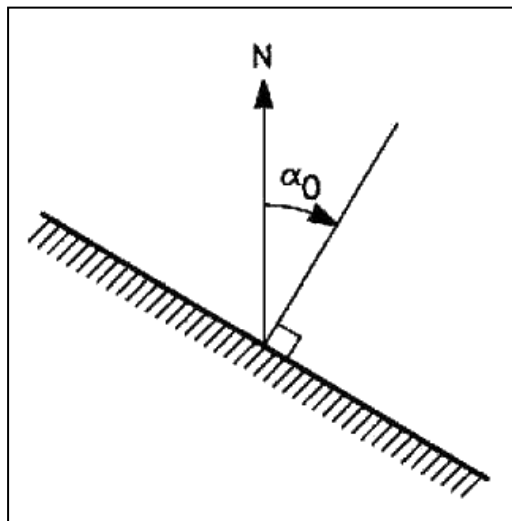
Figure 3.33: Definition of profile orientation
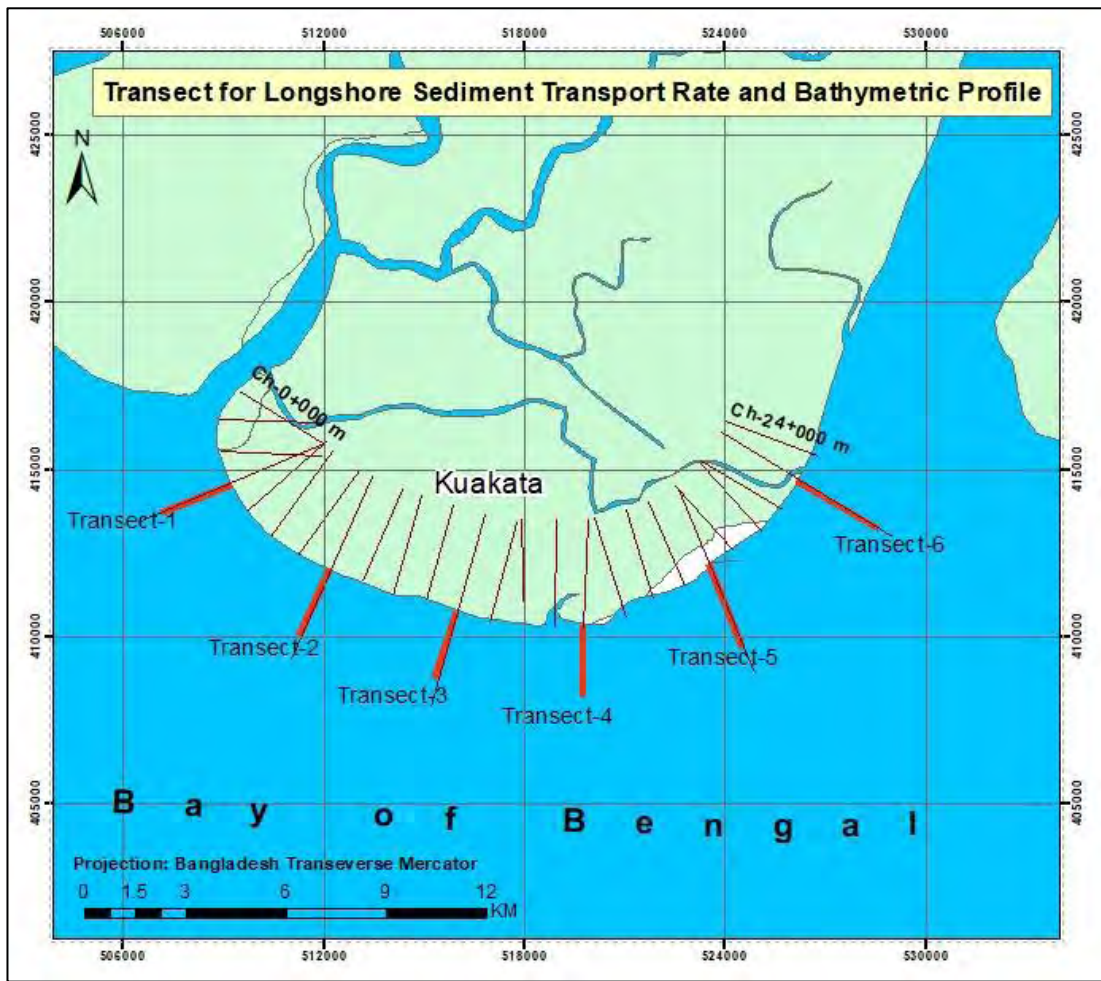
Figure 3.34: Transects perpendicular to the shoreline
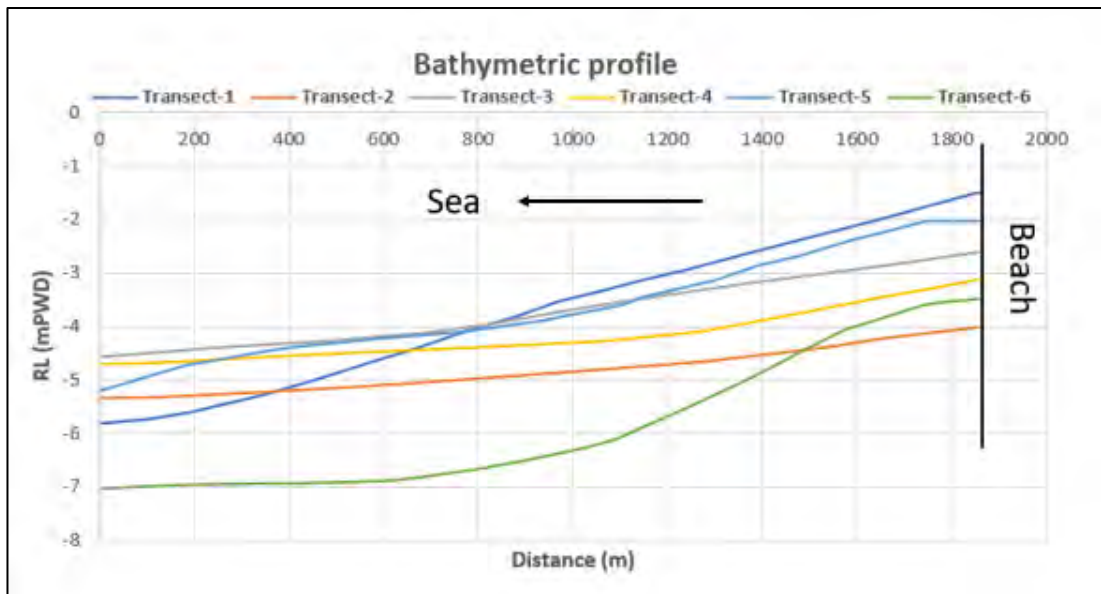
Figure 3.35: Cross-sectional profiles along the transects

The characteristics of the individual computation profiles are illustrated by **Table 3.9.** Length of the transect depends on the location of depth of closure. Depth of closure is that depth in the offshore of the sea, beyond which literally no littoral transport occurs. So, over the time no significant change in bottom elevation of the sea beyond depth of closure. Length of the transect should be equal or greater than the distance of depth of closure from coastline. There are several formulae exists to find the depth of closure. For Kuakata nearshore area, it is seen that depth of closure located within 2000 m. So, the length of the transect in this study is reasonable and appropriate.

Table 3.9: Overview of profiles used for computation of littoral transport

Profile ID	Δx (m)	Number of grid points in the transect	Position for wave climate extraction at the tip of the transect			Shore normal orientation (degrees)	Length (m)
			Easting	Northing	Depth (m)		
Transect-1	5	400	507116	413688	-5.8	250	2000
Transect-2	5	400	511205	410176	-5.3	210	2000
Transect-3	5	400	514909	408928	-4.5	203	2000
Transect-4	5	400	519677	408287	-4.7	182	2000
Transect-5	5	400	524490	409822	-5.2	157	2000
Transect-6	5	400	528617	413274	-7.0	120	2000

<u>Sediment Characteristics and Bed Roughness:</u>

Bed samples should be collected from different location in intertidal zone but in this study, it could not be done for limitation. So, bed parameters have been collected from previous literature.

Table 3.10: Bed parameters applied for all transects

Parameter	Value
Median Grain Size (d_{50})	0.2 mm
Geometrical spreading for grain sizes $\left(\sigma = \sqrt{\dfrac{d_{84}}{d_{16}}}\right)$	1.5
Nikuradse roughness coefficient	4 mm

After giving all necessary inputs (i.e., transects position and dimension, cross-sectional profiles, grid size, beachline orientation and transect orientation and sediment characteristics) in the LITDRIFT model, timeseries of longshore sediment transport has been simulated. Minimum 4/5 years' simulation needs to run for getting better result for LITDRIFT model.

3.6   Coastline Evolution Using LITLINE Model

This model type will calculate the movements of the coastline position with respect to a straight baseline. The model is, with minor modifications, based on a one-line theory, in which the cross-shore profile is assumed to remain unchanged during erosion or accretion. Thus, the coastal morphology is solely described by the coastline position (cross-shore direction) and eventual changes of dune geometry at a given long-shore position. The sediment transport information is derived from information in pre generated littoral drift transport tables. **Figure 3.36** represents the simple flow chart of LITLINE or coast evolution model.

Figure 3.36: Simple Flow chart of LITLINE model
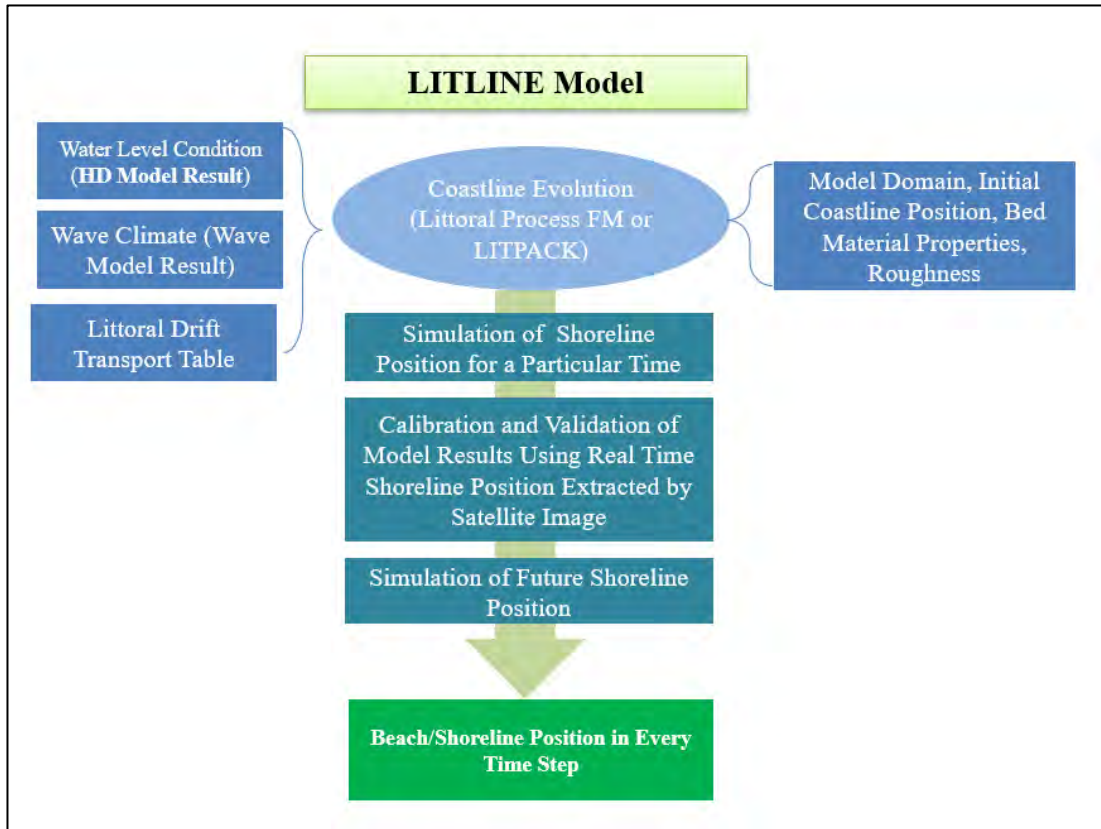
The coastline evolution calculations are based on a co-ordinate system in which the x-axis is a baseline that runs parallel to the primary coastline orientation, while the y-axis runs from the baseline in offshore direction (**Figure 3.37**) $y_c(x)$ is the distance from the baseline to the coastline.
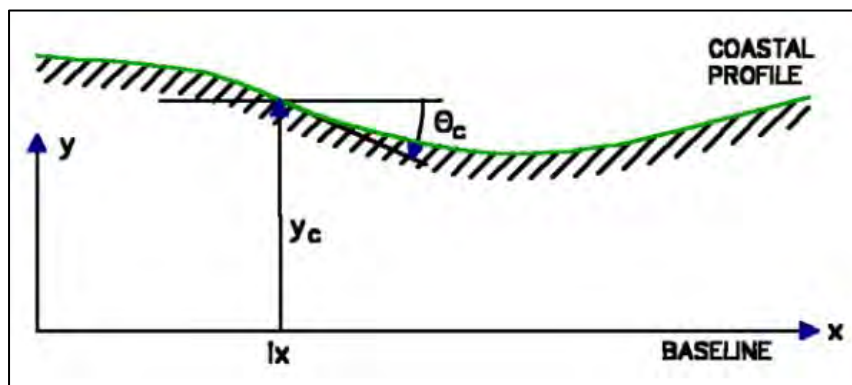
Figure 3.37: Coordinate system in coastline evolution calculation

Coastline profile is used to denote the variation of y_c in the longshore(x) direction, while the cross-shore profile denotes the water depth (bottom position) as a function of the cross-shore position relative to the coastline position y_c.

3.6.1 Governing Equation for LITLINE Model

The main equation in the coastline evolution model is the continuity equation for sediment volumes:

$$\frac{\partial yc(x)}{\partial t} = -\frac{1}{h_{act}(x)}\frac{\partial Q(x)}{\partial x} + \frac{Q_{sou}(x)}{h_{act}(x)\Delta x} \qquad\qquad \textbf{(3-18)}$$

In which the symbols are

$Y_c(x)$ distance from the baseline to the coastline

t   time

$h_{act}(x)$ height of the active cross-shore profile

$Q(x)$ longshore transport of sediment expressed in volume

x   longshore position

Δx longshore discretization

$Q_{sou}(x)$ source/sink term expressed in volume

$h_{act}(x)$ and $Q_{sou}(x)$ are calculated based on user specifications while longshore transport rate $Q(x)$ is determined from tables relating the transport rate to the hydrodynamic condition at breaking. Δx is user specified, while the internal timestep Δt is determined from stability criteria. From an initial coastline position $y_{init}(x)$, the evolution in time is determined by solving equation using an implicit Crank-Ncholson scheme.

The continuity equation for sediment volumes, equation (*3-18*, is solved through an implicit Crank-Nicholson Scheme. The discretization in longshore direction is sketched in **Figure 3.38**.
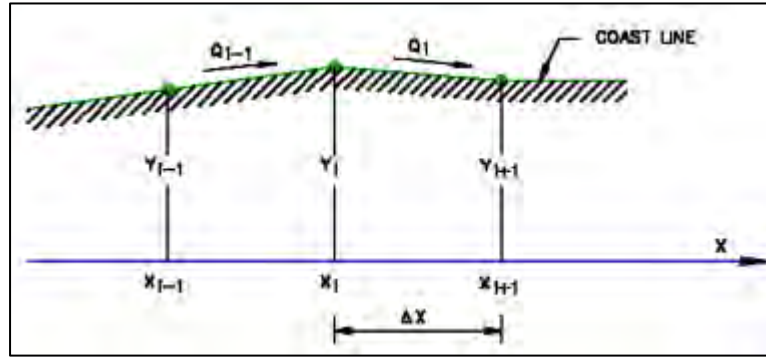
Figure 3.38: Longshore discretization

Qi denotes the transport rate between x_i and x_{i+1} while dQ_i denotes the change in the transport rate with respect to change in coastline orientation (for values of θ close the local orientation θ_0).

$$dQ(x) = \frac{\partial Q}{\delta \theta}(x, \theta_0) \qquad \text{(3-19)}$$

A subscript "t" denotes(known) values of the present time step, while subscript "t+1" denotes unknown values of the next time step. Transport rates corresponding to time step t+1 are estimated through:

Based on a crank-Nicholson scheme of the continuity equation can be written as

$$a_i y_{i-1,t+1} + b_i y_{i,t+1} + c y_{i+1,t+1} = d_i \qquad \text{(3-20)}$$

in which

$$a_i = (1-\propto)dQ_{i-1} \qquad \text{(3-21)}$$

$$b_i = \frac{\Delta x^2 . h}{\Delta t} - a_i - c_i \qquad \text{(3-22)}$$

$$d_i = a_i y_{i-1,t} + b_i y_{i,t} + c y_{i+1,t} - \Delta x . (Q_{i,t} - Q_{i-1,t} - QS_i) \qquad \text{(3-23)}$$

Where QS_i is the contribution from possible sources. a_i, b_i, c_i, and d_i can be found for the present time step and with two boundary conditions, the system of equation for all longshore positions can be solved by Gauss-elimination method.

The boundary conditions applied assume a zero-transport gradient through each boundary. This causes the coastline orientation at the boundaries to be constant. The

parameter α is the Crank-Ncholson factor. It determines how implicit the solution scheme is. A value of 0 gives a fully implicit solution. A value of 1 gives a fully explicit solution.

3.6.2 LITLINE Model Setup

Model domain can be provided in two ways. Either we can set a mesh file of our interested area (i.e., Kuakata) giving domain type as 2D bathymetry or we can set domain type as work area providing lower left corner and upper right co-ordinates. Here dedicated HD model bathymetry (.mesh file) is used to set model domain.

Under littoral processes module model definition is set as coastline evolution which is also known as LITLINE model. Time is set according to user and model requirement. In case of current research study coastline evolution model was run from year 2008 to year 2018. Constant roughness height (0.00040) is used for Bed Resistance for each profile in the model.

Water level condition needs to provide in the model. Model can be run without providing water level condition but for more accurate prediction (converging result with actual scenario in faster rate) it is necessary to incorporate water level condition of the study area. In this current study water level is extracted for the year 2008 to year 2018 in somewhere in the middle portion of Kuakata beach from BoB model and used in the model accordingly.

3.6.3 Baseline and Initial Coastline Preparation

A coastline under Bathymetry needs to be provided as dfs1 file (i.e., line series) which will be regarded as initial coastline. For this from satellite image of year 2010 the coastline of Kuakata is digitized by ArcGIS tool. Then shapefile is imported in Autocad. A baseline is set from which distance of the ordinates of the coastline is calculated with 50-meter interval. Again these 50-meter interval lines are imported in GIS again and length of those lines are calculated. Eventually a dfs1 file is created by MIKE using these values.

As the concern is about the erosion of Kuakata beach so only the segment, vulnerable to erosion, is considered for Litline model. Moreover, the orientation of beach is bidirectional so by a single baseline (i.e., one orientation angle) it is difficult to represent a coastline. Initial coastline is represented by **Figure 3.39**.
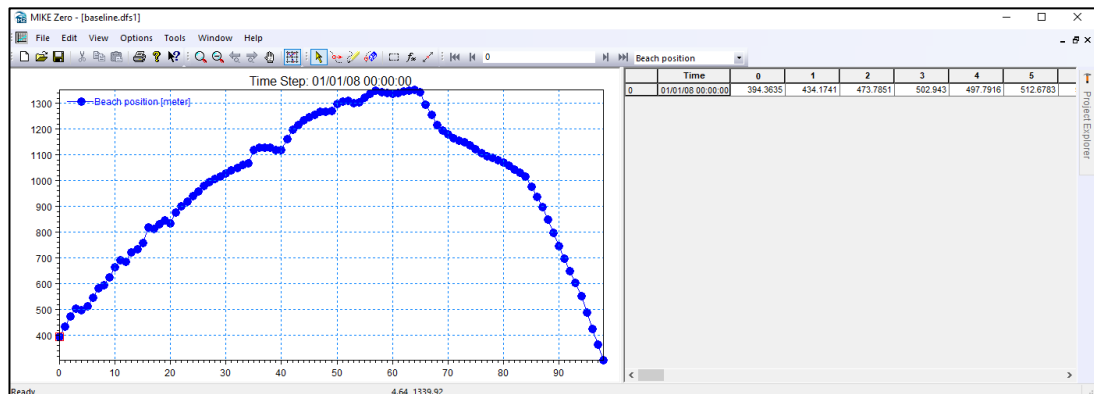
Figure 3.39: Beach position from baseline (Initial Coastline)

3.6.4　Wave Climate Input

Wave climate is derived from the dedicated wave model of Kuakata. Varying in time and space a representative dfs1 file is extracted from dedicated wave model result file and ultimately given as input to the litline model. The components of wave climates are wave height, wave period, mean wave direction and reduction factor. Here reduction factor is assumed to be 1 which means all incident waves are effective (i.e., the strength of wave is not reduced). Wave climate is shown in the following **Figure 3.40**.
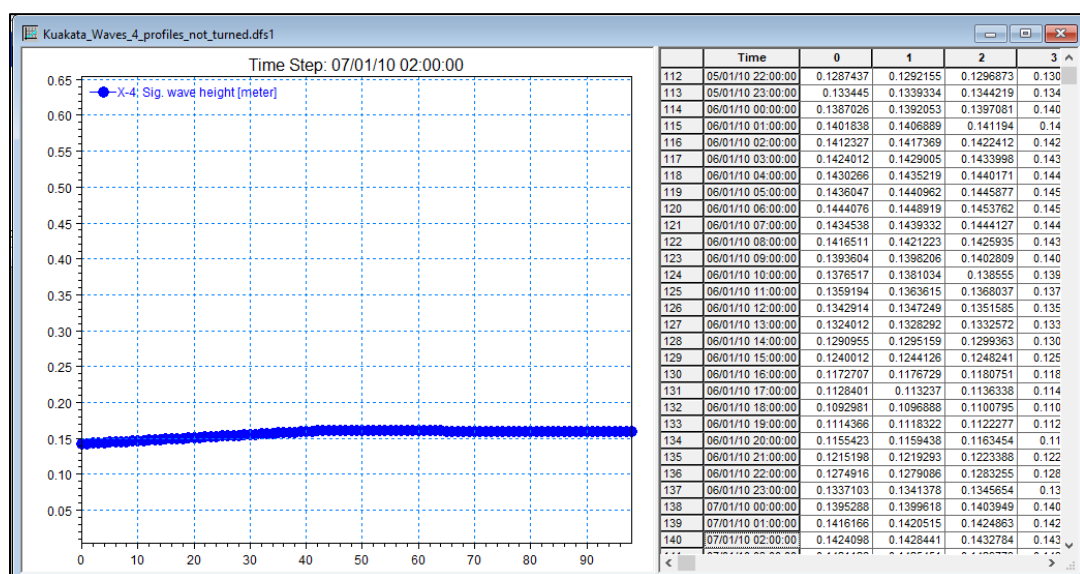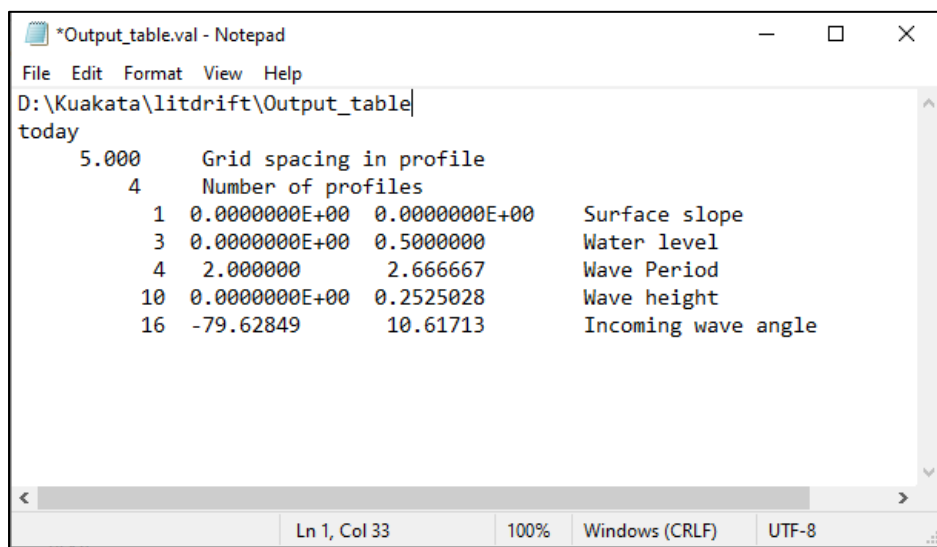
Figure 3.40: A dfs1 file represents wave climate

81

3.6.5   Littoral Drift Table Generation

A .val file is required to run Litline model. To create a .val file we use littoral drift table generation. Under bathymetry predefined cross-shore profiles (i.e., transect-1 to transect-6) are added. Bed resistance for each profile is given as 0.0040. grain diameter and fall velocity for each profile are set as 0.2000 mm and 0.0220 m/s respectively. Bed parameters and sediment calculation are set as default value. In Table Mode under Transport output_table.val file is saved in specified location. If we run this setup we will get .val file which is required for coastline evolution model. If the .val file is opened by notepad, it shows the following data as like **Figure 3.41**.

Figure 3.41: Output_table.val file required for LITLINE Model

Providing all essential inputs in the LITLINE model, time series of beach position is simulated. Future shoreline can also be predicted by this model adopting special technique which is described in the following chapter.

CHAPTER FOUR

DATA ANALYSIS, RESULT AND DISCUSSION

4.1 General

In this chapter erosion analysis (i.e., coastline shifting, quantifying erosion-accretion area, bathymetry comparison), current analysis from hydrodynamic model, wave rose analysis from wave model and detailed results from LITDRIFT model and LITLINE model are explained in the following sections.

4.2 Analysis of Shoreline and Bathymetry Change

Shoreline analysis for Kuakata beach is carried out by historical satellite imegaries (1978-2020) using ArcGIS tool. As bathymetry for the sea for year 2007 and 2014 have been collected so bathymetry change over the year is also observed. Bathymetry change in the vicinity of Kuakata beach and shoreline change are inter related to each which will be critically discussed in the subsequent article.

4.2.1 Historical Shoreline Change

Kuakata beach is 24 Kilometer long. The whole Kuakata beach can be subdivided into three parts by location. The western side is known as Lebur Char, the middle portion is known as Gangamatir Char and the eastern side is known as Kawar Char. The subdivisions of Kuakata beach are illustrated by **Figure 4.1**. In this study shoreline is subdivided into 24 divisions by 1 km chainage interval. Long term (10 years) shifting is measured in each chainage.

As it is mentioned earlier in Chapter 3 that all images are of 30 m resolution. All satellite images are downloaded with the assistance predicted tide by global tide model, essentially in dry season and low tide time which will give accurate coastline line position. Though 30 m resolution imageries can introduce up to 30 m erroneous result, yet it is acceptable for research purpose. Now a days 10 m resolution sentinel images are available by which coastline shifting assessment can be accomplished more correctly. Commercially available high-resolution images can also be used depending on the purpose.

Figure 4.1: Zonewise division along Kuakata beach
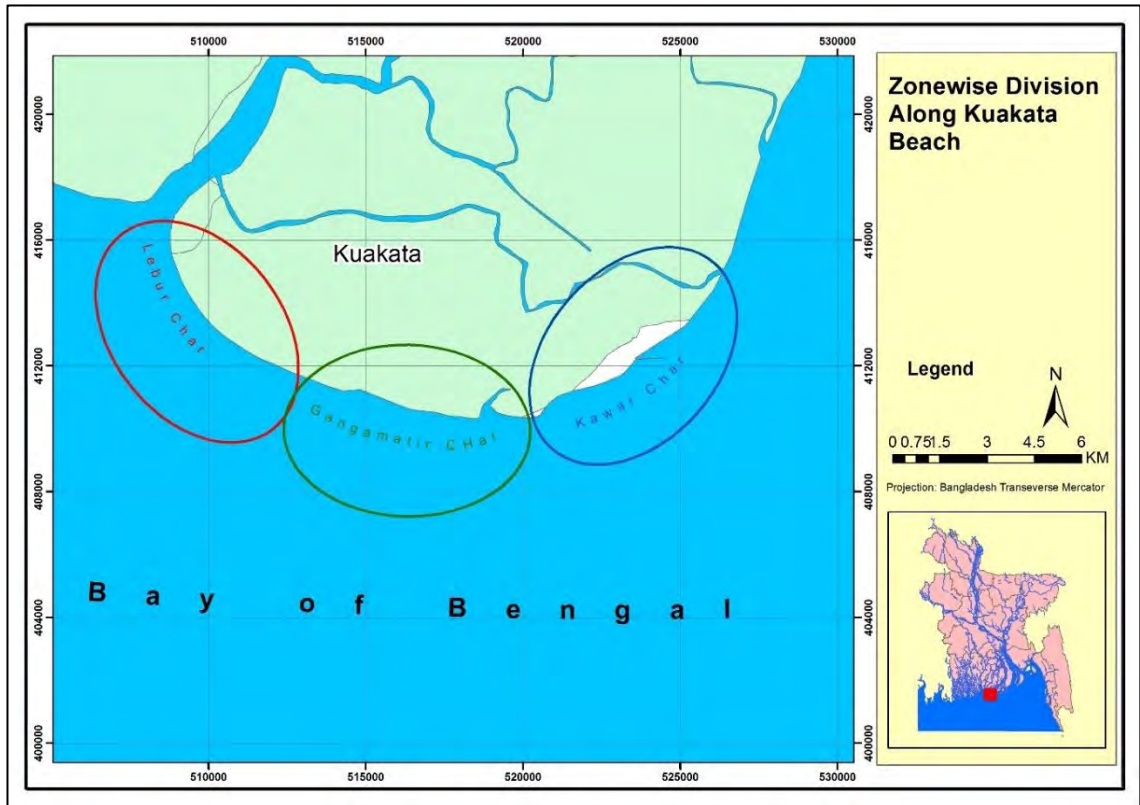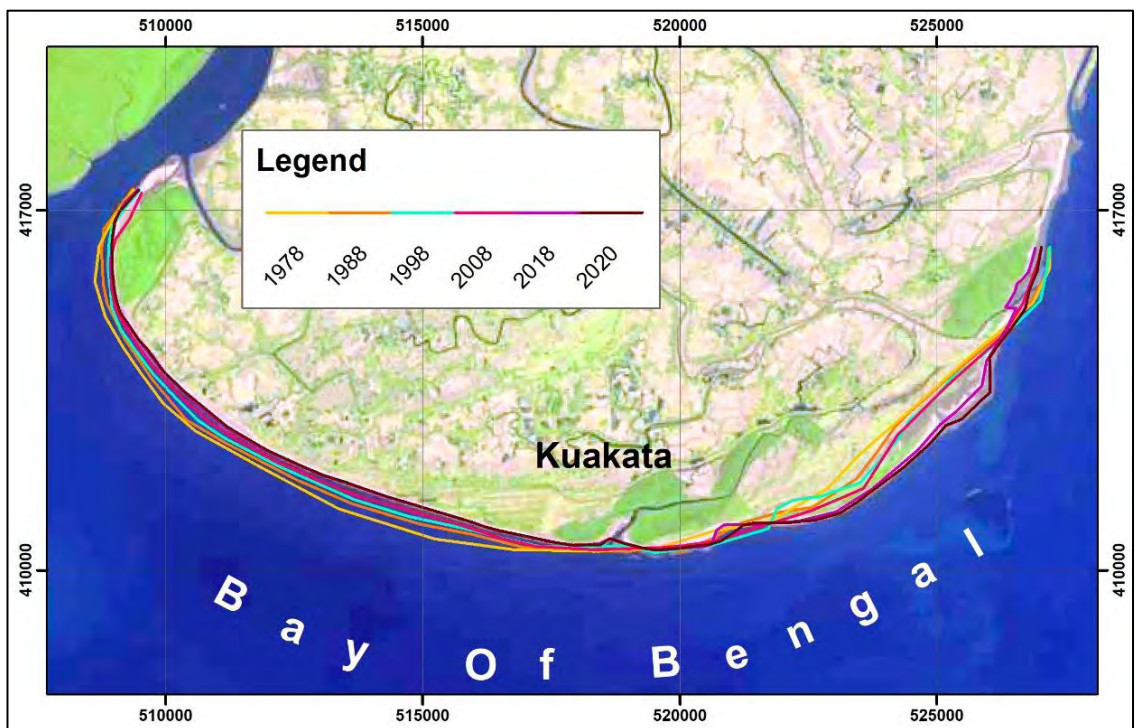

Figure 4.2: Coastline shifting (1978-2020) of Kuakata beach
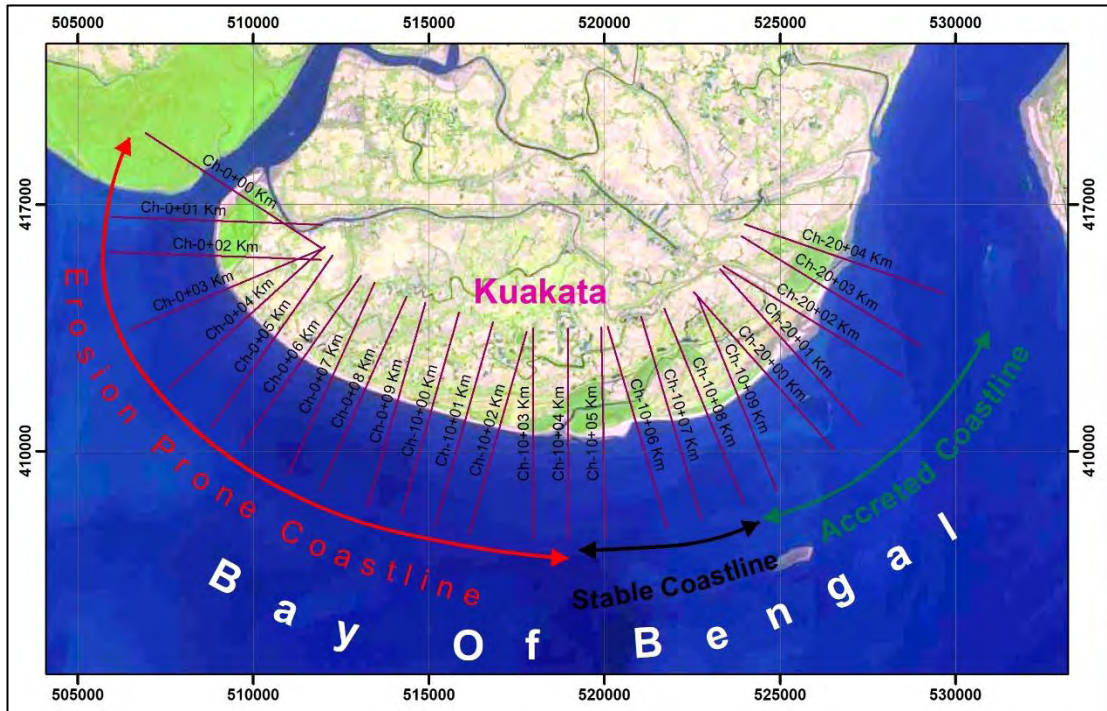
Figure 4.3: Erosion vulnerability of Kuakata beach with chainage
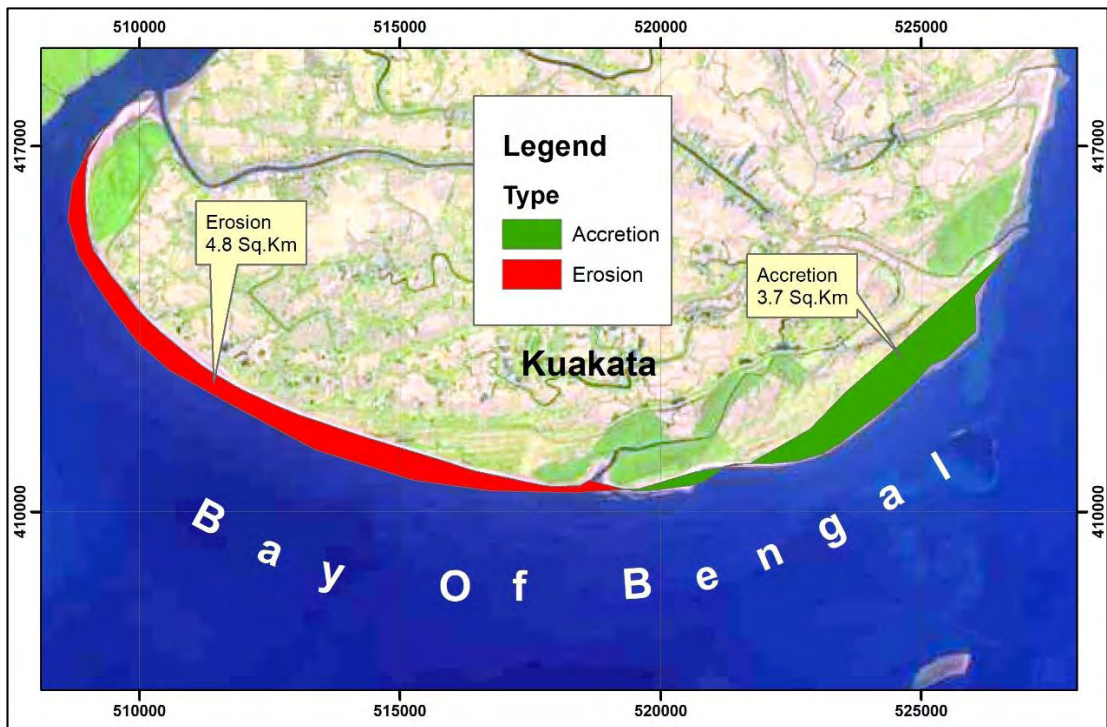
Figure 4.4: Total erosion and accretion of Kuakata beach

From the **Figure 4.3**. It is seen that left portion (Chainage-0 to chainage-13 km) is erosion prone coastline, Chainage 13 km to Chainage-17 km is more or less stable

85

over the time and Chainage-17 to Chainage-24 is accreted coastline.Total Erosion and accretion area have also been found out from 1978 to 2020. From **Figure 4.4** it is seen that 4.8 sq. km has been eroded and 3.7 sq. km has been accreted in 42 years. So, the erosion rate and accretion rate are 9 m/yr and 12.2 m/yr respectively. Though erosion area is higher than the accretion, but erosion rate is comparatively lesser than the accretion in Kawarchar area.

Table 4.1: Changes in shorelines in different locations

Chainage (km)	Change (m) (1978-1988)	Change (m) (1988-1998)	Change (m) (1998-2008)	Change (m) (2008-2018)	Change (m) (2018-2020)
0	18	-117	-66	100	-7
1	45	-143	-170	116	-6
2	-150	-125	-30	-40	-9
3	-112	-31	-111	-62	-11
4	-105	-87	-100	-83	-5
5	-57	-153	-106	-111	-25
6	-91	-75	-85	-86	-28
7	-115	-72	-65	-107	-10
8	-171	-92	-68	-139	0
9	-184	-80	-90	-127	-6
10	-202	-92	-89	-128	-5
11	-186	-82	-20	-116	-6
12	-50	-77	0	-150	-3
13	0	-43	-33	-30	-4
14	22	-97	58	-91	3
15	192	-40	-71	50	-7
16	32	190	-64	-245	40
17	-80	0	163	25	0
18	172	-95	194	197	42
19	273	139	93	203	43
20	74	184	0	430	67
21	0	147	0	442	140
22	50	63	22	393	160
23	67	52	-41	0	63
24	-48	123	-286	-240	270

NB: Positive Value and Green Colour denotes Deposition and Negative Value and Red Color denotes Erosion.

From **Table 4.1** it is seen that erosion occurs at Lebur Char area which is up to chainage-13 km. In the middle portion or Gangamatir Char bankline is bit dynamic, sometimes it is characterized by erosion and sometimes by accretion. In the east side of Kuakata, Kawar char, is characterized by accretion. Erosion rate is found from table for last 10 years is 11.7 m/yr where accretion in Kawarchar area is 21.2 m/yr.

4.2.2 Historical Bathymetry Change

Bathymetry of Kuakata beach area has been collected for two years. Bathymetric data for 2007 from C-Map and for year 2014 from GEBCO are superimposed on each other. Using bathymetry data 2007 a raster surface is created by IDW tool of GIS and same thing is done for GEBCO bathymetry data for the year 2014. Raster of 2007 is subtracted from the raster 2014 by raster calculator in GIS which eventually results another new raster and represents the bathymetry change in seven years in the vicinity of Kuakata beach.
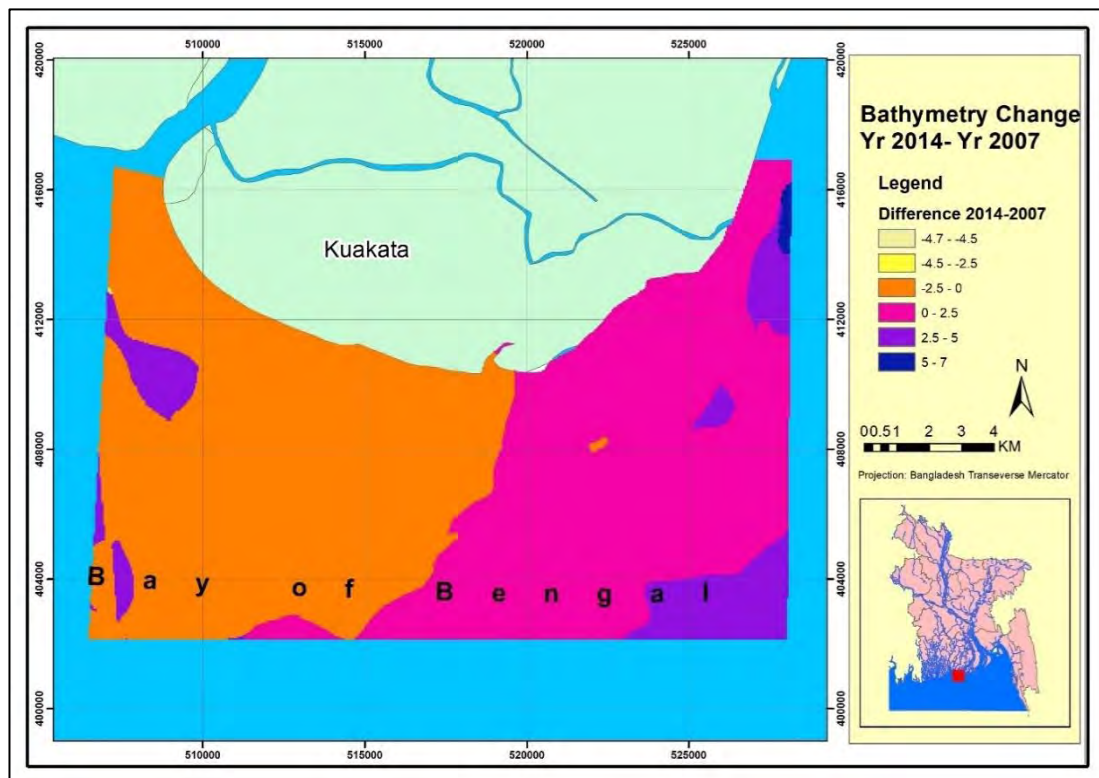

Figure 4.5: Bathymetry change year 2014- year 2007 in the vicinity of Kuakata beach

From the **Figure 4.5** it is identified that negative value indicates erosion whereas positive value indicates deposition. So, it can be said that western side is dominated by negative value and thus vulnerable to erosion which is shown by yellow color. On the other hand, eastern side is dominated by positive value and thus inclined to deposition phenomena which is shown by pink color. From the bathymetry change it is evident that in the western side of the beach erosion is occurring and on the other hand in eastern side sedimentation occurs which also conforms the result of satellite images analysis.

From historical satellite images analysis, it can be concluded that significant amount of erosion is occurring in the western Kuakata beach and deposition occurs in eastern part which confirms with bathymetry changes of the beach including nearshore. Maximum erosion occurs 202 m and maximum deposition occurs up to 442 m over different decade.

4.3   Nearshore Wave-tide Hydrodynamics

It is very important to analyze the current and wave properties to understand the reasons behind the coastal erosion at Kuakata beach area. Current direction and speed in different water level condition, current rose analysis from HD model and wave rose analysis from wave model result file will determine whether longshore or cross shore current is dominant in Kuakata. Moreover, current directions and magnitudes due to combined effect of tide and wave (i.e., coupled HD model with wave radiation stress) for both ebb tide and flood tide were analyzed for the existing condition (without incorporating protective structures) for different periods of the year 2017. The results from the simulations helped to understand the existing governing nearshore hydrodynamic conditions in the study area. This section will accomplish the 2nd objective of the study.

4.3.1   Current Analysis from HD Model Result

Current analysis has been carried out for three different periods like monsoon, dry and normal period. For every period water level was found out. Four points have been identified in water level hydrograph in day. Point-1 is identified as when water level

move from low tide to high tide. Point-2 is identified as when water level is in equilibrium condition (low tide to high tide). Point-3 is identified as when water level move from high tide to low tide and point-4 is identified as when water level is in equilibrium condition (high tide to low tide). These are illustrated in **Figure 4.6** and **Figure 4.7**.Current direction and speed were extracted in the vicinity of Kuakata beach for every point. It is found that for point-1 and point-2, the current direction is eastward and for point-3 and point-4 current direction is westward.
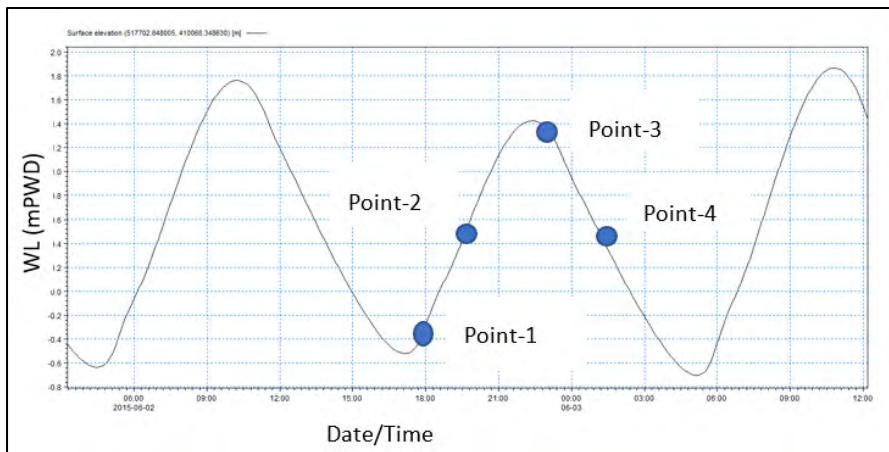
Figure 4.6: Current direction and speed at Kuakata Nearshore in monsoon period at different water level condition

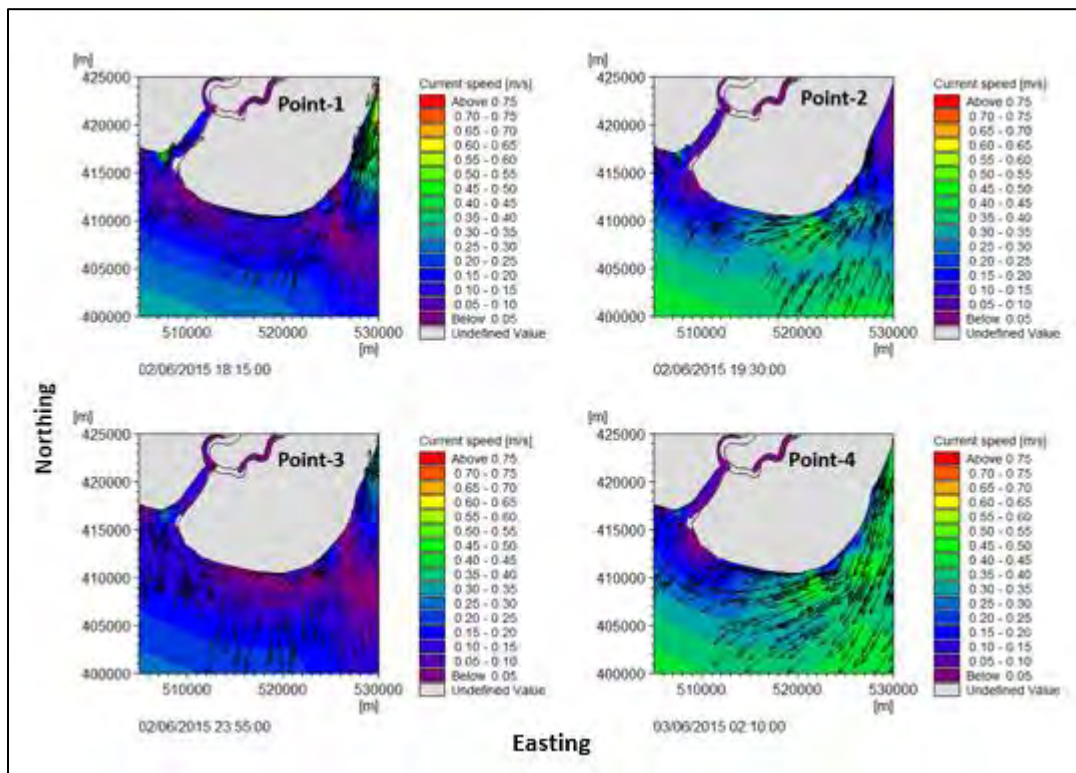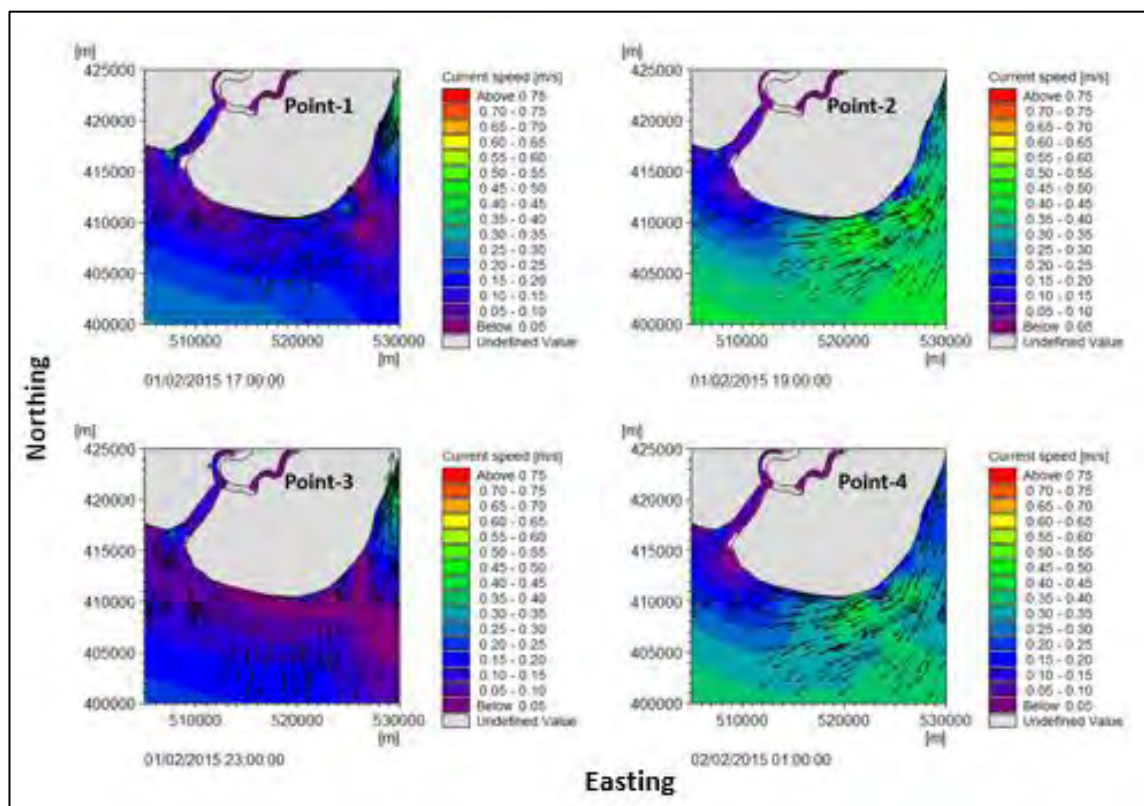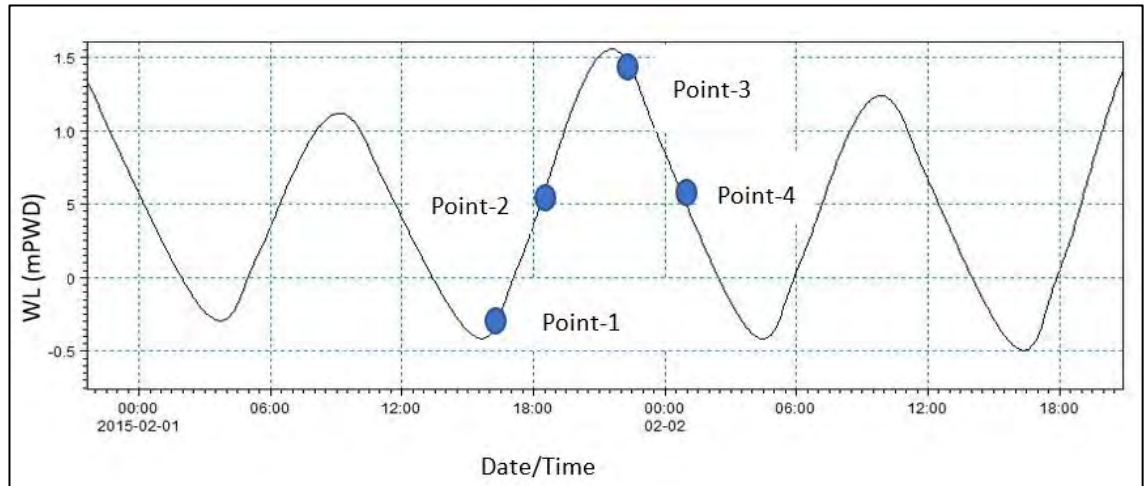**Figure 4.7: Current direction and speed at Kuakata nearshore in dry period at different water level condition**

It is because of the presence of tide is there and which is semi diurnal. It is also found from the analysis that eastward current speed is higher than westward current speed. So, sediment moves toward right, which means sediment transport occurs Lebur Char to Kawar Char.

In Data view manager of MIKE, there is a statistical analysis tool which show the maximum current speed in the Kuakata beach area.

4.3.2 Current Rose Analysis

From one-year hydrodynamic result file current speed and direction data are extracted in three different point. By plot composer tool of MIKE current roses are prepared for the study area which is shown in the **Figure 4.8**. There extraction points (i.e., point-1, point-2 and point-3) are shown in the map (**Figure 4.8**). This current rose for point-1 is in left portion of the beach which is marked by red dot on the map. Here eastward current is dominant. Current rose for point-2 is for the middle portion of the beach. Here current is in both directions. But in eastward direction current speed is higher. This current rose indicates that most of the currents are slightly angular to left direction in a year. We will see later, there will be very little annul drift in westward direction.
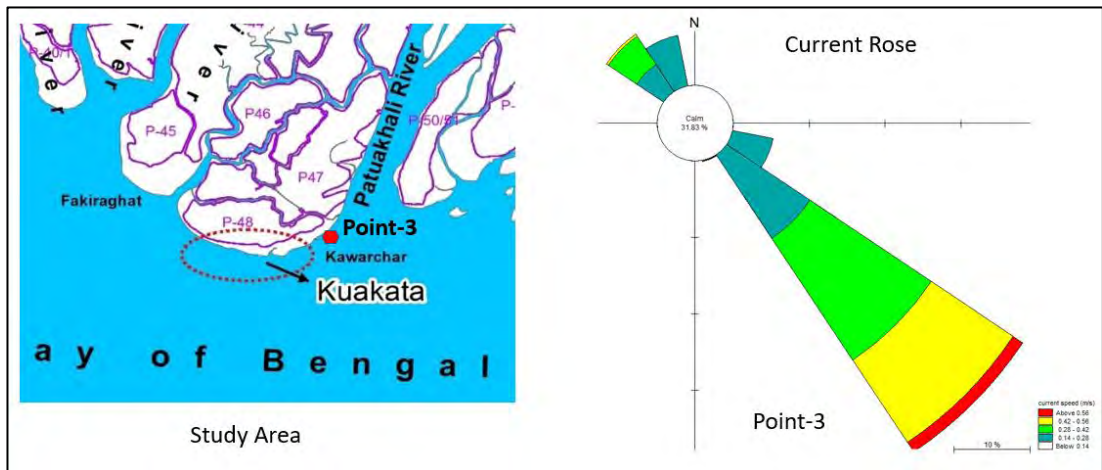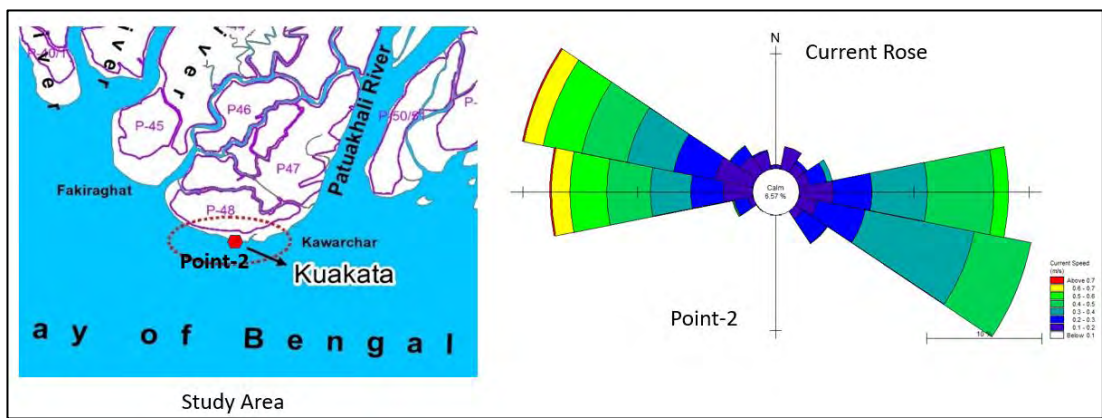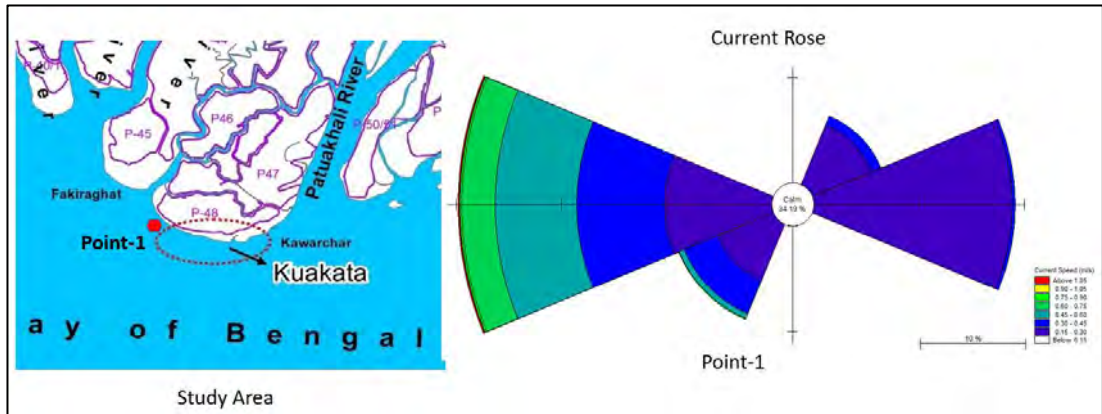
Figure 4.8: Current Rose at different location of the beach (i.e., Point-1, Point-2 and Point-3 shown on the left map)

4.3.3 Wave Rose Analysis from Wave Model Result

Waveroses are prepared from wave model result. The components of making a waverose are significant wave height and mean wave direction. From Plot Composer of MIKE waverose can be prepared. Wave result is extracted in three different location i.e. transect no. 2,4 and 6. From waverose analysis or pattern it is found that most of the waves come angularly and hit the beach. It is also found that right ward angular waves is more prominent which is also a indicator of transporting sediment more than the left.
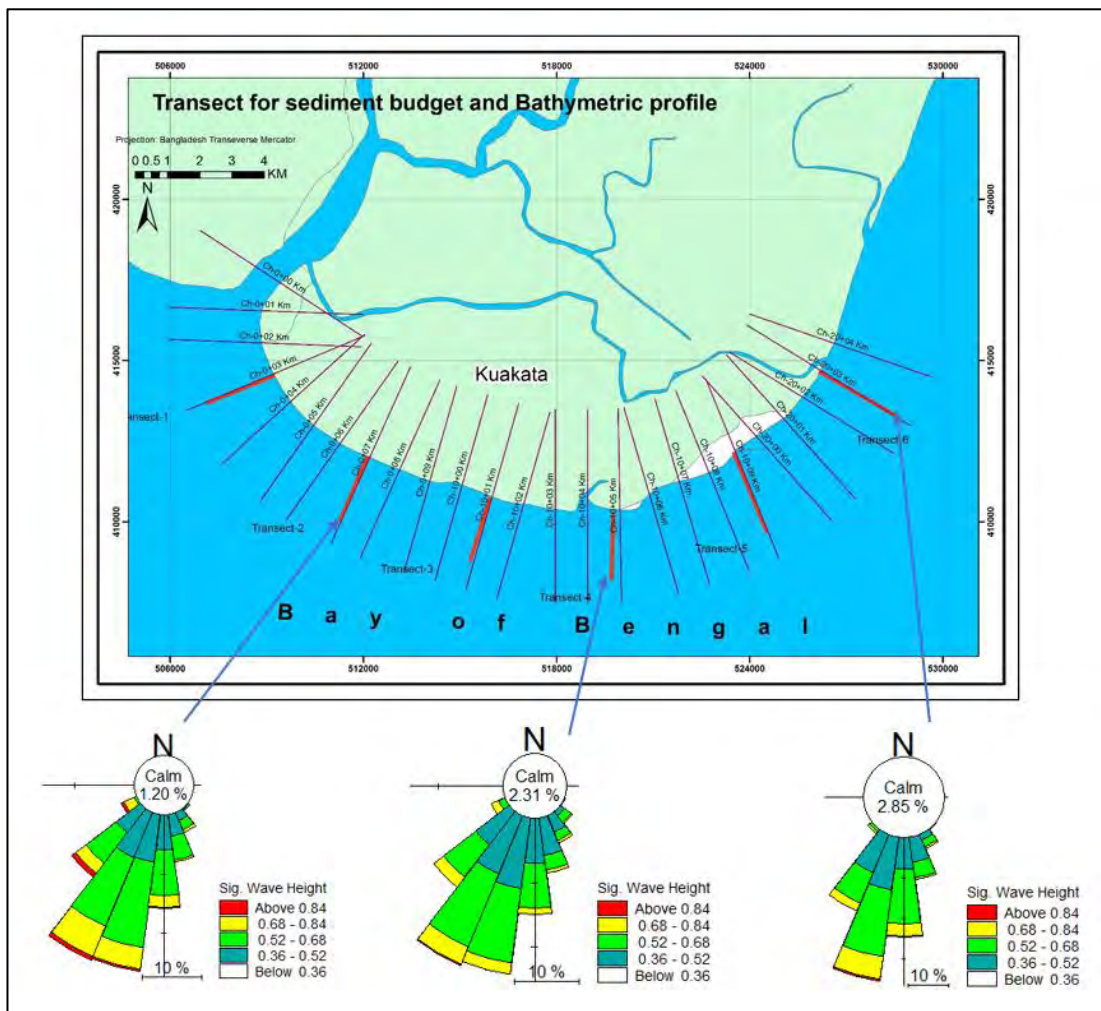
Figure 4.9: wave rose at different location, at transect no. 2,4 & 6

4.3.4 Current Speed Diagram Analysis

Current speed diagrams for Kuakata nearshore are prepared from hydrodynamic result file for spring tide and with wave action which shown in figure **Figure 4.10**. Tide and seasonal information are marked on each diagram. If we couple wave with HD model (i.e., incorporate wave radiation stress in pure tide model) current speed increases (**Figure 4.10**). In monsoon flood tide current speed varies 1.65 m/s to 1.95 m/s and ebb tide varies 0.3 m/s to 1.2 m/s. on the other hand for dry season flood tide current speed 0.6 to 1.8 m/s and ebb tide current speed varies from 0.1 m/s to 1 m/s.

By statistical tool of MIKE data manager maximum current speed and bed shear stress are found out for Kuakata nearshore in different wave and tide condition which are shown in the **Table 4.2**. Bed shear stress increases with the increase of current speed. During Flood tide current direction is eastward and during ebb tide current direction is left ward. Flood tide always govern here to cause longshore littoral transport to eastward (i.e., to east direction).
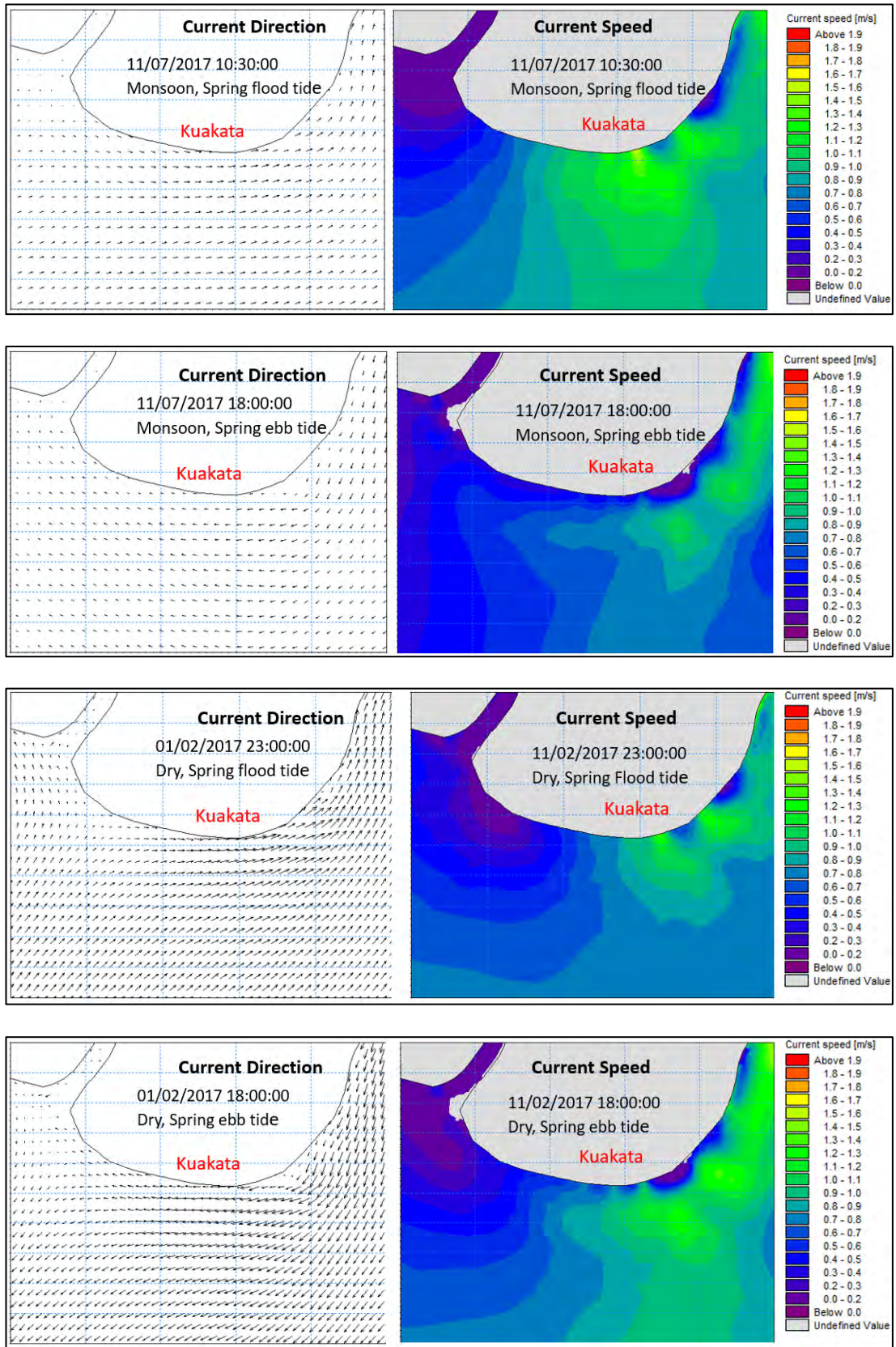
Figure 4.10: Current speed diagram with wave action at spring tide

Table 4.2: Maximum speed and maximum bed shear stress matrix

Season	Wave condition	Tide condition	Max Current speed(m/s)	Max bed shear stress (N/m²)
Dry (February-2017)	without	flood	0.8	1.4
		ebb	0.1	0.01
	with	flood	1.1	1.7
		ebb	0.2	0.1
Monsoon (July-2017)	without	flood	0.95	1.7
		ebb	0.15	0.05
	with	flood	**1.2**	**2.8**
		ebb	0.25	0.17

From the above **Table 4.2**, for spring tide, monsoon flood tide is with wave condition is governing for longshore current. Maximum current speed and Maximum bed shear stress are 1.2 m/s and 2.8 N/m², respectively.

It can be concluded from the above article 4.3 that current speed and direction for different water level condition and current speed analysis confirms that eastward (i.e., to east) littoral transport occurs. Current rose and wave rose analysis confirms longshore current is dominant in Kuakata. Wet season flood tide with wave action during spring tide is the governing situation for littoral transport. Bed shear stress increases with increase on current speed. Maximum current speed increases as we go offshore from the beach consequently maximum bed shear stress follow the same.

4.4   Assessment of Longshore Sediment Transport

The littoral transport has been calculated by the model LITDRIFT for a number of coastal profiles distributed along the coast which is described in the previous section. The littoral drift has been determined for the actual orientation of the coastline and for a range of different coastline orientations in order to find the sensitivity of the transport to variations in the coastline orientation and the dominant wave direction estimated from the wave simulations by MIKE21 SW. The calculations have also determined

the 'equilibrium orientation' of the coastline for each profile, which indicates how much the coastline will change its orientation if the transport rate is to be reduced considerably by coastal protection structures like groynes, and thereby make it possible to make an estimate of how long and/or how closely spaced protection structures would have to be in order to be effective.

Littoral drift model is simulated for four years (from 01/01/2015 to 31/12/2018). For getting better result litdrift model should be simulated at least for 4 years which is a prerequisite. Timeseries of wave climate at the end of a transect is extracted from the wave model result and given as input in the litdrift model which is essentially a dfso file. Sediment properties (D50) is given as 0.2 mm and other sediment properties are assumed based previous literature. By data extraction tool of MIKE cross-shore profile is generated along the transect which given in the input in the litdrift model as dfs1 file. Cross-shore profile, sediment properties, coastline orientation and model development are illustrated in the previous chapter 3.

The main results from the sediment transport estimation are shown in the **Figure 4.11**. It is observed that for transect-1, transect-2, transect-3 and transect-4 longshore sediment transport is toward east direction and found different value for each transect. And for transect-5 and transect-6 longshore sediment transport is toward west direction and here also found different value for each transect. The westward sediment transport is very low compared to eastward sediment transport. As eastward transport higher than the westward transport, the net sediment transport will be from western side to eastern side along the beach through the transect. Maximum erosion occurs in between transect-2 and transect-3 amounts 73,001 m^3 and maximum deposition occurs in between transect-4 and transect-5 amounts 226,094 m^3 which is explained in the **Figure 4.12**. Maximum littoral transport is found in transect-4 amounts 216,136 m^3/year. It is also evident that total amount of sediment that eroding from Lebur Char area is depositing in the eastern side and apart from that some sediment flow from the upstream also enters the system and being deposited in the eastern side of Kuakata.
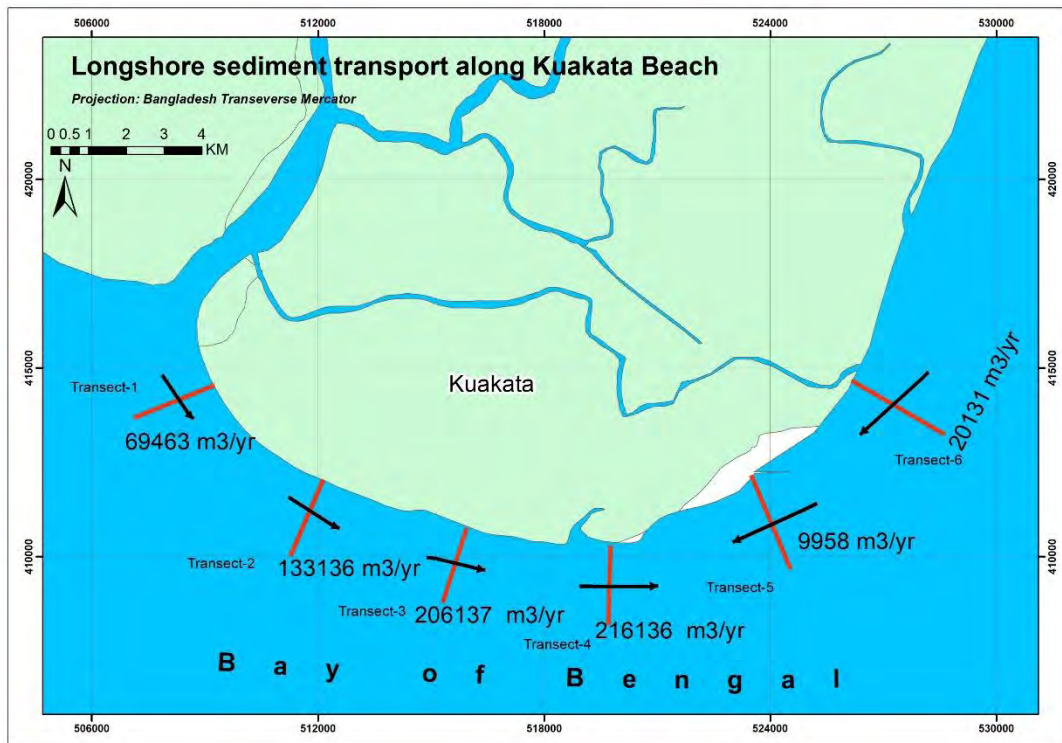
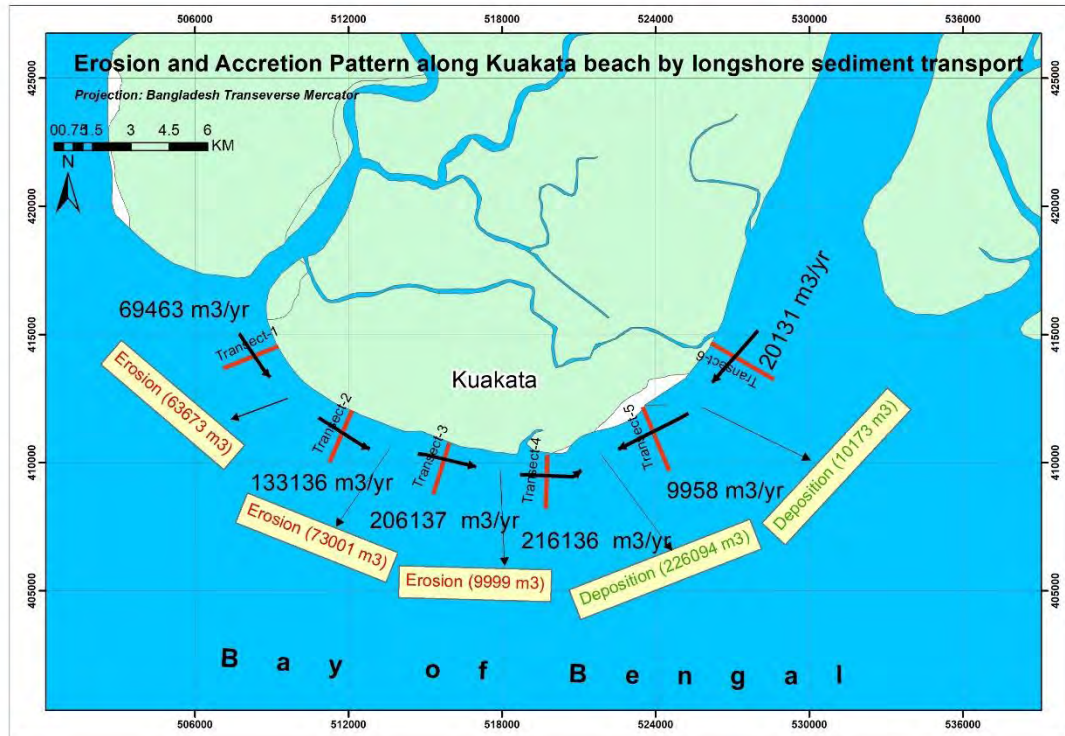**Figure 4.11: Yearly longshore sediment transport along Kuakata beach**

Figure 4.12: Erosion and accretion pattern by annual littoral transport along Kuakata beach

4.4.1 Calculation of Longshore Sediment Transport Using Empirical Equation

Several empirical formulas have developed by different authors and organizations like CERC (1984), Kamphuis (1991), Van Rijn (1993) and many others. Among them CERC and Kamphuis formula are popular. Here longshore sediment transport is estimated manually using these two formulas and Comparison is made with model result.

CERC Formula:

CERC (1984) suggests various methods of deriving longshore sediment transport rates for a site, including using the known transport rate at nearby site, measured sediment volume changes between two bathymetric surveys of the site or use the CERC formula for potential sediment transport. The CERC formula assumes that the longshore sediment transport rate depends on the longshore component of energy flux in the surf zone.

The CERC formula provides an estimate of the instantaneous (gross) sediment transport, ignoring the effects of currents and onshore-offshore processes. It should be noted that longshore sediment transport rates derived using the CERC formulation provide at best an order-of-magnitude estimate of the sediment transport, as there is considerable scatter in reported estimates of the dimensionless K value and as the formulation does not take the effect of wave period into account in the calculations.

The CERC formula is given by:

$$Q = \frac{K}{(\rho_s - \rho)ga'}P_{ls} \tag{4-1}$$

Where,

Q = Longshore sediment transport rate
K = dimensionless empirical coefficient, related to sediment grain size
ρ_s = sediment density
ρ = water density
g = acceleration due to gravity
a' = solids fraction of the in-situ sediment deposit (1-porosity)

and the longshore component of energy flux in the surf zone is given by:

$$P_{ls} = \frac{\rho g}{16} H_{sb}^2 C_{gb} \sin(2\theta_b)$$ **(4-2)**

Where

H_{sb} = nearshore breaking height of significant wave

C_{gb} = wave group speed at breaking

θ_b = angle breaking wave crest makes with shoreline

In shallow water,

$$C_{gb} = \sqrt{g d_b}$$ **(4-3)**

Where,

d_b = depth of wave breaking, which is assumed to be related to the wave breaking height $H_b = 0.78 d_b$

The values for the parameters in the CERC formula are given below:

The median grain size of sediment (D_{50}) in the surf zone at Kuakata beach from previous literature is found to be 0.20 mm. From Coastal Engineering Manual (2003), an empirically based value for K is around 0.9, based on the median grain size $D_{50} =$ 0.20 mm using **Figure 4.13**.
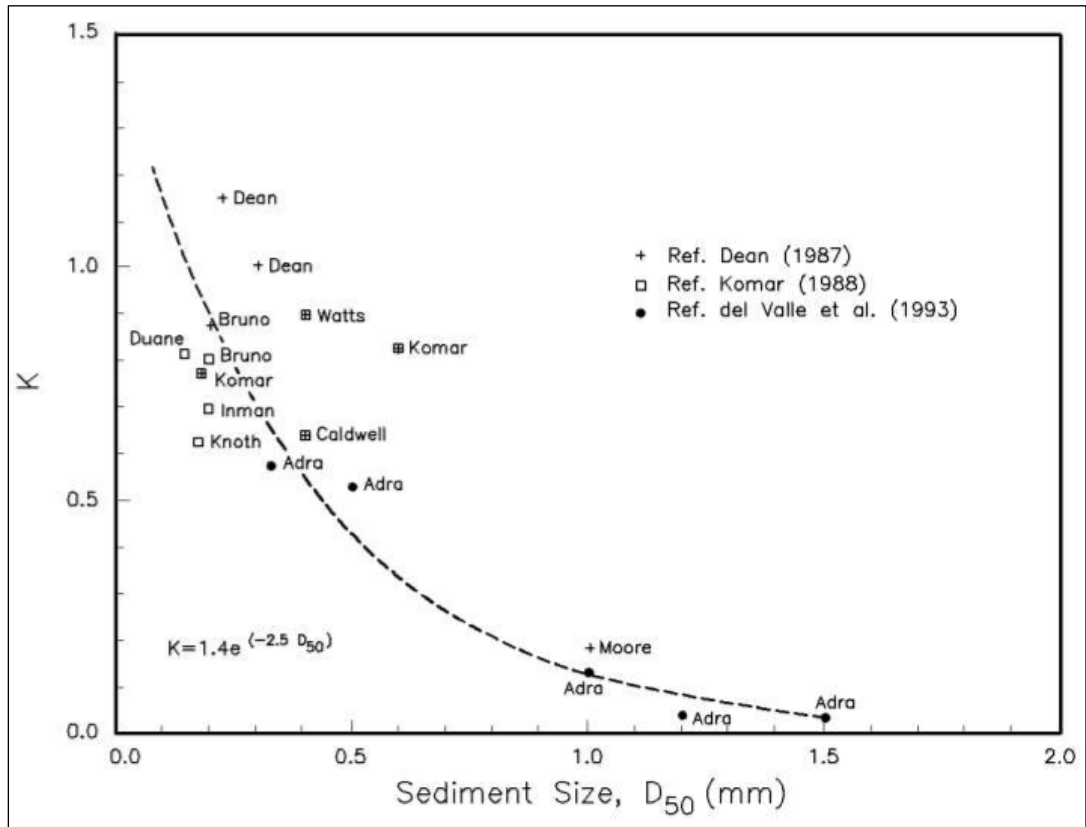
Figure 4.13: Determination of value of K parameter in CERC sediment transport formula (Source: Coastal Engineering Manual,2003)

ρ_s = sediment density=2650 kg/m^3

g   = acceleration due to gravity =9.81 m^2/s

a   = 1- porosity, Porosity of a typical beach berm is around 40% so a = 0.6

It is seen from model or wave rose analysis, Lebur Char to Gangamatir Char (i.e., transect 1, 2, 3 and 4) and Kawar Char to Gangamatir Char (i.e., transect 5 & 6) has opposite pattern of longshore sediment transport. From the wave model result file wave climate is extracted near transect 2. Breaking wave height can be calculated giving some input data showing in the **Figure 4.14**.

Figure 4.14: Online Surf wave Calculator (Source: https://swellbeat.com/wave-calculator/)

Water depth is given from 2D hydrodynamic result file near transect 2. Thus, H$_{sb}$ is found out.

C$_{gb}$ = wave group speed at breaking, which varies with the wave height in accordance with above equation. We get the value of C$_{gb}$ is 2.74.

θ$_b$ = angle breaking wave crest makes with the shoreline= $42.25^0 - 40^0 = 2.25^0$

P$_{ls}$ = ((1025*9.81)/16)*0.6^2*2.74*sin(2*2.25^0) =48.64

Q = (0.9/((2650-1025)*9.81*0.6))*48.64= 0.0045 m^3/s = .0045*1230*24*60*60= 142,327 m^3/yr

Kamphuis Formula:

For comparison purposes, the sediment transport direction and relative magnitude is also evaluated using the Kamphuis (1991) expression. This expression is based on an extensive series of hydraulic model tests and depends on breaking wave height, wave period, grain size, nearshore beach slope and nearshore wave approach angle. The expression is given by:

$$Q_k = (6.4x10^4)H_{sb}^2 T_{op}^{1.5} m_b^{0.75} D^{-0.25} sin(2\alpha_b)^{0.6} \qquad \textbf{(4-4)}$$

Where,

Q_k = sediment transport rate, m³/year

H_{sb} = breaking wave height

T_{op} = wave period

M_b = nearshore beach gradient

D = sediment grainsize (i.e., 0.20 mm according to previous literature)

α_b = angle breaking wave crest makes with the shoreline

If data used for the same location in the domain, following longshore sediment transport is found using above equation.

$Q_k = 6.4*10^4*0.6^{2}*8^{1.5}*0.0167^{0.75}*.0002^{-0.25}*\sin (2*2.25)^{0.6} = 127,227$ m³/yr

Kamphuis (1991) method also shows that the main potential is for sediment transport from west to east direction. It is noted that the Kamphuis equation takes into account wave period, which is not a parameter used by the CERC equation.

Kamphuis formula estimates lower littoral drift compared to CERC formula. Values are close to net sediment transport estimated from the model which validates the model result to some extent.

4.4.2   Longshore Sediment Transport by Bathymetry Data

In practical case it is difficult or cumbersome job to measure the actual longshore sediment transport through a cross-shore profile or a transect. But techniques or technologies are available to measure the transport which is very time consuming and high cost is also involved which can be found in literature review. Another way is there to verify the model estimated littoral transport or longshore sediment transport by comparing two set of bathymetry data (if available) of different time period in the nearshore area up to the depth of closure. This method is widely used to verify the LITDRIFT model. In this study, volume of erosion and accretion have been calculated

by GIS tool using bathymetry of 2007 known as C-map and the bathymetry of 2014 downloaded from GEBCO. So, the erosion and accretion volume in 7 years are found 1.3 Mm^3 and 1.5 Mm^3 respectively. From the model we get the net sediment transport transect-2 is 133,136 m^3/year Total erosion and accretion are found from littoral transport model is 146,673 m^3/year and 236,267 m^3/year. So, in 7 years erosion and deposition will be 1.03 Mm^3 and 1.65 Mm^3. Thus, the littoral drift model can be verified. Erosion-deposition volume is shown in the **Figure 4.15** .

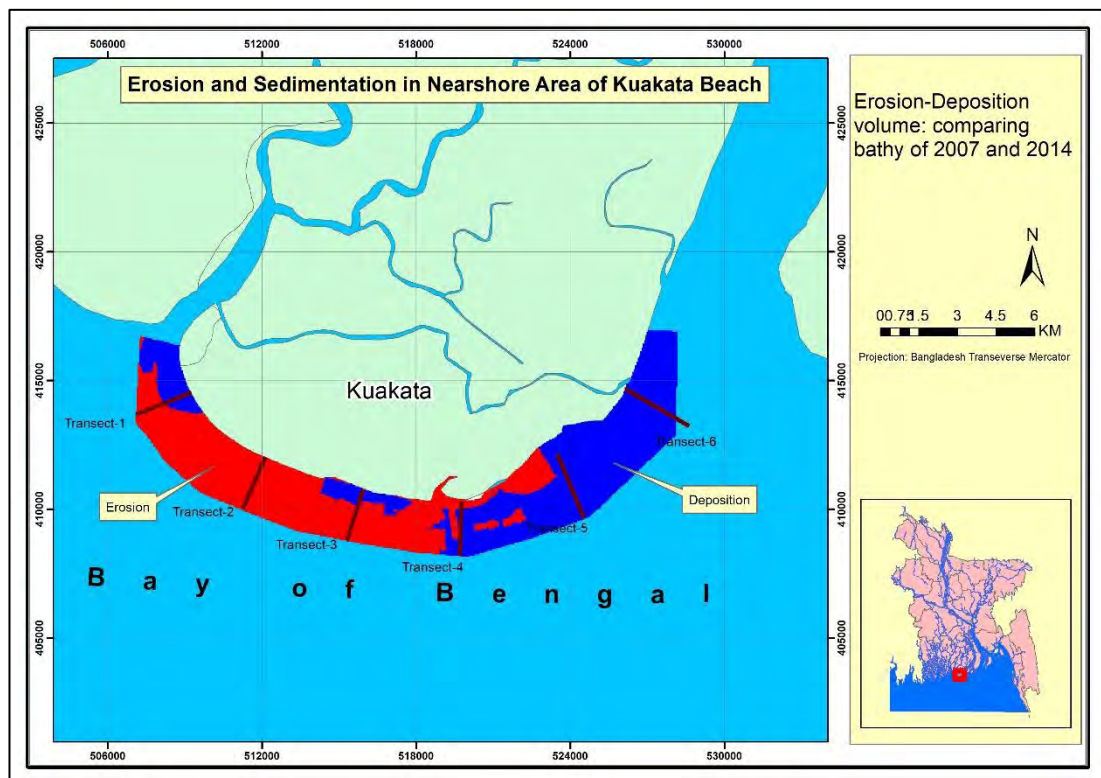**Figure 4.15: Volume calculation by bathymetry comparison in nearshore area of Kuakata beach using GEBCO bathy data of the year 2007 and 2014**

4.4.3   Comparison of Longshore Sediment Transport Obtained by Various Methods

So, we can compute longshore sediment transport for a coastline by different methods but data requirement to find out littoral transport varies method wise.   CERC or

Kamphuis does not provide us the accurate estimation for littoral drift always, but it can be helpful to have an idea. Using bathymetry comparison in nearshore area or the area up to the transect end (depth of closure) longshore sediment transport can be found out with promising result. Based on bathymetry comparison result litdrift model is calibrated to some extent. But most of the time bathymetry is not available for different year then we have to rely on manual calculation (i.e., CERC, Kamphuis, Van Rijn). The comparison of longshore sediment transport by different methods are illustrated by the bar chart in following **Figure 4.16**.
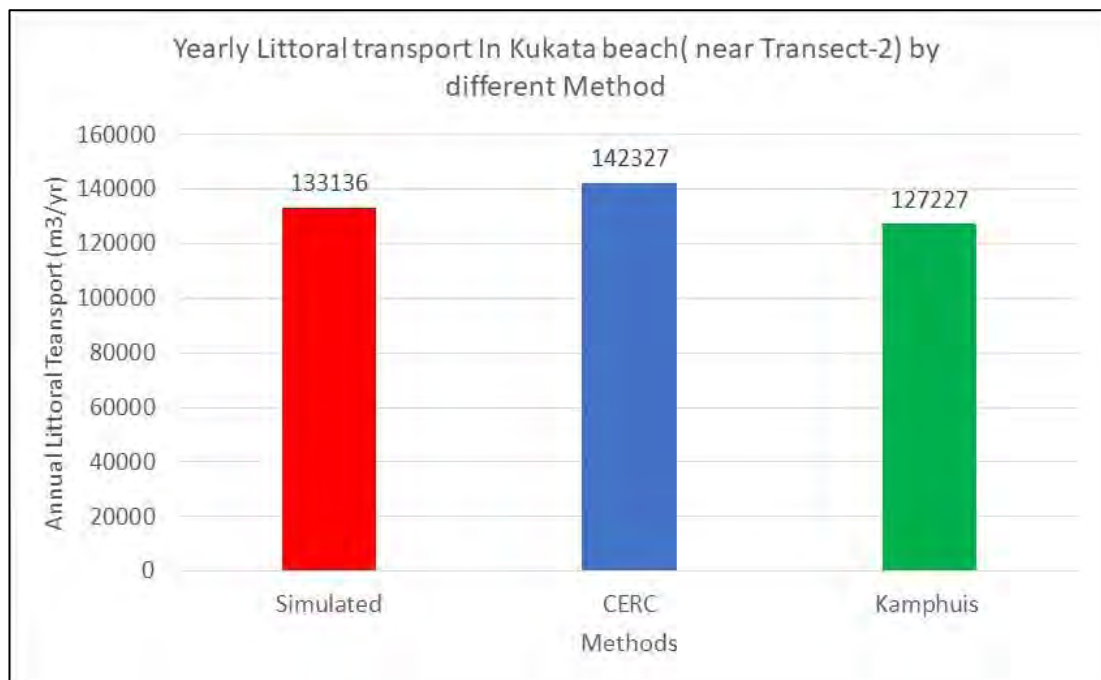
Figure 4.16: Comparison of simulated longshore sediment transport along Kukata beach with empirical method

So, it can be concluded that there is a significant longshore sediment transport along Kuakata beach which is the prime cause of erosion. Series of groyne can be constructed to arrest this transport, thus combat erosion. As tourism is very important for Kuakata beach, from aesthetic point of view any hard structure like groyne or breakwater might not be permissible. As a result, soft measurement could be undertaken rather than hard structure. In that case beach nourishment can be a good

idea to protect the beach from erosion. Estimated annual longshore drift can gives idea about the requirement of beach nourishment for the beach.

4.4.4 Seasonal Variation of Longshore Sediment Transport

One hydrological year is divided into three seasons for convenience. These are pre-monsoon (January-May), post-monsoon (June-September), and Post-monsoon (October-December). There must be upstream flow variation for different season. There is also impact of seasons in wave climate in the near shore which is the prime reason for longshore sediment transport. The simulation period of LITDRIFT model is 01/01/2015 to 31/12/2018 (i.e., 4 years). Output of the LITDRIFT model provides us timeseries of longshore sediment transport so we get the littoral transport in every time step, and we get accumulation of longshore sediment transport as well. Copying the result from the output (dfso file) into excel, the analysis of seasonal variation of longshore sediment transport.
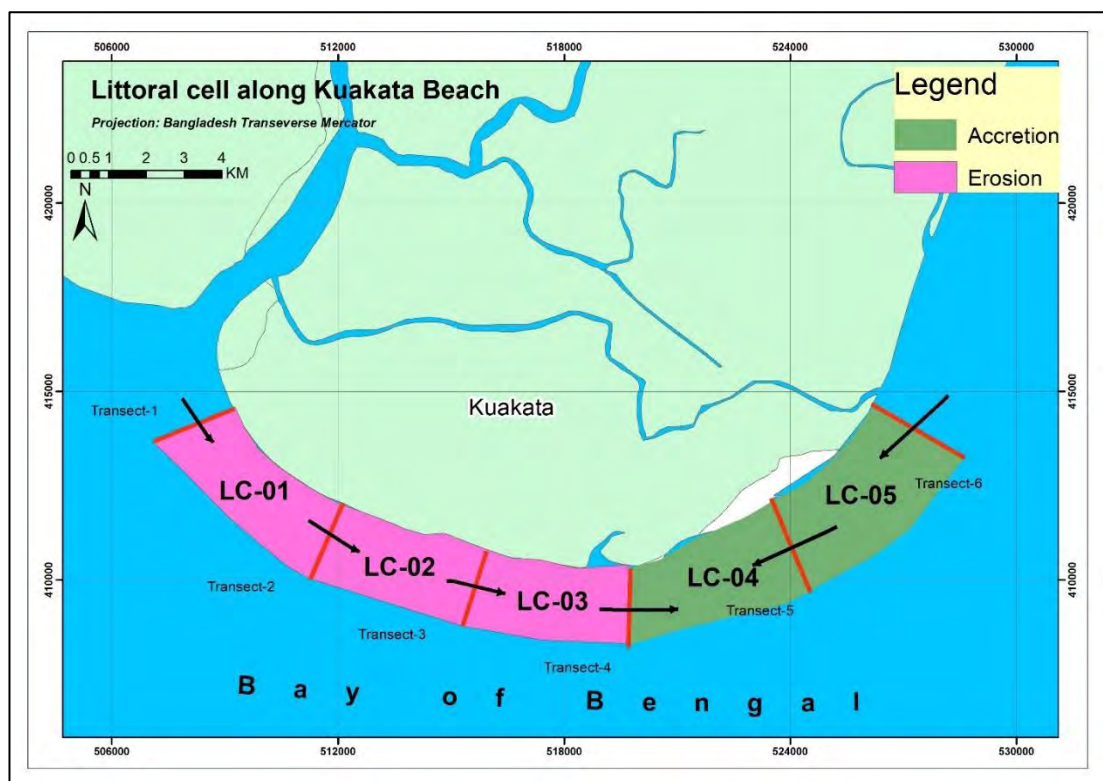

Figure 4.17: Littoral cell along Kuakata beach

As it is mentioned earlier that, here in Kuakata beach 6 transects are considered. In each transect littoral annual longshore sediment transport is estimated from the model and erosion-accretion pattern are observed and verified with bathymetry and empirical methods of estimating longshore sediment transport. Segment in between 2 transects is called littoral cell. There are total 5 littoral cells (i.e., LC-01 to LC-05) as we see in the **Figure 4.17**. Litttoral cell are the portion or segment in between 2 transects where erosion or accretion will be dominant based on the water level condition, wave climate, tidal current and upstream flow. Littoral cell 01 to 03 (red marked) are located on the western side of Kuakata whereas in Littoral cell 04 and 05 are accretion dominant cell. Maximum erosion occurs per year at LC-02 (73,001 m^3) and Maximum accretion occurs per year at LC-04 (226,094 m^3). The amount of erosion-accretion volume is found from **Figure 4.12**.

Month wise longshore sediment transport for each transect have been calculated from LITDRIFT result file which is illustrated by

Table 4.3 and **Figure 4.18**. It is evident that considering all 6 transects, there is maximum net longshore sediment transport occurs in June (i.e., 138,087 m^3/month) whereas minimum net longshore sediment transport (1552 m^3/month) occurs in January. Total net LSTR is from west to east direction and estimated value is 5.94 x 10^5 m^3/year.

Table 4.3: Month wise variation of longshore sediment transport

Station	Longshore sediment transport rate (LSTR) in m³/month												Net LSTR (m³/year)	Gross LSTR (m³/year)
	Jan	Feb	Mar	Apr	May	Jun	Jul	Aug	Sep	Oct	Nov	Dec		
Transect-1	214	632	4371	10065	6640	15947	14900	9497	4360	1695	823	319	69463	76409
Transect-2	410	1212	8378	19291	12726	30565	28557	18202	8357	3249	1578	611	133136	141124
Transect-3	634	1876	12972	29868	19704	47325	44216	28183	12939	5030	2443	946	206137	218505
Transect-4	665	1967	13601	31317	20660	49620	46361	29550	13567	5274	2562	992	216136	216136
Transect-5	-123	-364	-1010	-1530	-1046	-1777	-1421	-1066	-187	-721	-370	-343	-9958	9958
Transect-6	-249	-736	-2042	-3092	-2114	-3593	-2873	-2156	-378	-1457	-748	-693	-20131	21741
Net (m3)	1552	4589	36271	85919	56570	138087	129739	82209	38658	13069	6289	1832	594783	683874

Yearly longshore sediment transport is shown in the **Figure 4.19**. The highest transport occurs at transect no. 4 (i.e., 216,136 m^3/year). **Figure 4.20** reveals the seasonal variation of longshore sediment transport. It is observed that there is huge impact of season in the longshore sediment transport.

Figure 4.18: **Monthly longshore sediment transport rate along Kuakata beach**

Yearly longshore sediment transport is shown in the **Figure 4.19**. The highest transport occurs at transect no. 4 (i.e., 216,136 m^3/year).
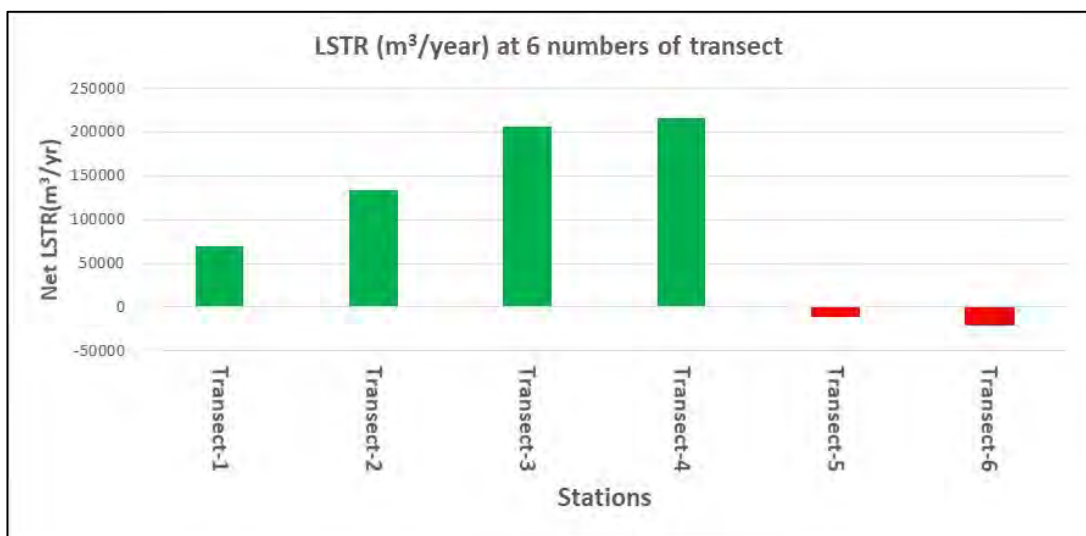
Figure 4.19: Net longshore sediment transport rate at each transect

Figure 4.20 reveals the seasonal variation of longshore sediment transport. It is observed that there is huge impact of season in the longshore sediment transpo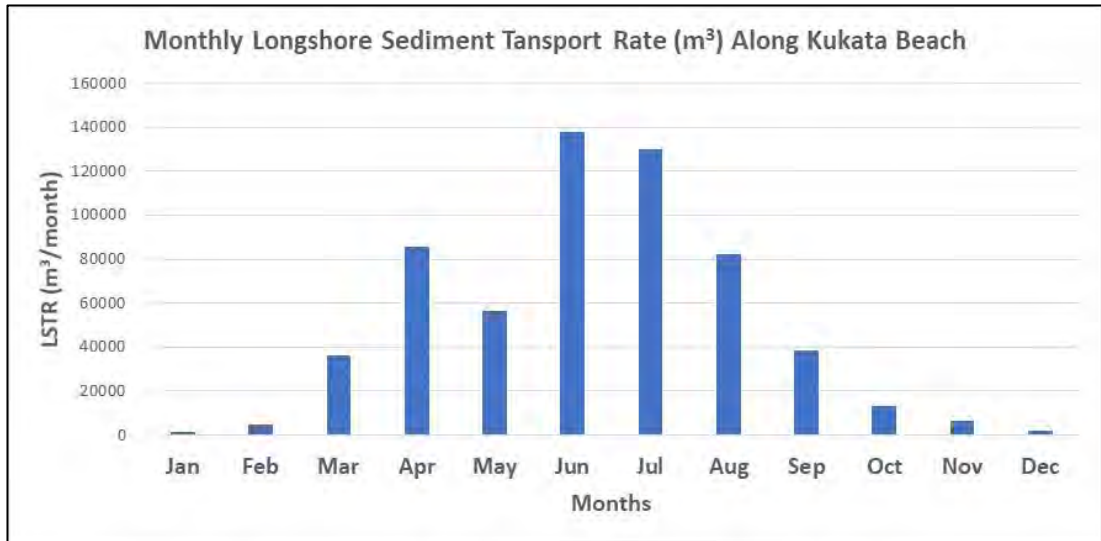rt. From the **Figure 4.20**, it is seen that maximum transport occurs at monsoon season, minimum transport occurs at post-monsoon and moderate amount of transport occurs at pre monsoon season. Seasonal longshore sediment transport for pre monsoon,
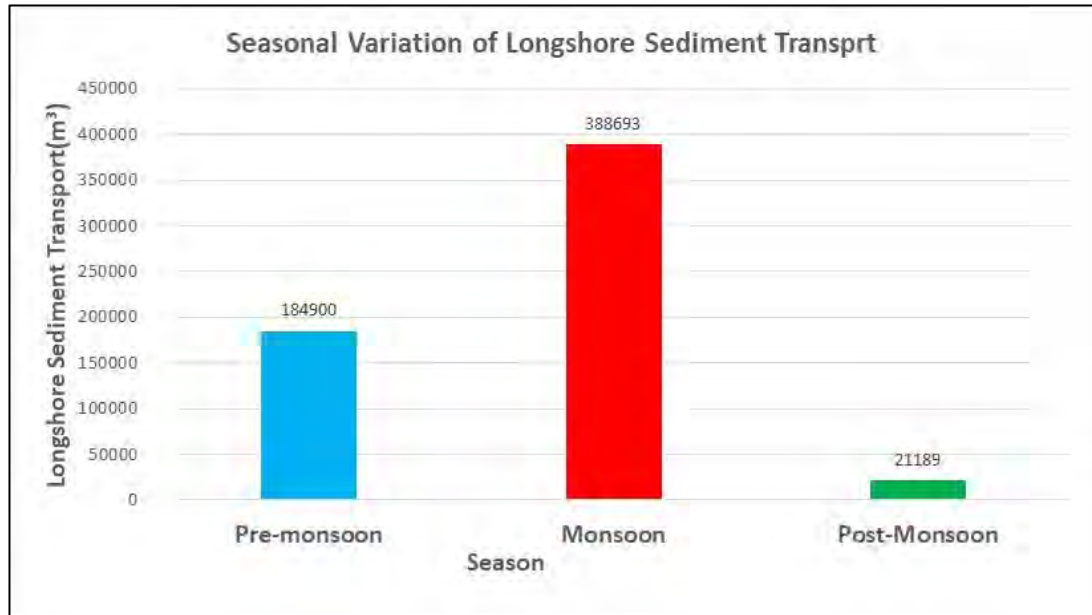
Figure 4.20: Seasonal variation of longshore sediment transport

monsoon and post monsoon are 184,900 m^3; 388,693 m^3 and 21,189 m^3 are respectively. So, it can be concluded that during monsoon nearshore is more susceptible to longshore sediment transport, hence beach will likely be eroded in monsoon.

4.5   Shoreline Evolution Using LITLINE Model Simulation

The objective no. 4 of this study was to simulate the shoreline evolution along the study area using LITLINE model which will be verified with real time coastline position for a particular year. In this section, it has been described.

Coastline evolution or LITLINE model is simulated over the time period 02-01-2010 to 01-01-2019 (i.e., for 9 years). Time step interval is considered as 3600 sec or 1 hour and real time formulation is checked. Under morphology module **Include morphology calculation** is check marked. Update scheme is given as update continuously. Under active profile section height of the active beach is assumed to be 3 m. For active depth baseline.dfs1 is given and active depth is shown accordingly. A dfs1 file is obtained as output of the model which indicate the beach position from the baseline at each time step. The output or result file is shown in the **Figure 4.21**.
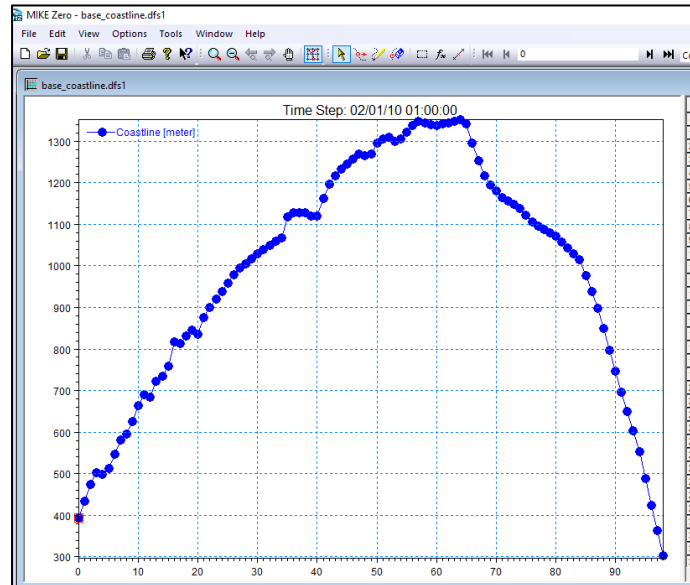
Figure 4.21: Simulated beach position (output of LITLINE model)

Baseline, initial coastline, and simulated coastline are illustrated in the **Figure 4.22**. It is observed that coastline is moving landward causing significant amount erosion in eastern side (Lebur Char area). The movement of coastline in the middle portion is not that prominent as like Lebur Char area. Erosion-accretion analysis by satellite images also confirms this phenomenon.
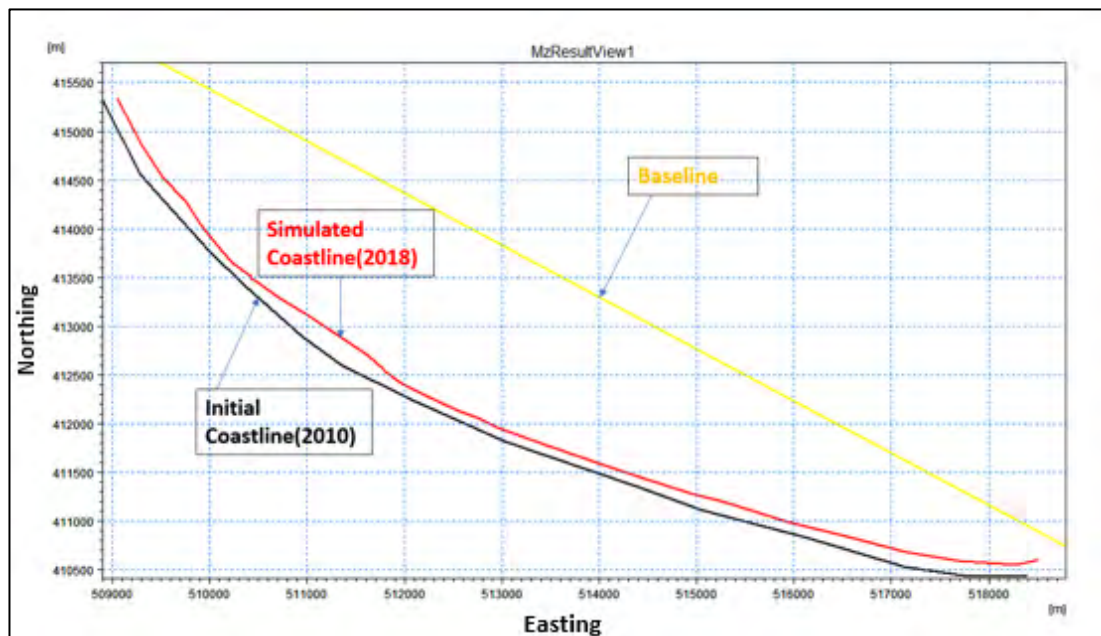
Figure 4.22: Baseline, initial coastline and simulated coastline

From LITLINE model result file it is possible to observe the beach position at any time step of any year whereas it could be done by analyzing satellite images with the aid of GIS tool also which is more accurate but cumbersome job.

4.5.1 Verification of LITLINE Model

The LITLINE model is calibrated for the year 2018 and validated for the year 2016 by Sentinel-2 satellite imageries. Sentinal-2 satellite images are found from year 2016 with high resolution (10 x10 m) compared to LANDSAT satellite images. It is good have high resolution images for calibration and validation purpose of LITLINE model. From USGS Sentinel-2 satellite images for dry season (clear image found for the month March) of mentioned year have been downloaded.

To calibrate and validate the coastline evolution model or LITLINE model, actual shoreline of Kuakata beach is digitized from satellite image of the year 2018 and 2016 by ArcGIS tool. Then it is superimposed in the Result Viewer of MIKE Zero with the simulated coastline by the model.
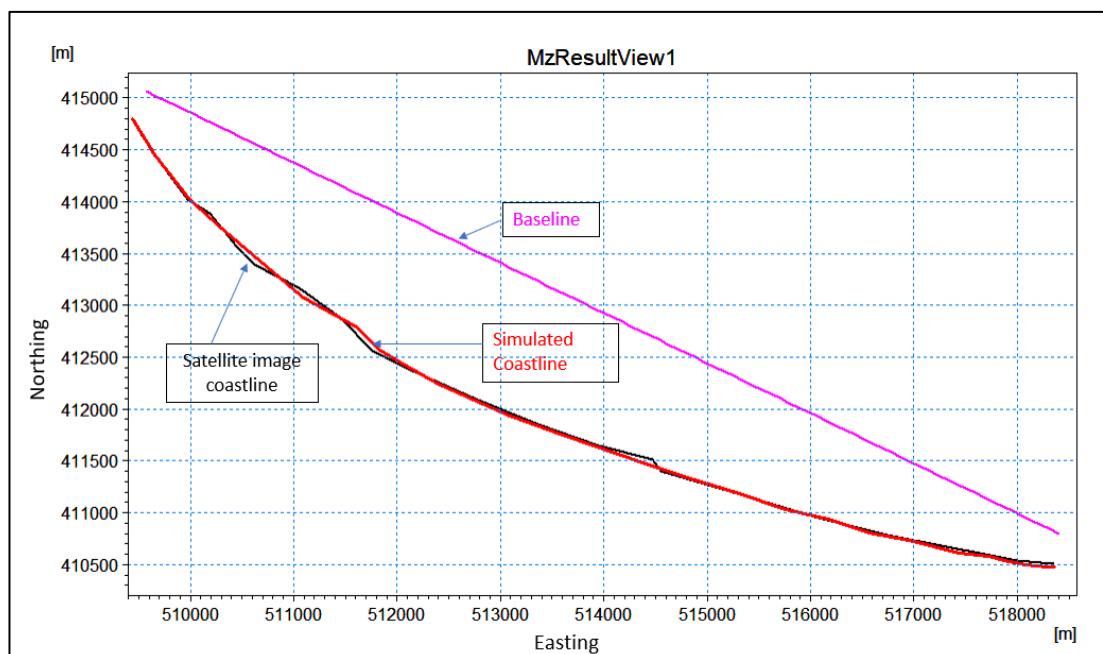
Figure 4.23: Calibration of LITLINE model for the year 2018
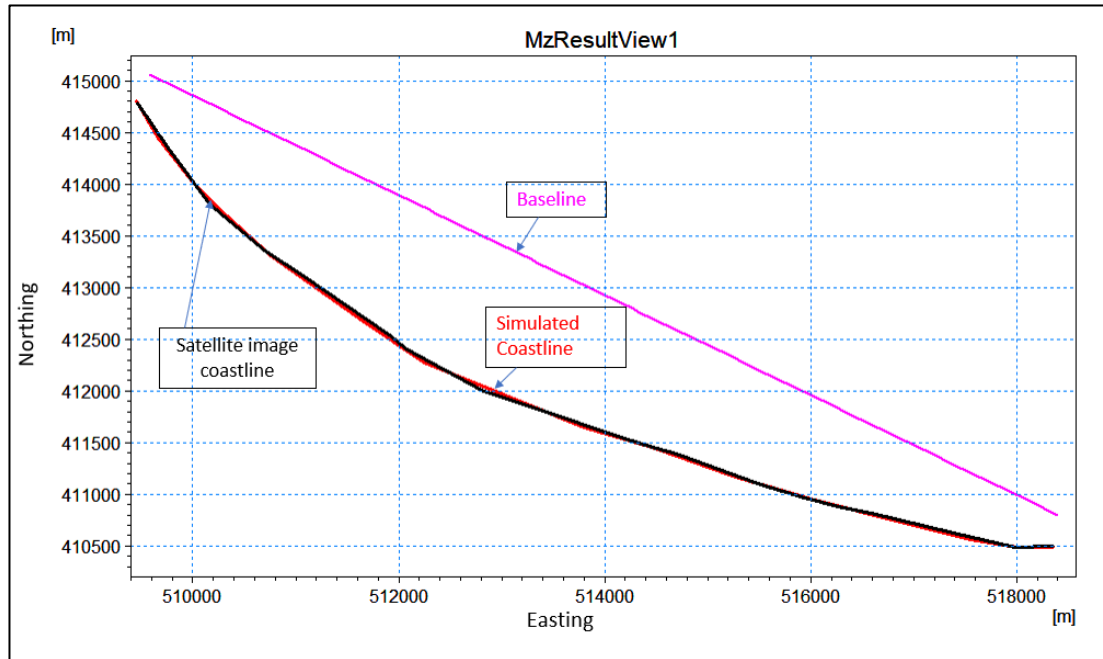
Figure 4.24: Validation of LITLINE model for the year 2016

The calibration and validation of the LITLINE model are shown in the following **Figure 4.23** and **Figure 4.24** which imply quite satisfactory model result. After calibration and validation of Litline model. A long-term simulation (i.e., 9 years) of beach position is conducted for erosion prone area only, the simulated beach position is shown in the **Figure 4.25**. It is observed from the simulation result that maximum erosion occurs 240 m in 9 years shown by circle on the map and other places erosion varies 100 to 145 m over simulation period.
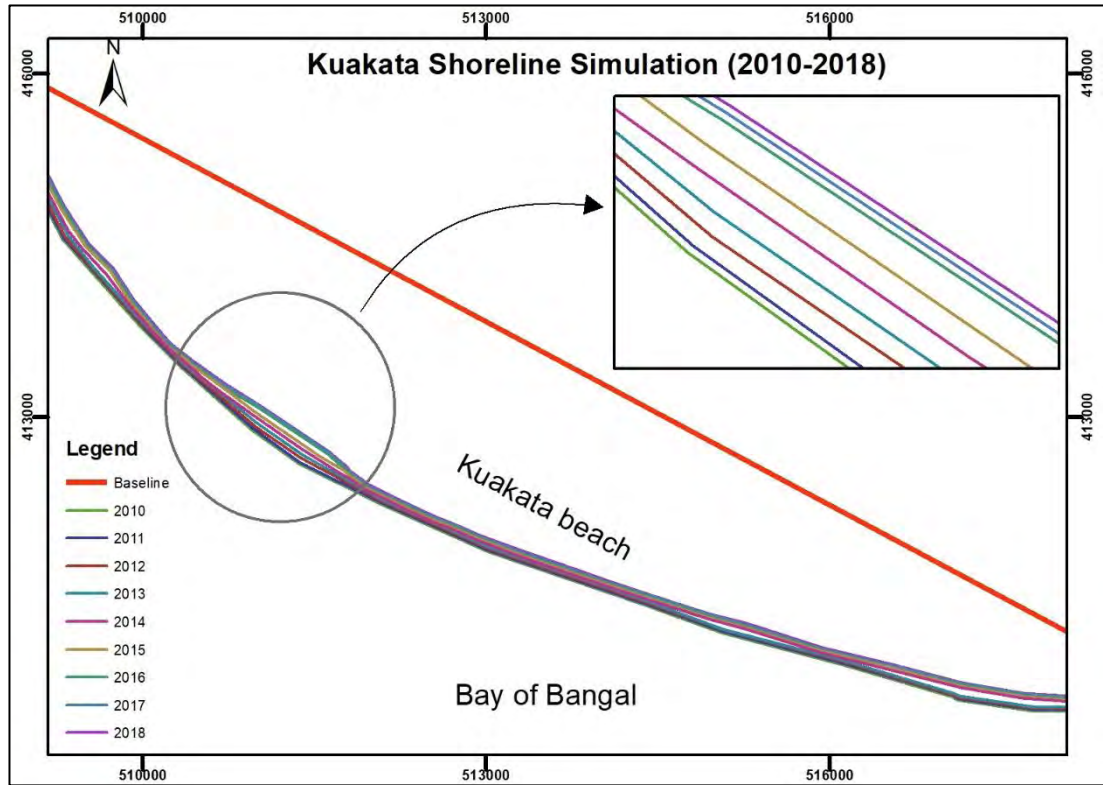
Figure 4.25: Simulated shoreline position along Kuakata beach using LITLINE model for period 2010 to 2018

4.5.2 Prediction of Future Shoreline in Eroding Zone

To predict or simulate future shoreline we require future wave climate data. And to have future wave climate data we require future wave field, wind field and tide level. Global tide model provides tide level at any geographical point on the sea at any time based on the tidal constituents.
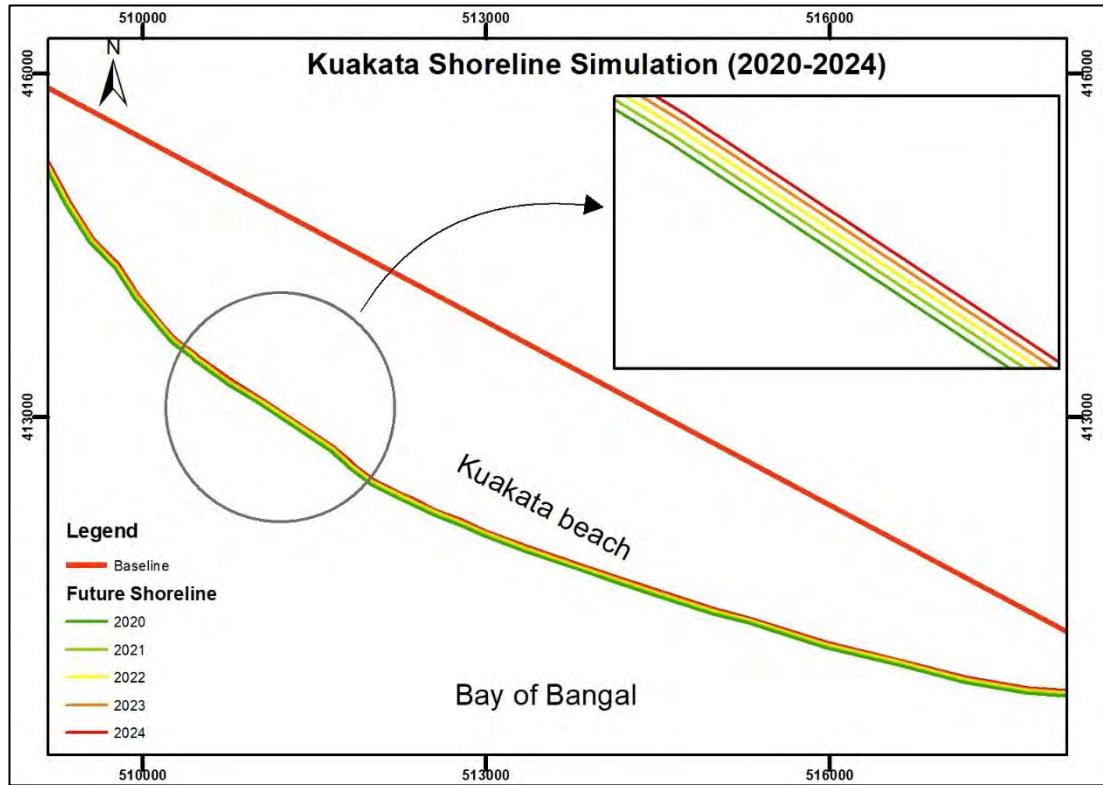
Figure 4.26: Future shoreline simulation (2020-2024)

But for future wave field and wind field data, it is not possible to have. If we make assumption that last 5 years wave climate will prevail for next 5 years in the study area, then changing the time series of wave climate to future we can predict future shoreline for next five years.

Shoreline evolution model can be used more effectively beach morphology study incorporating structures in the model (i.e., groyne and breakwater). Special technique is to be adopted to predict or simulate future shoreline. It is estimated for future shoreline simulation that shoreline will move further 9.6 m/year in next 5 years.

4.6   Summary of the Results

Following major findings have been found from this study:

i.   By satellite images analysis, amount erosion and accretion in the Kuakata beach are quantified. By using bank line of year-1978 and year-2020 erosion is 4.8 km^2 and accretion is 3.7 km^2. Most of the erosion occurred in Lebur Char area and accretion occurred in Kawar Char area.

ii.   Long-term (10 years) bankline shifting has been also analyzed. It is seen that chainage 0+00 to chainage 13 km (west part of beach) is erosion prone coastline. Chainage 13 Km to chainage-17 km is more or less stable coastline which is the middle portion of the kuakata. And in rest of the part (i.e., chainage-17 km to Chainage-24, east part) sedimentation occurs.

iii.   Chainage wise changes of shorelines in different location have been estimated. Erosion rate is found from analysis for last 10 years is 11.7 m/yr where accretion in Kawarchar area is 21.2 m/yr.

iv.   From 2D hydrodynamic model current analysis is done in the vicinity of Kuakata beach two seasons like monsoon and dry period. In four scenarios current direction and magnitude is observed in a day in monsoon and dry season. It is seen that current direction is eastward at starting point of flood tide and equilibrium condition during flood tide. It is also seen that current direction is westward at starting point of ebb tide and equilibrium condition during ebb tide because of tidal characteristics of the sea. During flood tide current direction is eastward and during ebb tide current direction is westward. The magnitude of eastward current is higher than westward current, so sediment is transported from west to east. Maximum current speed and Bed shear stress occurs during monsoon spring flood tide considering wave action and values are 1.2 m/s and 2.8 N/m^2, respectively.

v.   From wave roses it is seen that most of the time wave direction is eastward in angel. That means longshore current is dominant. Sediment is transported from west to eastward. Current rose prepared from HD model also conforms the same.

vi.   Result from the wave model is used in LITDRIFT model. Longshore sediment transport is calculated from LITDRIFT model which is shown in previous chapter. The overall net sediment transport or resultant transport is eastward. 5.94×10^5 m^3/yr sediment transport is seen eastward. Total amount of erosion and accretion are 1.46×10^5 m^3 and 2.36×10^5 m^3 per year which is justified with bathymetry data of Kukata beach area.

vii.   By coastline evolution model, it is also observed that up to chainage 13 km shoreline is eroding with time and it is verified with real satellite images

coastline where same wave climate is used as in littoral drift model which confirms the accuracy of longshore sediment transport estimation. Shorelines of Kuakata are simulated from the year 2020 to 2024. During this period further migrating of shoreline is predicted as 48 m towards the land.

CHAPTER FIVE

CONCLUSION AND RECOMMENDATION

5.1   General

Erosion and accretion along Kuakata beach have been analysed by Landsat satellite images. 4 (four) types of models have been used in this study. These are 2D hydrodynamic model, wave model, littoral drift model and coastline evolution model (LITLINE). Wave model is coupled with hydrodynamic model. Result from wave model is used in littoral drift model and LITLINE model. Eventually from littoral drift model sediment budget is estimated and from LITLINE model shoreline changes along beach are observed.

5.2   Conclusion

Following major findings have been found from the current study:

1. Around 13 km western side of Kuakata beach (i.e., Lebur Char) faces serious erosion and on the other hand 7 km eastern side (i.e., Kawar Char) accretes over the last 4 decades which is found from historical satellite images.

2. A dedicated hydrodynamic and a wave model are setup, calibrated and validated for the Kuakata study area and nearshore wave-tide hydrodynamics analyzed. It is found that longshore current governs in the nearshore of Kuakata and wet season, spring tide, flood tide with wave action is the governing condition for littoral transport.

3. Longshore sediment transport is estimated from LITDRIFT model. It is seen that overall net longshore sediment transport is 5.94×10^5 m^3/yr towards east. Erosion occurs at Lebur Char area is 1.46×10^5 m^3/yr and deposition occurs at Kawar Char area is 2.36×10^5 m^3/yr.

4. Coastline evolution model simulated for eroding western side of Kuakata beach and it is verified with real satellite images coastline where same wave climate

is used as in littoral drift model which conforms the accuracy of longshore sediment transport estimation. At the same time future shoreline simulation is done where it is seen that eroding beach will erode further at 9.6 m/yr.

5.3 Recommendation

Based on this study some recommendations have been summarized below:

1. As we know the dominant current direction and wave direction in the Kuakata beach, mainly longshore current occurs here. Groynes can be incorporated in the model. Nearshore hydraulics can be studied after incorporating groyne in the hydrodynamic and wave model.

2. Kuakata beach morphology study can be done incorporating series of groynes in the coastline evolution model (LITLINE) and different options or scenarios can be analyzed with further studies.

3. Beach nourishment study can further be enhanced using littoral drift model result of this thesis work.

4. Coarser bathymetry is used from C-map and GEBCO in the vicinity of Kuakata beach. Better result can be expected if fine bathymetry would be used. Further study can be carried out using fine bathymetry (if available) and compared with present result.

REFERENCES

Appendini, C.M., Salles, P., Mendoza, E.T., and Lopez, J. (2012), "Longshore sediment transport on the Northern Coast of the Yucatan Peninsula", *Journal of Caoastal Research*, Vol. 28 (6), pp. 1404–1417.

Ariya, D.S., Kori, S., and Vaidya, A.M. (2013), "Simulation of shoreline changes along Muthalapozhy Harbour, India", *11th International Conference on Hydroinformatics.*

Bushra, N. (2013), "Detecting changes of shoreline at kuakata coast using RS-GIS techniques and participatory approach", *M.Sc. Thesis*, IWFM, BUET, Dhaka, Bangladeh.

Corbella, S. and Stretch, D. D. (2012), "Predicting coastal erosion trends using non-stationary statistics and process-based models", *Coastal Engineering*, Vol. 70, pp. 40-49.

DHI. (2017), *Scientific document and user guide on Littoral Process FM*, Danish Hydraulic Institute, Denmark.

DHI. (2017), *Scientific document and user guide on MIKE 21 FM,* Danish Hydraulic Institute, Denmark.

DHI. (2017), *Scientific document and user guide on MIKE 21 SW*, Danish Hydraulic Institute, Denmark.

Frihy, O. and Deabes, E. (2012), "Erosion chain reaction at El Alamein Resorts on the western Mediterranean coast of Egypt", *Coastal Engineering*, Vol. 69, pp. 13-18.

Haque, A. (2018), "A mathematical model study on the hydraulics for the design and construction of a closure in a tidal channel", *M.Sc. Engg. Thesis*, Department of Water Resources Engineering, BUET, Dhaka, Bangladesh.

Hendriyono, W., Wibowo, M., Hakim, B.A., and Istiyanto, D.C. (2015), "Modeling of sediment transport affecting the coastline changes due to infrastructures in Batang - Central Java, Procedia", *Earth and Planetary Science*, Vol. 14, pp. 166-178.

Hossain, S. (2015), "Assessment of sediment movement pattern along nearshore coastal water of cox's bazar", *M.Sc. Engg. Thesis*, Department of Water Resources Engineering, BUET, Dhaka, Bangladesh.

Islam, M.R. and Ahmad, M. (2004), *Living in the coast: Problems, opportunities and challenges*, Working Paper WP011, PDO-ICZMP, Dhaka

IWM. (2014), *Coastal hydraulic and morphological study and design of protection measures for marine drive road*, Institute of water modeling, Dhaka, Bangladesh.

José, M., Cáceres, A.I., Brocchini, V. M. and Baldock, T. E. (2012), "An experimental study on sediment transport and bed evolution under different swash zone morphological conditions", *Coastal Engineering*, Vol. 68, pp. 31- 43.

Nahiduzzaman, S. (2018), "Simulation of storm surge level at a tidal channel due to coastal cyclone along the Bangladesh coast", *M.Sc. Engg. Thesis*, Department of Water Resources Engineering, BUET**,** Dhaka, Bangadesh.

Noujas,V., and Thomas, K.V.(2018), "Shoreline management plan for a medium energy coast along west coast of India" *Journal of Coastal Conservation*, Vol. 22, pp. 695-707.

Paul, B. K. (2009), "Human injuries caused by Bangladesh's cyclone sidr: an empirical study", *Natural Hazards*, Vol. *54*(2), pp. 483-495.

Kobayashi, N., Agarwal, A. and Johnson, B. (2007), "Longshore current and sediment transport on beaches", *Journal of Waterway, Port, Coastal and Ocean Engineering*, Vol. 133(4), pp. 296-304.

Rahman, M.A., Mitra, M.C., and Akter, A. (2013), "Investigation on erosion of Kuakata sea beach and its protection by artificial beach nourishment", *Journal of Civil Engineering (IEB)*, Vol. 41(1), pp. 1-12.

Rajab, P.M., and Thiruvenkatasamy, K. (2017), "Estimation of Longshore Sediment Transport Along Puducherry Coast, Eastcoast of India; Based on Empirical Methods and Surf Zone Model." *Indian Journal of Geo Marine Science*, Vol. 46(07), pp. 1307-1319.

Rashid, M.B., and Mahmud, A. (2011), "Longshore currents and its effect on Kuakata beach, Bangladesh." *Bangladesh Journal of Geology*, Vol. 29-30, pp. 30-40.

Safak, I. (2006), "Numerical modeling of wind wave induced longshore sediment transport", *M.Sc. Engg. Thesis*, Department of Civil Engineering, Middle East Technical Universitsy, Turkey.

Sarwar, M., and Woodroffe, C.D. (2013), "Rates of shoreline change along the coast of Bangladesh", *Journal of Coastal Conservation*, Vol. 17(3), pp. 515-526.

Shetty, A. and Jayappa, K.S. (2020), "Seasonal variation in longshore sediment transport rate and its impact on sediment budget along the wave-dominated Karnataka coast, India", *Journal of Earth Syst. Science*, Vol. 2020, pp. 129-234.

Shi, B., Wang, Y.P., Yang, Y., Li, M., Li, P., Ni, W. and Gao, J. (2015), "Determination of critical shear stresses for erosion and deposition based on in situ measurements of currents and waves over an intertidal mudflat", Journal of Coastal Research, Vol. 31, pp. 1344–1356.

Thach, N.N., Truc, N.N., and Hau, L.P. (2007)," Studying shoreline change by using LITPACK mathematical model (case study in Cat Hai Island, Hai Phong City, Vietnam)", *VNU Journal of Science*, Vol. 23 (2007), pp. 244-252.

Uddin, M., Alam, J.B., Khan, Z.H., Hasan, G.M.J., and Rahman, T. (2014), "Two-dimensional hydrodynamic modelling of northern Bay of Bengal coastal waters", *Computational Water, Energy, and Environmental Engineering*, Vol. 3, pp. 140-151.

Yadav, A.K., Dodamani, B.M., and Dwarakish, G.S. (2016), "Estimation of Longshore Sediment Transport Rate: A Review ", Proceedings *of International Conference on Hydraulics, Water Resources and Coastal Engineering (Hydro2016),* CWPRS Pune, India.